MECHANISTIC STUDIES FOR IMPROVED UNDERSTANDING OF LOW SALINITY

WATERFLOODING BASED ENHANCED OIL RECOVERY AND POTENTIAL

APPLICATION TO THE ALASKAN NORTH SLOPE RESERVOIRS

By

Mukul N. Chavan

RECOMMENDED: _____

Dr. Shirish Patil

_____

Dr. Santanu Khataniar

_____

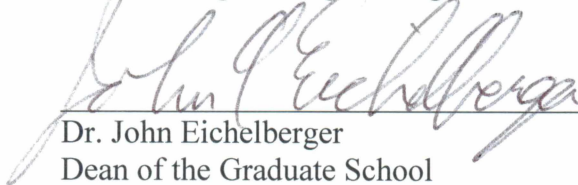Dr. Abhijit Dandekar
Advisory Committee Chair

_____

Dr. Abhijit Dandekar
Chair, Department of Petroleum Engineering

APPROVED: _____

Dr. Douglas Goering
Dean, College of Engineering and Mines

_____

Dr. John Eichelberger
Dean of the Graduate School

_____

Date

MECHANISTIC STUDIES FOR IMPROVED UNDERSTANDING OF LOW SALINITY

WATERFLOODING BASED ENHANCED OIL RECOVERY AND POTENTIAL

APPLICATION TO THE ALASKAN NORTH SLOPE RESERVOIRS

A

THESIS

Presented to the Faculty

of the University of Alaska Fairbanks

in Partial Fulfillment of the Requirements

for the Degree of

MASTER OF SCIENCE

By

Mukul N. Chavan, B.E.

Fairbanks, Alaska

May 2015

Abstract

Improvement in the recovery of oil by low or reduced salinity water has been reported by many researchers. However, a consistent mechanistic explanation behind low salinity waterflood has not yet emerged. A thorough literature review was conducted that pertains to low salinity water based enhanced oil recovery and preliminary screening criteria were proposed which may help in narrowing down the responsible mechanisms and identifying suitable candidates for low salinity waterflood. Altogether nine different variables, such as clays, oil characteristics, salinity ranges etc. were considered in developing the screening criteria.

With the exception of some tests on standard Berea sandstone cores, all other experimental studies were carried out on representative Alaska North Slope (ANS) reservoir core samples and oil and brine samples. Experimental studies involved a direct visualization of the release of crude oil from the clay surface with low salinity waterflood as observed through a simple substrate type test. Amott type spontaneous displacement tests were performed to quantitatively determine the effect of low salinity water using core materials containing different types of clays. Two sets of low salinity water coreflooding experiments were conducted in the tertiary recovery mode; first using dead oil and the second using recombined oil at pseudo reservoir conditions to examine the potential in improving oil recovery. Oil recoveries were also compared with continuous injection vs slug-wise injection of low salinity water. Finally, surface level investigation was performed using an optical microscope to visually analyze the impact of low salinity water on core samples. All the experiments performed with low salinity water on Alaska North Slope (ANS) reservoir core samples consistently showed anywhere between a 3-30 % increase in oil production with the use of low salinity brine. The literature review identified wettability alteration, cation exchange

capacity, clay type and clay content as some of the dominant mechanisms influencing low salinity

waterflooding.

Table of Contents

List of Figures

List of Tables

List of Appendices

Disclaimer

Acknowledgements

Chapter 1 Introduction

1.1   Background

Waterflooding and gas injection into the reservoir are the most common secondary recovery mechanisms (Ahmed 2010). As the gas to oil ratio (GOR) and water cut increase during secondary recovery stage, the field reaches an economic threshold. In this case other artificial methods are implemented which is known as improved or enhanced oil recovery (EOR). EOR methods include thermal recovery, alkaline flooding, polymer flooding, artificial lift techniques, miscible injection and combination of these techniques. There has been a declining trend in the production of hydrocarbons over the years and it is essential to maintain the production with a suitable EOR technique to meet exponential demand in energy.

In the present work, the Alaska North Slope (ANS) reservoir with a specific focus on low salinity waterflooding for enhancing the oil recovery is considered. ANS is located in the northern-most region of Alaska and contains the National Petroleum Reserve – Alaska (NPRA), Prudhoe Bay oil field discovered in 1968, followed by the Kuparuk oil field in 1969. The ANS contributes 15-20% of oil production in the U.S.A. Since achieving its peak oil production in 1988, the crude oil production from the ANS has declined rapidly. Figure 1.1 shows the declining production trend of the ANS over time.
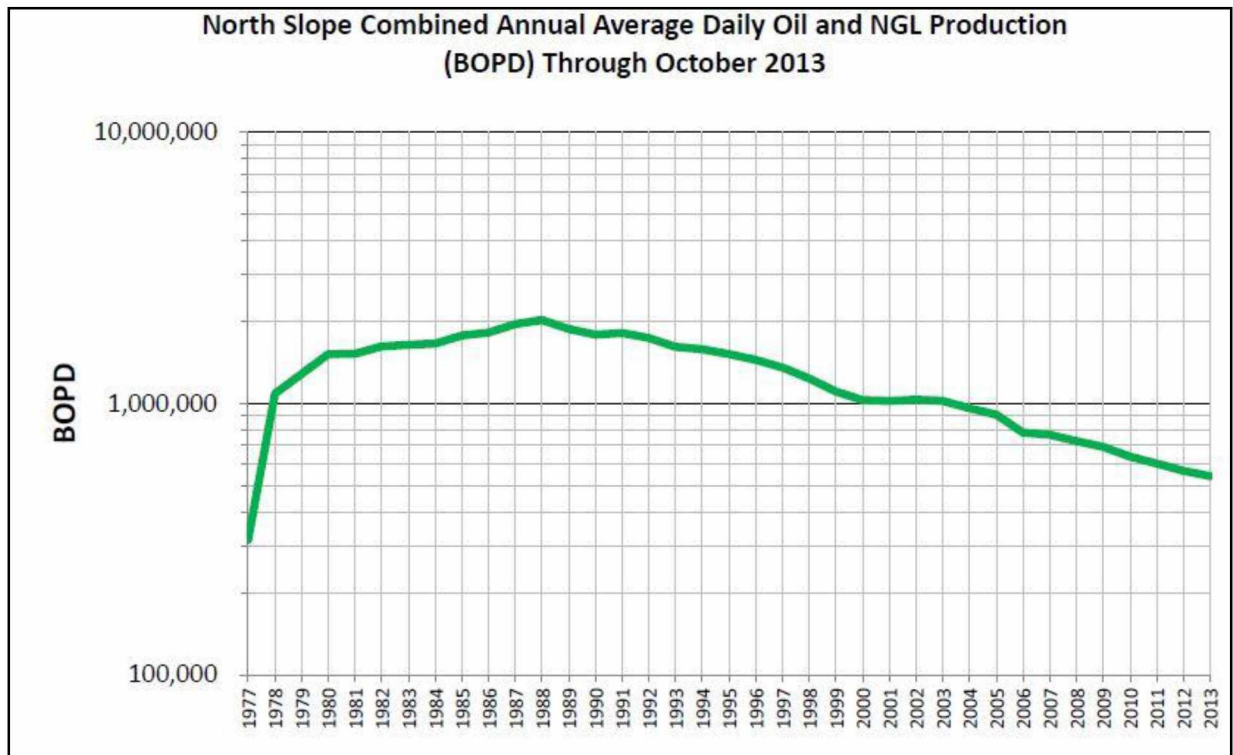
Figure 1.1 Declining Crude Oil Production Trend in ANS (Source: DNR Division of Oil and Gas 2013 Annual Report)

1.2   Low Salinity Waterflooding (LSWF)

Traditional waterflooding techniques are the oldest and most common methods to improve oil recovery beyond reservoir depletion. In contrast, low salinity waterflooding (LSWF) is a relatively new enhanced oil recovery method in which injection water salinity is reduced to further improve oil recovery. Improvement in the recovery of oil by low or reduced salinity water was first reported by Bernard back in 1967. The interest in LSWF picked up again in the mid-nineties with many publications that appeared from Dr. Morrow's research group, primarily based on laboratory corefloods. In 2004, Webb was the first to publish the results on a single-well test and provided field evidence of reduction in residual oil by low salinity water. However, up until 2005 the interest in low salinity waterflooding remained at a fairly low level but later years saw an almost exponential increase in this area with 25 papers appearing in the literature in 2010, Morrow and

2

Buckley (2011). A histogram similar to Morrow and Buckley's, shown in Figure 1.2 indicates that authors continue to investigate LSWF. Table A-1 shows a list of publications and indicates sources of information discussed in the present work. Data from the Table A-1 indicates that clay type, wettability, and water chemistry are the most discussed topics (see Figure A.1).

According to Morrow and Buckley (2011), despite growing interest in low salinity water effects, a consistent mechanistic explanation has not yet emerged. In part, this may be the result of the use of different materials (especially rocks and crude oils) and variations in test procedures. The complexity of the minerals, crude oils, and aqueous-phase compositions and the interactions among all these phases also may contribute to confusion about the cause of low salinity water effect. The variety of circumstances under which low salinity water effect may or may not be observed suggests that more than one mechanism may be in play.
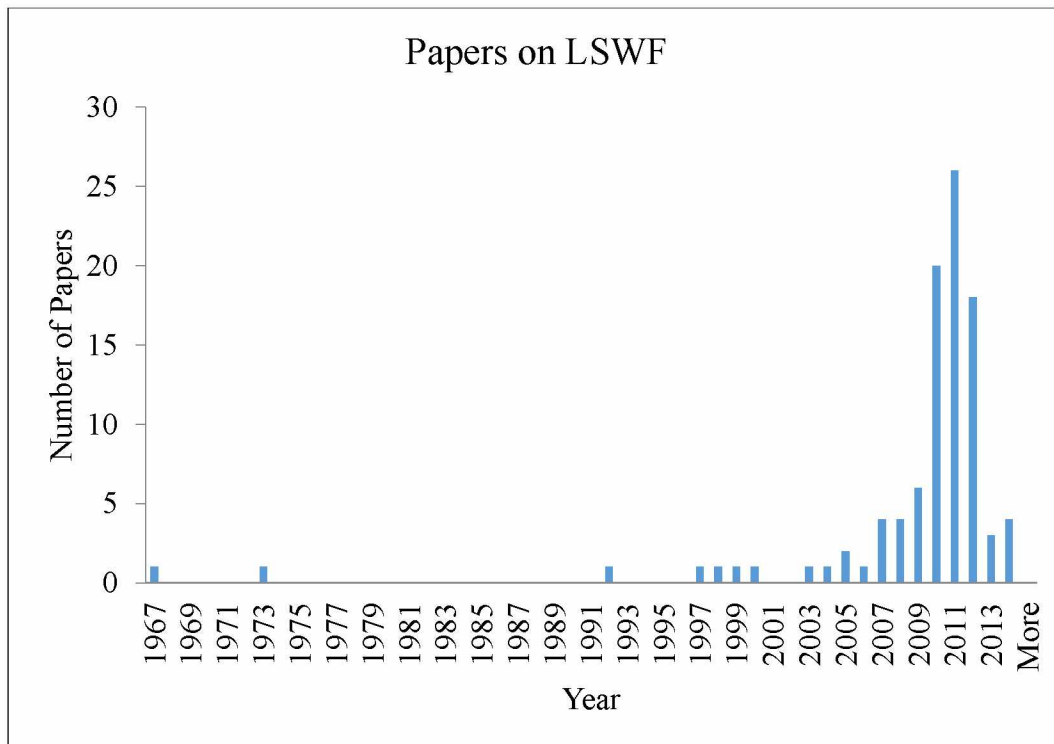
Figure 1.2 Society of Petroleum Engineers (SPE) Publications on LSWF

LSWF has been extensively studied, and many authors have documented the benefits on oil recovery, but the governing mechanisms for the enhanced recovery technique are not yet fully agreed upon. It is believed that certain conditions are necessary to observe an effect from low salinity water injection, but no one mechanism has been accepted as contributing the most to the observed benefits. Most of the literature studied showed an increase in oil recovery by LSWF in laboratory core sample experiments. Benefits have also been realized in the field, including on ANS (Webb et al. 2004). Cuong et al. (2013) presented a review on the topic of LSWF in which the mechanisms behind the LSWF in last two decades have been discussed and also made a comparison of the laboratory and field studies. Furthermore important simulation results discussed by Cuong et al. (2013) provides a comparison in LSWF-CO_2-Water alternating gas (WAG) and high salinity CO_2 WAG and it has been seen that LSW-CO_2 WAG yields higher ultimate oil recovery than high salinity-CO_2 WAG.

1.3   Investigation of the Role of Clay Type and Its Response to Low Salinity Water through
       Simple Clay Substrate Type Tests

Berg et al. (2009) carried out direct visual experiments to determine the effect of low salinity water

and reported on the successful use of montmorillonite clay substrates to study oil released by low

salinity water. Figure 1.3 is a basic sketch of the experiment in which a substrate was prepared by

attaching an oil droplet to clay particles. The use of low salinity water causes detachment of oil

droplet from the surface of clay. Low salinity water leads to wettability change of the sandstone

rock which then causes release of oil. These types of tests do provide a good qualitative indication

of the response of clay type to low salinity water.
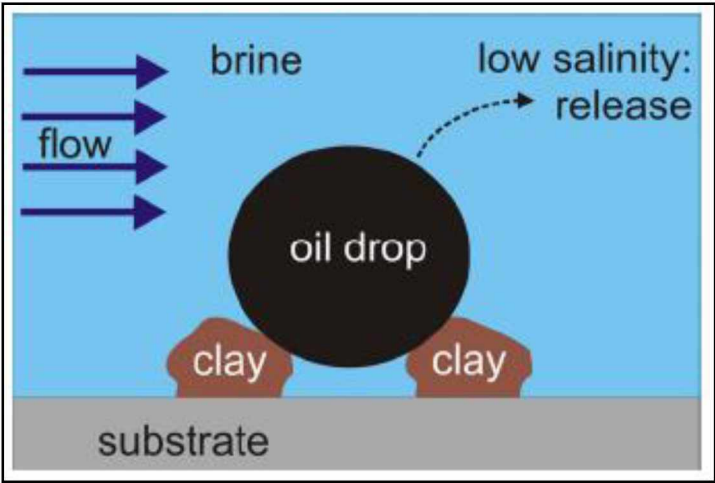
Figure 1.3 An Oil Droplet Attached to Clay Particles on a Substrate (Berg et al. 2009)

1.4   Investigation of the Role of Clay-type and its Response to Low Salinity Water through
      Amott Type Spontaneous Displacement Tests

The Amott wettability test is one of the traditional methods used to determine reservoir wettability by studying spontaneous fluid displacement. It works on the principle that the wetting fluid will imbibe spontaneously into the core thus displacing the non-wetting fluid. In other words, the core will spontaneously imbibe a higher volume of the wetting phase than the non-wetting phase. Core plugs used in this test are either 1" or 1.5" in diameter with lengths ranging from 2-3" (Dandekar 2013). Amott (1959) proposed this method, which involves a series of spontaneous and forced displacement of water and oil by each other. The process involves a five-step procedure that includes establishment of residual oil saturation by waterflooding an oil-aged core, spontaneous and forced displacement of water followed by spontaneous and forced displacement of oil. In the present work, the Amott test procedure involved an establishment of initial water saturation by oil flooding a core sample followed by spontaneous displacement of high salinity as well as low salinity water.

1.5   Low Salinity Water Corefloods

In general, coreflood experiment consists of a flow of fluid (gas or liquid) through a core sample at controlled temperature and pressure to measure the flow parameters. These coreflood experiments are used on a lab scale to develop and evaluate the concepts of oil recoveries on core level that will help improve the production in the field. The low salinity water coreflood is a relatively new technology which is used to determine the benefits of low salinity waterflood over high salinity waterflood.

1.5.1 Determination of Oil Recovery as a Function of Progressively Decreasing Injection Water Salinity

In this type of coreflood experiment, the core is cleaned and dried, saturated with high salinity brine and flooded down to initial water saturation (S_{wi}) using dead oil. Routine core analysis data on porosity, absolute permeability is determined. The first waterflood is conducted using the high salinity brine and residual oil saturation (S_{or}) is determined. The salinity of water is progressively reduced and injected in tertiary recovery mode.

1.5.2 Continuous vs. Slug Wise Injection

Given the fact that most reservoirs have undergone some form of waterflooding (typically high salinity), it seems logical to test the potential of low salinity water injection under tertiary mode to target the "low salinity S_{or}". However, incremental oil recovery benefits using low salinity water are typically seen after continuous injection of many pore volumes (PV's) of water (Morrow and Buckley 2011 and Agbalaka et al. 2009). In a field application this may be impractical as producing large volumes of low salinity water to recover the incremental oil and may result in an unfavorable cost to benefit ratio. However, smaller or optimized "slugs" of low salinity water followed by the typical high salinity water may obtain similar low salinity waterflood benefits. The investigation of slug wise injection of low salinity water can be conducted in two different modes: (1) in a secondary mode, i.e., inject a certain slug of low salinity water and follow that with high salinity water injection and (2) in a tertiary mode where low salinity water injected after high salinity water.

1.6   Reservoir Condition Corefloods and Surface Level Investigation

In this task, the low salinity water benefits on the core sample at full reservoir conditions, i.e. using recombined oil (pseudo live oil) sample at reduced conditions is determined. The pseudo live oil is prepared by recombining methane with the dead oil. Residual oil saturations are measured for progressively decreasing water salinities under tertiary injection mode. The data obtained are compared with the dead oil core floods mentioned in section 1.5.

Although, the benefits of low salinity water injection have been documented in numerous research reports, the exact mechanism is still not confirmed. However, some of the studies (Chen et al. 2010 and Sorbie and Collins 2010) have made an attempt to investigate the mechanism on a pore level. Chen et al. (2010) based on their nuclear magnetic resonance (NMR) studies have stated that there are two pore filling mechanisms for low salinity waterflooding, i.e., a pore center filling mechanism and a pore-corner filling mechanism. The invading low salinity water displaces oil from pore-centers and from pore-corners, and strips out adsorbed oil from pore surfaces and therefore changes wettability to an increased water wet condition.

In the present work, photographic optical microscope studies are used for surface level investigation after the Amott tests are performed as described in section 1.4 to determine the mechanism behind it. The microscope was used to reveal the differences in the fate of the clays as the high salinity water is known to stabilize the clays, while the low salinity water does not. This study is based on the qualitative analysis of the effect of low salinity as well as high salinity water.

1.7   Objectives

The primary aim of this research was to conduct mechanistic studies for improved understanding of low salinity waterflooding (LSWF) for the ANS reservoirs to determine the potential benefits in improving oil recovery. Currently used EOR methods in Alaska include miscible gas injection and waterflooding. Despite the application of these EOR methods, significant hydrocarbon volume is still in place in the ANS reservoirs. Therefore, a better understanding in LSWF for ANS reservoirs is necessary as this technique is relatively new, at least from a field application standpoint. Consequently, understanding the mechanism behind LSWF will help improve oil recovery.

Based on aforementioned background, the plan was to conduct low salinity waterflooding experiments on representative core samples from ANS reservoirs. Also the overall aim of this research was as follows-

1. Determine the preliminary screening criteria for LSWF based on the literature review.

2. Directly visualize a detachment of crude oil from clay mineral surface using substrate type test. Another important aspect of this experiment was to compare the effect of low salinity water on different types of clays (for example, Montmorillonite, Kaolinite and Glauconite, which is a predominant clay type in ANS).

3. Observe the role of Glauconite clay in low salinity water using Amott type spontaneous displacement test. Compare the oil recovery by spontaneously displacing oil with high salinity water followed by low salinity water for different types of clays. Quantitatively determine the amount of oil recovered with low salinity water.

4. Determine the oil recovery with low salinity waterflooding on ANS reservoir cores using dead oil.

5. Compare the above coreflood results with the coreflood at pseudo reservoir conditions, i.e. using recombined oil at corresponding reservoir temperature.

6. Observe the low salinity water effect at surface level using an optical photographic microscope technique. This method provides a qualitative analysis to find out a mechanism behind LSWF.

Chapter 2 Literature Review

A thorough literature review was conducted that pertains to low salinity based enhanced oil recovery (EOR). This was meant to be a comprehensive review of all the refereed published papers, conference papers, master's and doctoral theses and other reports in this area. The review was specifically focused on establishing various relations/characteristics or "screening criteria" such as:

1. Clay minerals potential mechanism that benefits low salinity waterflooding;

2. Clay types vs. range of residual oil saturations;

3. API gravity and down hole oil viscosity range that is amenable for low salinity water;

4. Salinity range for EOR benefits;

5. Pore sizes, porosity, absolute permeability and wettability range for low salinity EOR;

6. Continuous low salinity injection vs. slug wise injection;

7. Grouping of possible low salinity mechanisms;

8. Contradictions or similarities between lab experiments and field evidences;

9. Compositional variations in tested low salinity waters.

The current research work introduced various mechanisms and reservoir properties that contribute to additional oil recovery by LSWF, as found through an extensive literature review. Topics include clay types, oil properties such as API gravity and viscosity, injection water salinity ranges, pore size, porosity, permeability, wettability and compositional variation in low salinity waters. The literature review portion concludes by discussing comparisons between lab and field studies and by providing screening criteria for LSWF.

It can be concluded that either one or more of these mechanisms, or combination thereof, may be "case-specific", i.e., depending on the particular oil-brine-rock (OBR) system rather than something that is "universal" or universally applicable. Therefore, every OBR system that is unique or specific ought to be investigated to determine the benefits (if any) of low salinity water injection; however, the proposed screening criteria given in Table 6-1 may help in narrowing down some of the dominant responsible mechanisms.

2.1 Clay Minerals Potential Mechanism that Benefits Low Salinity Waterflooding

Many authors state that clay must be present in order to see benefits from LSWF, and studies have been conducted that show LSWF is effective in various types of clays. To determine what types of clays mostly benefit LSWF, it is necessary to understand the interactions between clay particles, water, and oil. Most sandstone reservoirs are made up of a mixture of sand and clay particles, and contain a mixture of water and oil in the pore space.

Tchistiakov (2000) suggests that in water environments, clay hydration reduces the strength of bonds between a clay surface and exchangeable cations. While part of the cations remains attached to the clay surface and form the adsorbed cation layer, another part of the cations transits at some distance from the clay surface and form the diffuse ionic layer. The distribution of the dissociated cations near a clay particle surface is determined by the balance between electrostatic attraction of the clay surface and thermal motion of the cations, tending to spread the cations away from the surface and equalize their concentration in the solution. Consequently the concentration of the dissociated cations decreases with distance from the particle. The concentration of the anions on the contrary decreases in direction towards the surface. An increase of valence exchangeable cations strengthens bonds between the cations and the clay surface and consequently reduces the potential and the diffuse layer thickness. In general, the clay stability in sandstone decreases with

12

the decrease of the exchangeable cation charge and radius. Thus mono-valent cations can easily desorb from a clay surface and go to the diffuse layer around the clay particle (Tchistiakov 2000).

Lager et al. (2008) describes the connection between oil and clays from a chemistry perspective, and conclude that the oil molecules are held on the surface of the negatively charged clay particles mainly by divalent cations. These are positively charged ions, such as calcium (Ca^{++}) or magnesium (Mg^{++}), which act as tethers to hold the oil molecules onto the rocks. When flooded with water that has a lower salinity than the reservoirs formation water, free cations in the displacing fluid, for example monovalent sodium ions (Na^+), exchange with the divalent cations holding the oil in place and release the oil molecules, allowing these to be swept out of the rock pores. It has been observed that the more clay present in the reservoir, the greater will be the benefit of using low salinity water (Jerauld et al. 2008).

Lee et al. (2010) refers to the structural layers as an electric double layer, which consists of an inner adsorbed layer of positive ions (the adsorption layer), and an outer diffuse layer (the osmosis layer) consisting of mainly negative ions. The thickness of the double layer depends on the ion concentration in the surrounding water. In the case of high salinity water containing more ions, the double layer is more compact, and the oil release from the clay surface is inhibited. However, when low salinity water is introduced, the double layer expands. The adsorption layer contains divalent calcium or magnesium ions, which act as tethers between the clay and oil droplets. Injecting reduced salinity water opens up the diffuse layer, enabling monovalent ions such as sodium, carried in the injected water, to penetrate into the double layer. Here, the monovalent ions displace the divalent ions, breaking the tethers between oil and clay particles, thus allowing the oil to be swept out of the reservoir.

13

Many of the research papers studied show that the presence of active clay minerals is necessary to obtain low salinity EOR effects. Clay minerals are often characterized as cation exchange material, because of structural charge imbalance, either in the silica or in the aluminum layer and also at the edge surfaces, causing a negative charge on the clay surface. The magnitude of the selectivity of different cations toward different clays varies considerably. The impact of low salinity waterflooding depends on the mineralogy of the rock. Many low salinity water flood experiments include sandstone with kaolinite clay. Among the clays usually present in reservoir sandstones, kaolinite has the lowest cation exchange capacity and is therefore probably the least favorable clay material for low salinity flooding. Based on the cation exchange capacity, the order of favorable type of clay minerals should be: kaolinite < illite/mica < montmorillonite (Austad et al. 2010). According to this classification montmorillonite, or clays with high cation exchange capacity, would be the most favorable clay for low salinity water flooding benefits. However some studies have been conducted where additional oil recovery was observed for which kaolinite is the dominant pore coating material and can be amenable for LSWF benefits (Jerauld et al. 2008; Seccombe et al. 2008; Hadia et al. 2011).

2.2   Clay Types vs. Range of Residual Oil Saturations

There are three main types of clays: discrete particle clays, pore-lining clays, and pore-bridging clays. Discrete particle clays are attached to sand grains, randomly scattered throughout the pore walls and do not form a connected clay particle framework. Kaolinite is an example of discrete particle clay. Pore-lining clays are attached to pore walls and form relatively continuous thin clay mineral coating. Chlorite is an example of pore-lining clay. Pore-bridging clays are attached to the rock mineral skeleton, and extend far into or completely across a pore or pore throat. Montmorillonite is an example of pore-bridging clay (Tchistiakov 2000).

Many authors agree that clay must be present to benefit from LSWF, but there has been a lack of study on clay type versus residual oil saturation. The crude oil type and rock type, particularly presence and distribution of clay types, both play a dominant role in improving residual oil saturation (Robertson et al. 2003). The LSWF was performed after establishing residual oil saturation (S_{or}) following high salinity water flooding and it was found that S_{or} was reduced by about 20%. Seccombe et al (2008) showed through data obtained from core analysis and single well chemical tracer tests (SWCTT) that additional recovery from LSWF increased as the Kaolinite concentration increased. Morrow and Buckley (2011) showed that oil recovery increased as a result of LSWF using Berea sandstone cores containing kaolinite clay.

Boussour et al. (2009), observed an oil recovery of up to 15% of OOIP with kaolinite free sandstones, but contained 9-10% of clays composed of illite, mica and chlorite. Cissokho and others (2010) observed additional oil recovery of 10% from LSWF in sandstone cores not containing any Kaolinite, but did contain Chlorite, Muscovite and Illite. There are also examples of LSWF benefits in clay free carbonate reservoirs (Zahid et al. 2012; Yousef et al. 2012).

2.3   API Gravity and Down Hole Oil Viscosity Range that is Amenable for Low Salinity Water

There is little evidence relating oil API gravity and oil viscosity to LSWF. The existing data is a result of reporting oil properties used in experiments, not from studies that specifically relate oil properties to LSWF benefits. Some oil property data used in LSWF experiments is presented in Table 2-1. There are wide ranges of API gravity and viscosity for the oils used in LSWF experiments where additional oil recovery was observed, thus indicating that these properties may not be playing any specific role in LSWF.

Many researchers have found out that the oil composition influences the incremental oil recovery (Tang and Morrow 1997 and 1999; Lager et al. 2008). Oil type is an important parameter and it

15

must contain a significant amount of polar components in it, i.e. relatively high acid or base number to observe the benefits with LSWF (Tang and Morrow 1999; Austad et al. 2010; Ashraf et al. 2010; Fjelde et al. 2014). Oil having higher concentration of polar components is bonded to clay surfaces by divalent cation which makes it less water-wet and LSWF can alter the wetting state of the rock which ultimately improves oil recovery (Fjelde et al. 2012; Fjelde et al. 2014).

Table 2-1 Properties from Various LSWF Tests

Source/ Paper	Incremental Oil Recovery	Porosity	Permeability	API Gravity	Viscosity	Salinity (TDS)	p^H
	(%)	(%)	(mD)		(cP)	(ppm)	
Tang and Morrow (1997)	NR	23	487-614	NR	0.52-1.05	3000	6.9-7.3
Webb et al. (2004)	25-50	20-30	200-700	33-12	0.45-50	3000	7.1
McGuire et al. (2005)	13	16-24	NR	NR	NR	1500	>9
Zhang and Morrow (2006)	7	17-24	60-1100	23-25	8-58	NR	>9
Loahardjo et al. (2007)	16-29	20-27	400-800	25	56-112	3500	7
Lager et al. (2008)	10	NR	NR	NR	NR	2600	10.5
Patil et al. (2008)	14	19	65	NR	NR	5500	NR
Pu et al. (2010)	NR	10-20	0.25-250	24-31	20-50	3000	NR
Robertson (2010)	NR	19-21	90-130	NR	NR	3300	NR
Vledder et al. 2010	10-15					2200	
Cissokho et al. (2010)	10	16-20	400-800	37	5.42	1000	>7
Hadia et al. (2011)	8	16-22	10-4800	39	5.96	4300	NR
Fjelde et al. (2012)	NR	27-28	70-170	NR	1.5	2000	>7
*NR = Not Reported							

2.4 Salinity Range for EOR Benefits

The literature review suggests that oil recovery increases by decreasing the salinity of injected water; however, the optimum injected water salinity will depend on the composition of the reservoir brine. Drastic changes in salinity have been found to cause formation damage, fines migration and permeability reduction (Vaidya and Fogler 1992). Sorbie and Collins (2010) concluded that additional recovery due to LSWF requires high salinity reservoir brine. A high salinity brine causes the reservoir to be more oil wet, which provides a greater opportunity for LSWF to be effective. Also, Jerauld et al. (2008) and Austad et al. (2010) mentioned that initial water saturation is required to observe LSWF effect.

Webb et al. (2004) reported that laboratory results show additional oil recovery in injection water salinity of 3,000 ppm TDS and field experiments have shown the same effect in near wellbore environments. McGuire et al. (2005) reported that SWCTTs on four Alaska North Slope fields (two Ivishak, one Kuparuk, one Kekiktuk) showed low salinity benefits and concluded that salinity up to 5,000 ppm TDS or less is more effective for a large percentage of oil recovery. A SWCTT in the Ivishak reservoir, with 7,000 ppm TDS, showed no improvement in oil recovery (McGuire et al. 2005). Morrow and Buckley (2011) reported benefits from LSWF for injection brine compositions of up to 5,000 ppm total dissolved solids (TDS) in laboratory tests, and injection waters with compositions in the range of 2,000 to 3,000 ppm TDS, in field tests. In addition, Table 2-1 shows the range of salinities for EOR benefits.

2.5   Porosity, Pore Sizes, Absolute Permeability and Wettability Range for Low Salinity EOR

Other perceived factors that may affect benefits from LSWF include porosity, pore sizes, absolute permeability, and wettability. The literature review produced little evidence directly correlating porosity, pore size, and permeability to LSWF. Like the oil properties mentioned above (API gravity and viscosity), these properties are reported as part of experiments, but there have been no sensitivity studies conducted to determine their effect on LSWF; again indicating that these properties may not be playing any specific roles in LSWF. Some of these properties are listed in Table 2-1. On the other hand, wettability, and its relation to LSWF, has been studied in detail.

It is widely agreed that the wetting state of a reservoir affects recovery of oil by LSWF (Rivet et al. 2010; Sorbie and Collins 2010; Vledder et al. 2010; Skrettingland et al. 2011; Hadia et al. 2011; Shiran and Skauge 2012). Wettability modification is proposed as a microscopic mechanism based on p^H and salinity (Tang and Morrow 1997) and it results from interaction between crude oil components and reservoir rock (Buckley et al. 1998). Berg et al. 2009 provided direct experimental evidence that wettability alteration of clay surfaces is a microscopic mechanism for LSWF.

Agbalaka (2006) and Kulathu et al. (2013) carried out an experiment to observe the change in residual oil saturation in a core after low salinity water flooding, and found that low salinity water flooding causes the more oil-wet rock to become water-wet. This change from oil-wet to water-wet corresponds to decreasing residual oil saturation, thus a higher recovery. Wettability alteration towards increased water-wetness during LSWF is the widely suggested case of increased oil recovery and experimentally it has been found out that LSWF has a significant effect on the shape and the end points of the relative permeability curves, resulting in lower water relative permeability

and higher oil relative permeability (Webb et al. 2004; Rivet et al. 2010; Vledder et al. 2010; Morrow and Buckley 2011; Fjelde et al. 2012).

Seccombe et al. (2008) described the adsorption of crude-oil components onto reservoir rock as the mechanism that renders parts of reservoir rock oil-wet. The desorption of polar organic compounds from the clay surface causes wettability to change from oil-wet to water-wet. Hadia et al. (2011) performed experiments on neutral wet cores and showed increase in recovery due to LSWF, and Sorbie and Collins (2010) demonstrated that LSWF has little effect on strong water wet systems. Based on experiments performed by Spildo et al. (2012) and Alotaibi and Naser-El-Din (2011) mixed-wet system considered as more favorable than water-wet systems. Some authors noticed that LSWF made core samples more oil-wet (Sandengen et al. 2011; Fjelde et al. 2012). Ashraf et al. (2010) carried out corefloods with oil having different wetting tendencies and reported that LSWF improved recovery under oil-wet, water-wet and neutral-wet conditions, with water-wet and neutral-wet conditions showing maximum effect. The LSWF EOR effect is attributed to the wettability alteration, mainly because of the expansion of the electric-double layer (EDL) (Ligthelm et al. 2009). Formation of micro-dispersions when low salinity water comes in contact with crude oil can be another reason of wettability alteration and also it depends on crude oil composition, characteristics, sulfate ion concentration and temperature (Mahzari and Sohrabi 2014; Kasmaei and Rao 2014).

2.6   Continuous Low Salinity Injection vs. Slug Wise Injection

While it is known that continuous low salinity water flooding is the optimum method for producing the highest recovery factor, it may not be economically viable. However, slug-wise injections produce similar results and require much less fresh water and make low salinity water flooding a realistic option in enhanced oil recovery. Seccombe et al. (2008) found that the most effective and economical method, from core injection analysis, is a slug wise injection of 40% of the pore volume (PV). A 10% PV slug showed no additional recovery and 30% PV was the smallest slug necessary to flow through the entire core plug. The 40% PV showed to have recovered 87% of the oil recovered by continuous low salinity injection. Vledder et al. (2010) reported an incremental oil recovery of 10% to 15% due to a 40% PV low salinity injection in the Oman field in Syria. Kulathu et al. (2013) observed that S_{or} is achieved as early as 3-4 pore volumes (PV) of injected low salinity water with cyclic injection as compared to 6-7 PV's in continuous injection.

LSWF in the secondary mode refers to the injection of low-salinity water at the irreducible water saturation (S_{wi}) whereas tertiary mode low-salinity waterflood means injection of low salinity water after high salinity brine. Most of the experiments performed showed increase in oil recovery in both modes (Zhang and Morrow 2007; Agbalaka et al., 2009). But in some other studies, LSWF did not show any incremental oil recovery in tertiary mode (Rivet et al. 2010; Nasralla and Nasr-El-Din 2011).

2.7   Grouping of Possible Low Salinity Mechanisms

There are various macroscopic and microscopic mechanisms for low salinity waterflooding in the literature and still the exact mechanism is unknown. Boussour et al. (2009) analyzed possible mechanisms for LSWF and presents experimental counter-examples for most of them; including the presence of kaolinite, divalent ions in injected brine, and the effect of temperature. However, there are a number of papers that support these mechanisms and are presented in the literature as follows:

1. The increase in cation valency of a brine solution, which can be achieved with decrease in brine salinity, impacts increased oil recovery (Salathiel 1973).

2. The first explanation for LSWF effects was from migration of fines (Tang and Morrow 1999; Zhang and Morrow 2007).

3. The detachment of mixed-wet clay particles from the pore walls (Tang and Morrow 1997). Also with the use of low salinity brine the fine materials become mobile and which results in exposure of underlying rock surfaces and increases water wetness of the system (Tang and Morrow 1999).

4. The increase in p^H has been proposed as a driving mechanism in LSWF by saponification mechanism of elevated p^H, the mineral surface exchange of H^+ in the liquid with cations and dissolution of carbonates (McGuire et al. 2005; Zhang and Morrow 2007; Lager et al. 2008).

5. Mechanism based on forces and molecular interaction between charged surfaces separated by liquid (Adamson and Gast 2007).

6. Detachment of clay particles, cation exchange capacity (CEC) between clay minerals and invading brine has improved effect in oil recovery with low salinity water (Lager et al. 2008).

21

7. Low salinity water leads to wettability change of the sandstone rock which then causes release of oil (Berg et al. 2009; Rivet et al. 2010; Skrettingland et al. 2011; Sorbie and Collins. 2010; Vledder et al. 2010; Hadia et al. 2011; Shiran and Skauge 2012; Kasmaei and Rao 2014).

8. In many sandstone fields the change in ionic strength of water alters the wettability of rock and hence improves oil recovery (Alotaibi and Naser-El-Din 2011).

9. Multi-component ionic exchange (MIE) between mineral surface and invading brine is proved to be the primary mechanism underlying the improved recovery with low salinity water flood. It explains the importance of presence of clay minerals and its cation exchange capacity with low salinity water (Lager et al. 2008; Omekeh et al. 2012).

10. Salting-in effect has been suggested which contributes to desorption of some organic materials loosely bonded to clay surface. (RezaeiDoust et al. 2009; Austad et al. 2010).

11. Electric-double layer expansion is proved to be primary mechanism in LSWF as it changes the electrical charge at both oil/brine and rock/brine interface to highly negative charge which causes repulsion force between the interface and changes wettability (Lee et al. 2010; Ramez and Nasr-El-Din 2014).

12. Hamouda et al. (2014) observed from the experiments that for chalk formations, possible mechanism was the presence of cations which alters wettability and for sandstone rocks, MIE, mineral dissolution and rock weakening causing fines migration.

2.8 Contradictions or Similarities between Lab Experiments and Field Evidences

Numerous experiments have been conducted on LSWF on a core scale; however, the number of field tests is considerably less. Many of the reviewed papers indicate that field wide benefits are slightly lower than laboratory studies. Robertson (2007) provided anecdotal evidence, through historic records, that field-wide LSWF can be a successful EOR method by analyzing the injection history of several water floods in the Powder River Basin, Wyoming. His results indicate that oil recovery increased as the salinity ratio of injected water decreased.

Webb et al. (2004) demonstrated through log-inject-log tests that LSWF increased oil recovery in the near wellbore environment. Single well chemical tracer tests (SWCTT) have also been used to evaluate whether LSWF results from the field represent laboratory results. SWCTTs have been completed in the Kuparuk C Sand to determine the effectiveness of LSWF. The thickness in the test well is 20 feet and has an average porosity of 16%. Measured S_{or} prior to LSWF was 0.21 ± 0.02 and measured S_{or} after LSWF was 0.13 ± 0.02. The tests resulted in an additional 8% PV of oil displacement due to LSWF (McGuire et al. 2005).

Endicott field tests showed that LSWF works equally well at inter-well distances as it does in core floods and single well tests. Using an Endicott core flood and SWCTTs, a linear relationship between reduced-salinity, additional recovery and clay content was defined. Based on clay content in the pilot area, it was predicted that final pilot oil recovery would be 13% of the total PV swept with reduced-salinity water. Actual pilot recovery after 1.6 PVs of reduced-salinity water injection was 10% of the total PV swept. Comparison of the pilot recovery profile with the scaled core-flood recovery profile indicates that the pilot is on-track to recover the original estimate of 13% (Seccombe et al. 2010).

23

In Oman field tests, and concurrent experiments, it was shown that the laboratory model showed additional recoveries within the range of what they expected and observed in the field tests. High-salinity water injection was performed and the recovery factors were recorded. Analog fields were tested and the ultimate recovery factor for those fields was also recorded. A field-wide increase in the ultimate recovery factor of 5-15% was observed. Laboratory tests modeling the water flood showed a range of 9-23% additional recovery. The data shows a range of overlap of expected results, indicating that laboratory models could help achieve an estimation of how the water flood will perform on a field-wide scale (Vledder et al. 2010).

There is also evidence that LSWF benefits are unique to each reservoir, and that benefits may not be realized. Skrettingland et al. (2011) conducted both laboratory and field tests to investigate the effectiveness of LSWF for the Snorre Field. They reported that LSWF would be ineffective, due to the existing wettability of reservoir being near optimum for seawater injection. The work by Skrettingland et al indicates that if laboratory tests do not show additional recovery by LSWF, then LSWF will also be ineffective on a field scale.

2.9   Compositional Variations in Tested Low Salinity Waters

Lee et al. (2010) observed that modifying the brine chemistry of the injection water can significantly impact the observed recovery, and provides support that for clay like surfaces low concentration of monovalent cations are preferred to high concentrations of divalent ions, which would indicate that increased clay content gives a greater response and lower divalent cation concentrations in the injection brine to connate brine also gives a higher low salinity EOR response. Cissokho et al. (2010) reported that additional recovery due to LSWF occurred when there were no divalent ions present in the low salinity brine.

Vaidya and Fogler (1992) give evidence of fine migration and formation damage due to changes in water composition. They found that in a system having exchangeable cations, the salinity and p^H of the medium have some correlation, and observed that for a p^H value of 2.0 there is no effect on permeability but as p^H increases there is a slight variation in permeability and at a value of p^H greater than 11.0 there is a rapid and drastic decrease in permeability due to zeta potential between surfaces produces a significant repulsive force that causes colloidally induced detachment of fines which is explained by DLVO theory. Similarly it is found that p^H of permeating fluid increases as salinity decreases (Vaidya and Fogler 1992).

Lager et al. (2008) presented evidence that injected low salinity water should be optimized to achieve the maximum benefit of LSWF. Only when the water was "optimized" to the reservoir, improvements of 6~12% recovery occur. They propose that it is important to model salinity changes within the reservoir to keep the salinity at an optimum level for maximum recovery. Omekeh et al. (2012) developed a model that describes multi-component ion exchange and the dissolution of carbonates contained within sandstones. They concluded through their analysis that calcite dissolution and ion exchange can alter the composition of the brine and that the carbonate chemistry may reduce the potential for beneficial low salinity water.

Austad et al. (2010) proposes that the composition of the low salinity injection water is of less importance, but that the formation water must contain active cations. The understanding of composition of formation water is more important in low salinity waterflooding which contains divalent cations at low p^H (e.g. Ca^{2+}). Reaction of low salinity water and this formation water causes desorption of organic material from clay. The water wetness of rock improves and hence increases in oil recovery. The clay type/properties, its amount in rock, polar components in oil, the

25

initial formation water composition and its p^H are the important factors proposed in low salinity mechanism.

Nasralla and Nasr-El-Din (2011) demonstrated that sodium ions (Na^+) change the electrical charge at both oil/brine and rock/brine interface to highly negative, which results in repulsion forces between the two interfaces, and hence wettability alteration (from oil wet to water wet) and improvement in oil recovery. The cations in the injected water have more dominant effect on the recovery factor than water salinity (cation concentration) and the water chemistry is the dominant factor in determining the oil recovery factor. NaCl cation type showed the highest oil recovery over $CaCl_2$ and $MgCl_2$ (Nasralla and Nasr-El-Din 2011).

There is evidence that the generation of surfactants from residual oil at high p^H level may be the cause of low salinity recovery mechanism and this can be accomplished by eliminating high concentration chemicals found in high salinity water. When injecting low salinity water, the reaction of water and minerals from reservoir takes place and hydroxyl ions gets generated which increases the p^H value up to 9 or more. The compositional change in water salinity reduces the interfacial tension between oil and water, it changes the properties of crude oil, and the elevated p^H level generates surfactants which ultimately alter the surface tension (Webb et al. 2004; McGuire et al. 2005; Mahzari and Sohrabi 2014).

Chapter 3 Experimental Setup

3.1 Overview of the Substrate Type Test

The substrate type experiment conducted here was a modification of Berg et al. (2009) experiment in which a new flow cell is designed. This was essentially an open flow cell that allows direct visualization of the release of oil droplets from clay surface. The main objective of this experiment was to directly visualize the release of crude oil and see the effect of clay type on low salinity waterflood.

3.1.1 Experimental Setup for Substrate Type Test
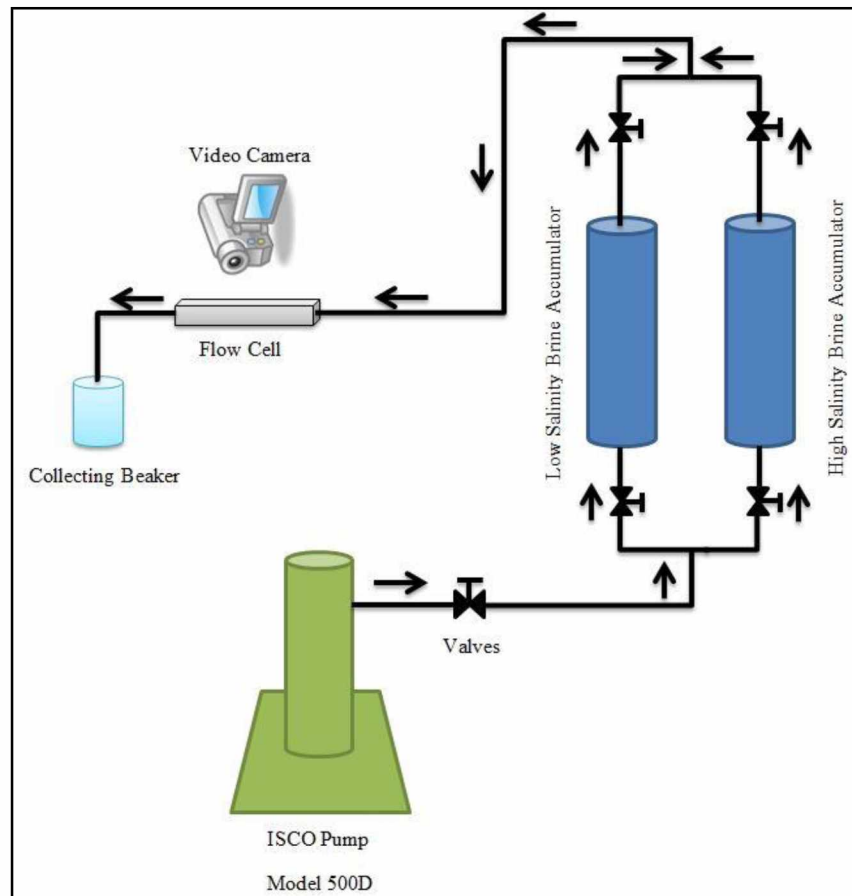
Figure 3.1 Schematic of Substrate Type Test (Modified after Berg et al. 2009)

Figure 3.1 is a schematic of a substrate type test which is a modified version of Berg et al.'s (2009) experiment. The setup consists of several different components as follows,

3.1.2 Teledyne ISCO Pump Model 500D

The Teledyne ISCO D-Series pump (model 500D) was utilized for the fluid flow through the system. The ISCO pump is a positive displacement pump and can operate at two different conditions, the constant pressure mode which maintains fluid delivery at a constant pressure by varying the flow rate whereas, in the constant flow mode, the flow rate remains constant by varying the pressure. Automatic and manual refill mode allows for the refilling of the pump cylinder with the displacing fluid (de-ionized water). The model 500D is capable of displacing fluid at a flow rate ranging from 0.001 ml/min to 204 ml/min and pressure up to maximum of 10,000 psi. Figure 3.2 shows the photographic representation of the model used in experiment.
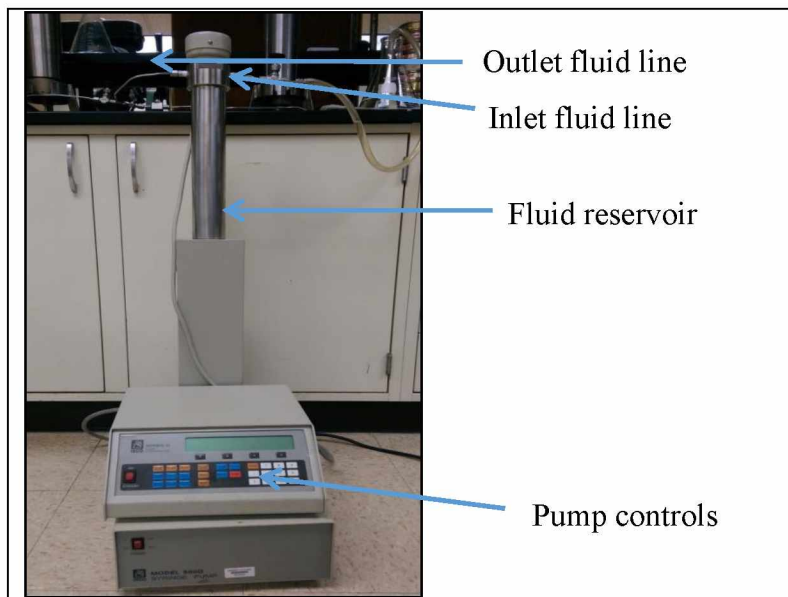
Figure 3.2 Photographic Representation of Teledyne ISCO Pump (model 500D)

3.1.3   Fluid Accumulators

An accumulator is a cylindrical vessel used for displacing fluids for core floods and similar displacement tests. For this work, two (high salinity water accumulator and low salinity water accumulator) floating piston accumulators, manufactured by TEMCO were utilized. Both of them were rated at an operating pressure of 2500 psi. They can only be subjected to temperatures up to 350 $^\circ$F. One of the accumulators containing low salinity water has a capacity of 1000 ml and the other has a capacity of 500 ml containing high salinity water (see Figure 3.3).
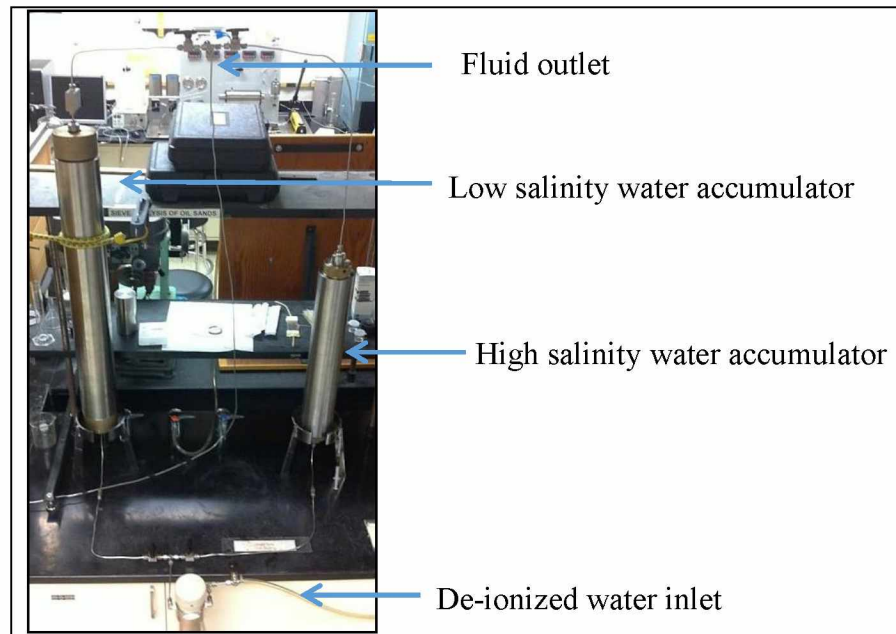
Figure 3.3 Photographic Representation of Fluid Accumulators

3.1.4 Fluid Lines, Fittings and Valves

Swagelok tubings and fittings were used to construct all the flow lines, Swagelok ball valves, needle valves were used to open and close the accumulators.

3.1.5 Flow cell – Slide Holders, Glass Slides and Plastic Tubing

Flow cell was constructed using microscopic glass slide (75mm x 25mm, available through VWR), microscope glass slide holders to keep the slide inside and to ensure a closed system fluid flow. Plastic tubing was utilized as an inlet and outlet to the slide holder.

3.1.6 Video Camera

A high quality video camera was used to continuously monitor detachment of crude oil (if any) from the substrate.

3.1.7 Syringe Needle (ϕ 0.65 x 0.80 mm)

A syringe needle was utilized to inject small drops of oil on a clay surface.

3.1.8 Different Clay Minerals- Glauconite, Kaolinite and Montmorillonite

Montmorillonite and Kaolinite clays were used from the clay mineral society. Glauconite clay (Greensand) was obtained from Delaware Geologic Survey, University of Delaware. Greensand is primarily composed of the mineral Glauconite - a potassium, iron, aluminum silicate. In some Delaware greensands, the Glauconite content exceeds 90%. The remaining 10% is mainly quartz (Delaware Geologic Survey).

3.2   Overview of the Amott Type Spontaneous Displacement Test

Figure 3.4 shows the experimental set-up for the Amott type spontaneous displacement test. This method mainly works on the principle of spontaneously displacing the non-wetting phase. Standard Amott cells made from glass were utilized for the experiment. In the present work, Amott cells were used to spontaneously displace oil with high salinity brine followed by low salinity brine.
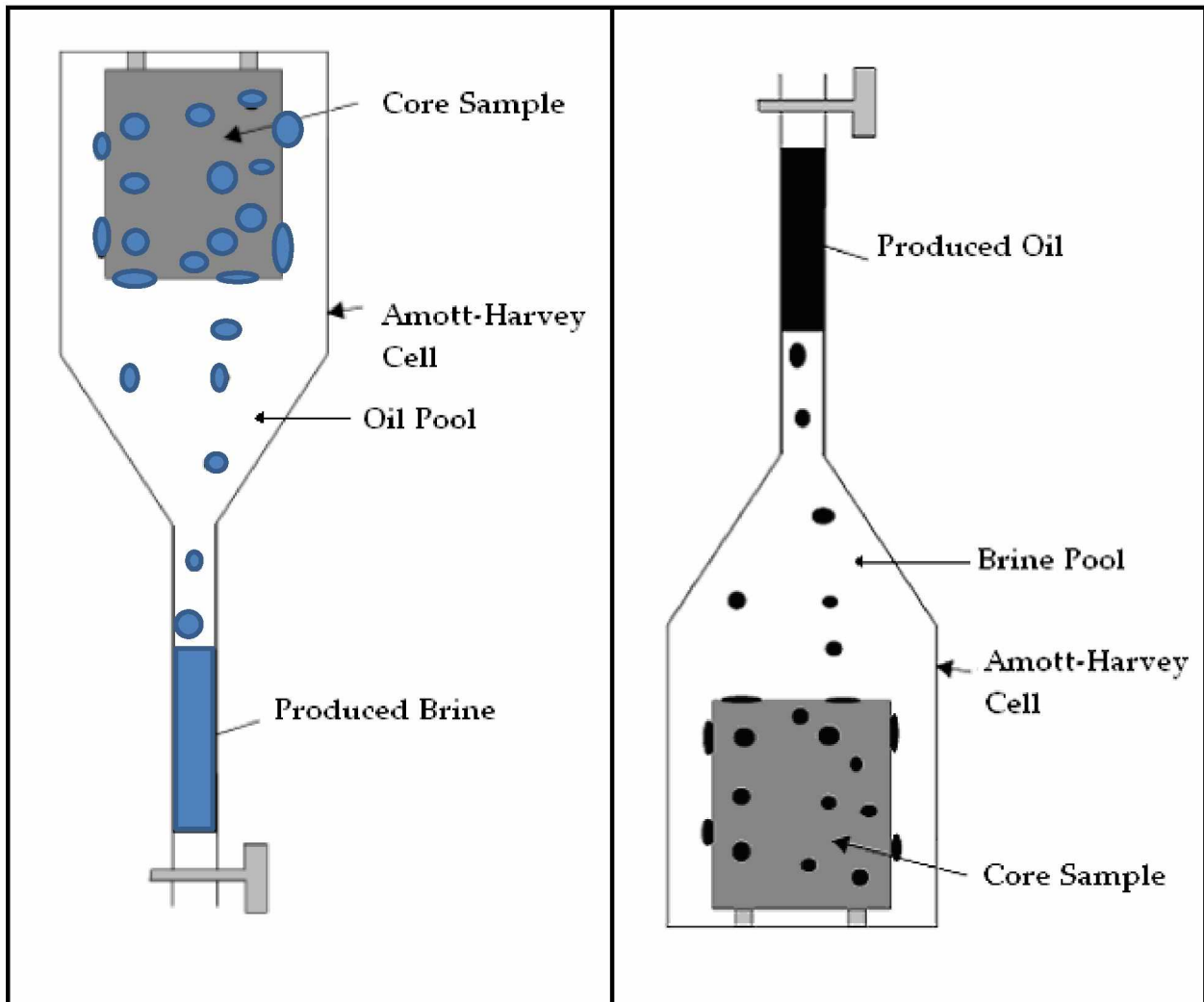
Figure 3.4 Schematic for Spontaneous Displacement of (a) Brine and (b) Oil

(Modified after Karabakal and Bagchi 2003)

3.3   Overview of the Low Salinity Water Coreflood Rig

As stated earlier, the primary objective of this work was to experimentally evaluate, on the core level, the effect of low salinity waterflooding on oil recovery. A modified version of the coreflood rig designed by previous researchers Agbalaka (2006), Patil (2007) and Kulathu (2009) who worked on the similar study was utilized to conduct coreflooding experiment on (a) ANS reservoir core samples, (b) Berea core samples and, (c) cores prepared in the lab. All the coreflooding experiments were performed in tertiary recovery mode. The design of the reservoir condition coreflood rig was adapted similar to the dead oil coreflood rig with some modifications to incorporate reservoir temperature and pressure.

3.3.1   Description of Coreflood Rig

Figure 3.5 shows the schematic representation of the coreflooding rig used in the experiment with all the necessary components. The coreflooding rig consisted of a Temco, Inc. RCHR series Hassler type core holder to accommodate core samples. The condition of overburden pressure was simulated by applying radial pressure on the rubber sleeve (annular space filled with hydraulic oil). This was achieved by pressurizing the hydraulic oil using a hand pump. There were spacers, distributers, and retainers that complete the core holder setup and help in holding the core plug in position within the rubber sleeve. Table 3-1 shows the maximum working pressure and temperature rating of the equipment used in the experiments. The pressure and temperature values used in actual experiments are given in Table 3-2.
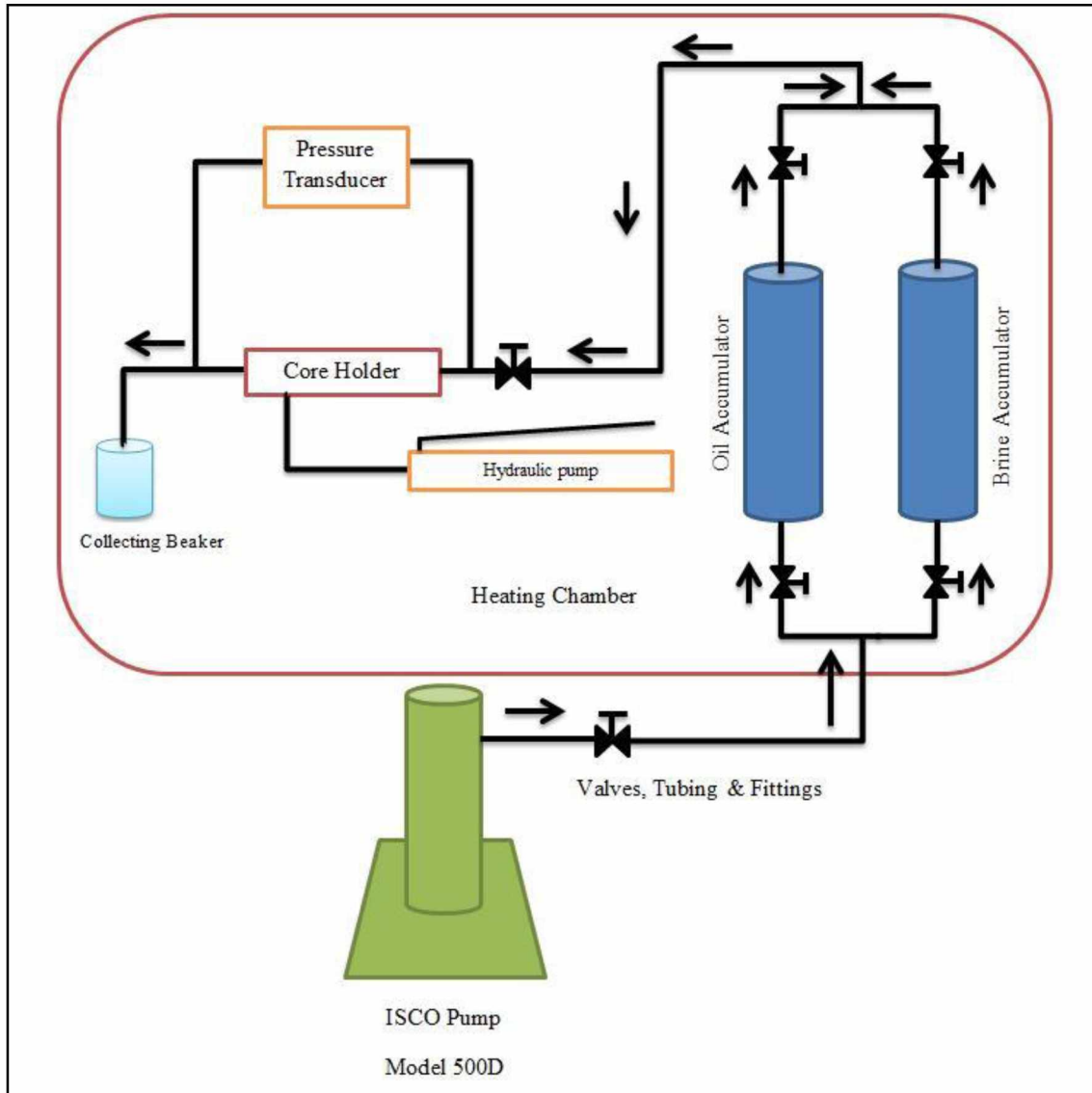
Figure 3.5 Schematic of Coreflood Set-up

An ISCO pump was used to pump the fluid (brine/crude oil) at either constant flow rate or constant pressure from the accumulators (brine/crude oil) in to the core holder. There were two accumulators (500 cc volume), rated at operating conditions of 2500 psi and 350 °F, that contain brine and oil, respectively. The brine/oil and de-ionized water (ISCO pump fluid) in the accumulator were separated by a floating piston in the cylinder. The fluid (brine and oil) pushed from the accumulator flows to a core holder. Valves were utilized accordingly to facilitate the flow

33

of either brine or oil. The Heise type digital pressure transducer (maximum working pressure of 10,000 psi) was used to measure the differential pressure across the core. The produced fluids were collected in the beaker and measurement of brine and oil was done by weighing balance. Thermotron heating chamber (temperature range of -94 °F to 356 °F) was utilized to accommodate all of the above assembly to conduct experiment at reservoir temperature (see Figure 3.6).
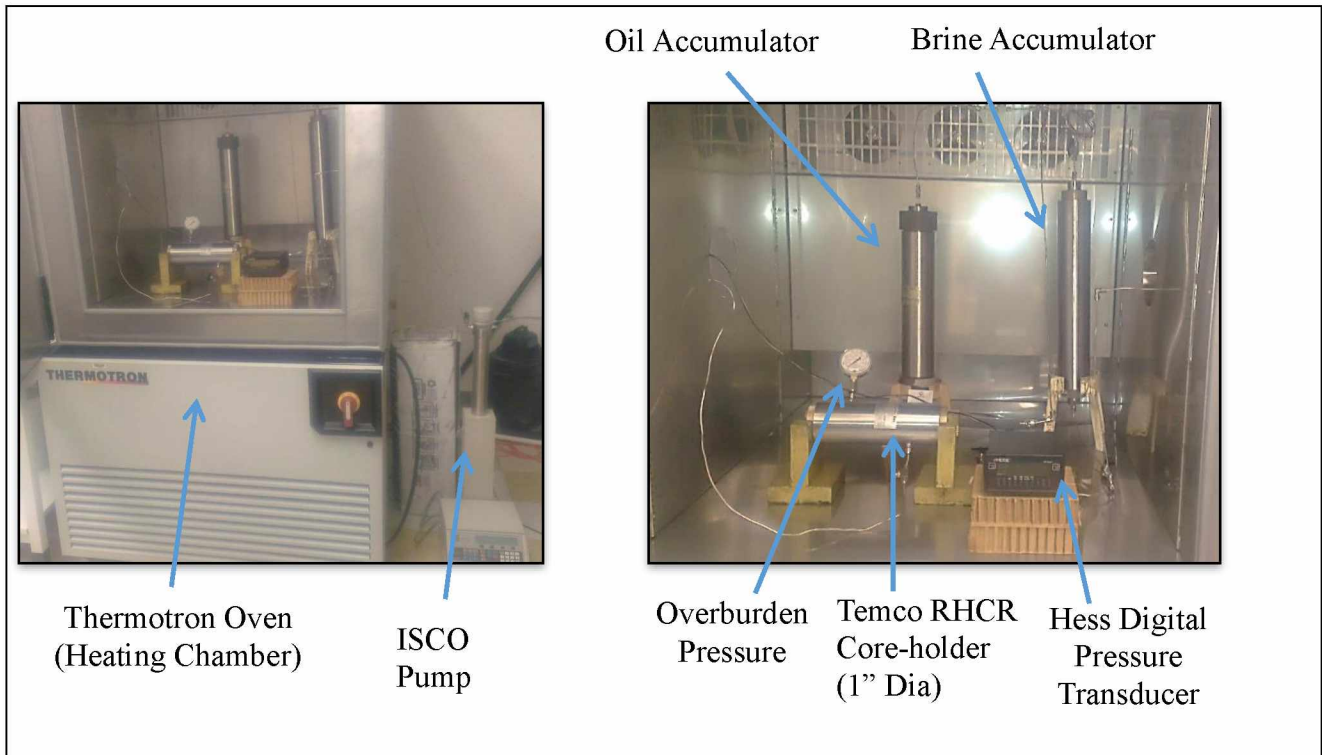
Figure 3.6 Photographic Representation of the Low Salinity Water Coreflood Rig

Table 3-1 Summary of Maximum Pressure and Temperature Rating

Equipment	Maximum Working Pressure Rating (psi)	Maximum Working Temperature Rating (^{o}F)
Core Holder	2500	350
Accumulators	2500	350
Teledyne ISCO Pump	10000	104
Digital Pressure Transducer	10000	Unknown
Fluid Lines, Fittings and Valves	6000	250
Hand Pump	10000	150
Back Pressure Regulator	10000	350

Table 3-2 Summary of the Pressure and Temperature used in the Experiment

Equipment	Maximum Pressure (psi)	Maximum Temperature (^{o}F)
Core Holder	500	155
Accumulators	500	155
Teledyne ISCO Pump	500	60
Digital Pressure Transducer	700	155
Fluid Lines, Fittings and Valves	500	155
Hand Pump	500	60
Back Pressure Regulator	110	155

3.3.2 Modified Setup for Reservoir Condition Corefloods

Figure 3.7 shows schematic of the modified setup (from section 3.3.1) used for flooding recombined oil. In this case, one of the accumulators contains recombined oil (pseudo live oil) under pseudo reservoir conditions. To maintain reservoir temperature, the accumulator, core holder, and tubing were accommodated in a heating chamber (Thermotron oven). Additionally a back pressure regulator was incorporated to maintain the recombined oil in single phase conditions. Nitrogen gas was used to pressurize the backpressure regulator. Rest of the description of coreflood rig is similar to section 3.3.1.
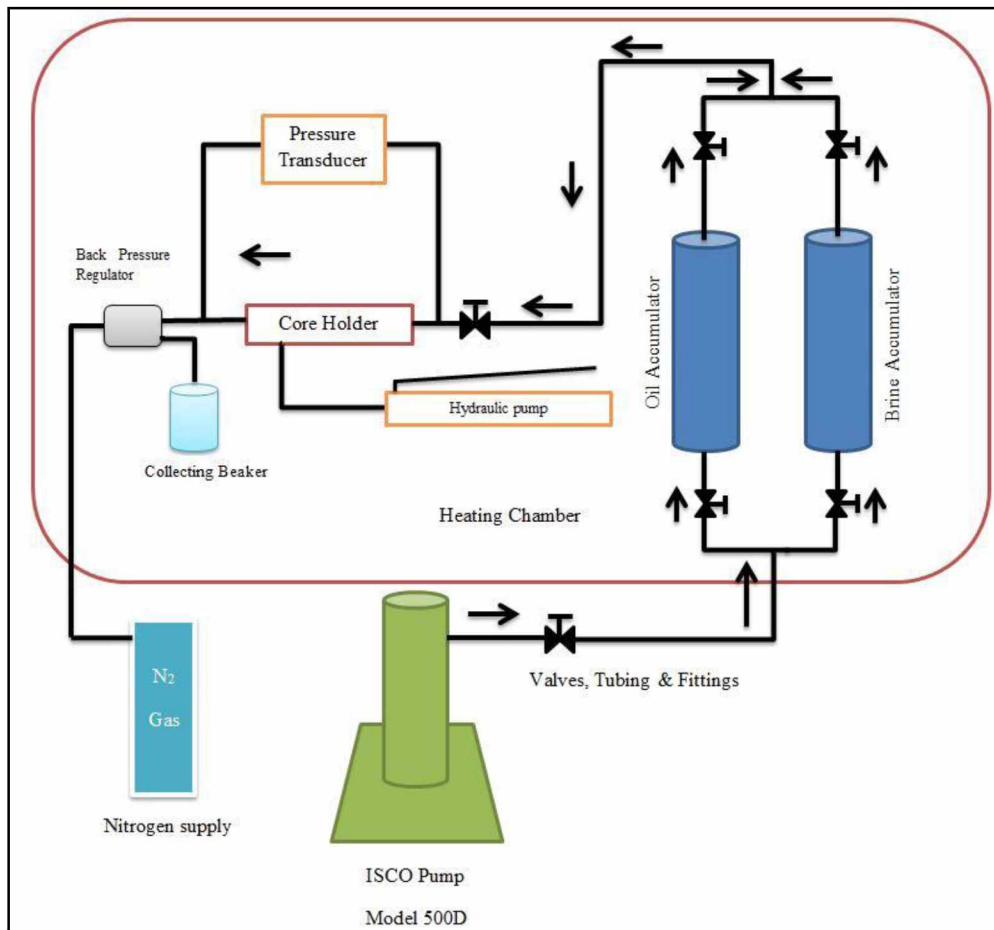
Figure 3.7 Schematic of Coreflood Rig used for Coreflooding at Reservoir Conditions

3.3.3   Recombination of Oil

Recombination of oil and gas above bubble point conditions was necessary for the fluids to remain in a single phase for the coreflooding at reservoir condition. Oil was recombined with methane gas at reservoir temperature and pressure in an accumulator (see Figure 3.8). Oil and methane gas at the desired gas-oil ratio (GOR) were injected into an accumulator. The accumulator was pressurized to a high pressure using an ISCO pump. The sample was kept pressurized for 2 days to form recombined oil. The accumulator was then heated to reservoir temperature before conducting a pseudo live oil coreflood experiment.
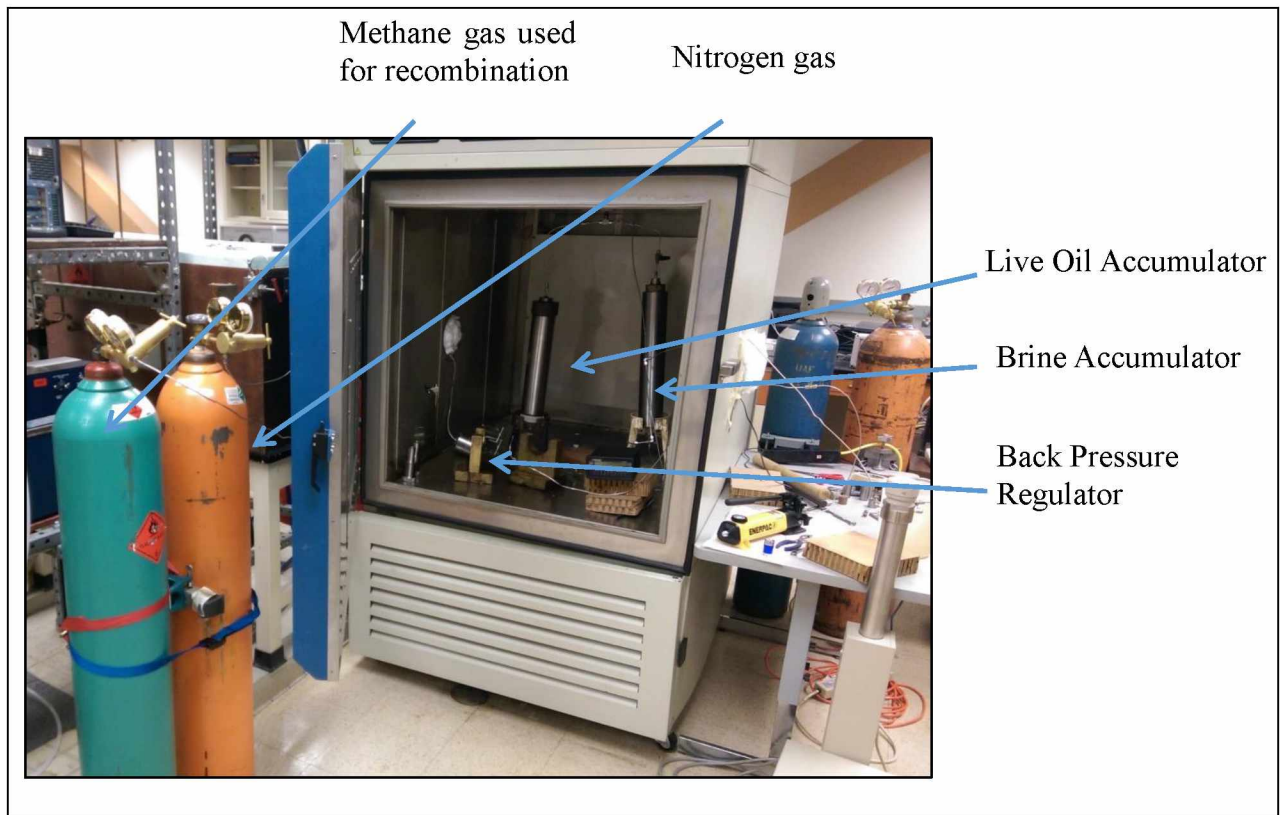
Figure 3.8 Photographic Representation of the Reservoir Condition Coreflood Rig

A brief description of some the components (ISCO pump, accumulators and valves, fittings and fluid lines) used in the coreflood rig is similar to the section 3.1.2 through 3.1.4. The detailed description of the setup, equipment used, and the principle of operation can be found in Agbalaka (2006). Descriptions of the remaining components are given in the following sections.

3.3.4   Core Holder

Temco, Inc. RCHR series Hassler type core holder rated at a maximum working pressure of 2,500 psi and temperature of 350 °F was utilized for the coreflooding studies. It consists of an outer metal jacket and an inner rubber sleeve placed concentric to each other. The rubber sleeve holds the core plugs (1-1.5" in diameter and up to 6" in length). The application of overburden pressure was in radial direction. This confining pressure ensures that the core sample was held within the sleeve (see Figure 3.9).
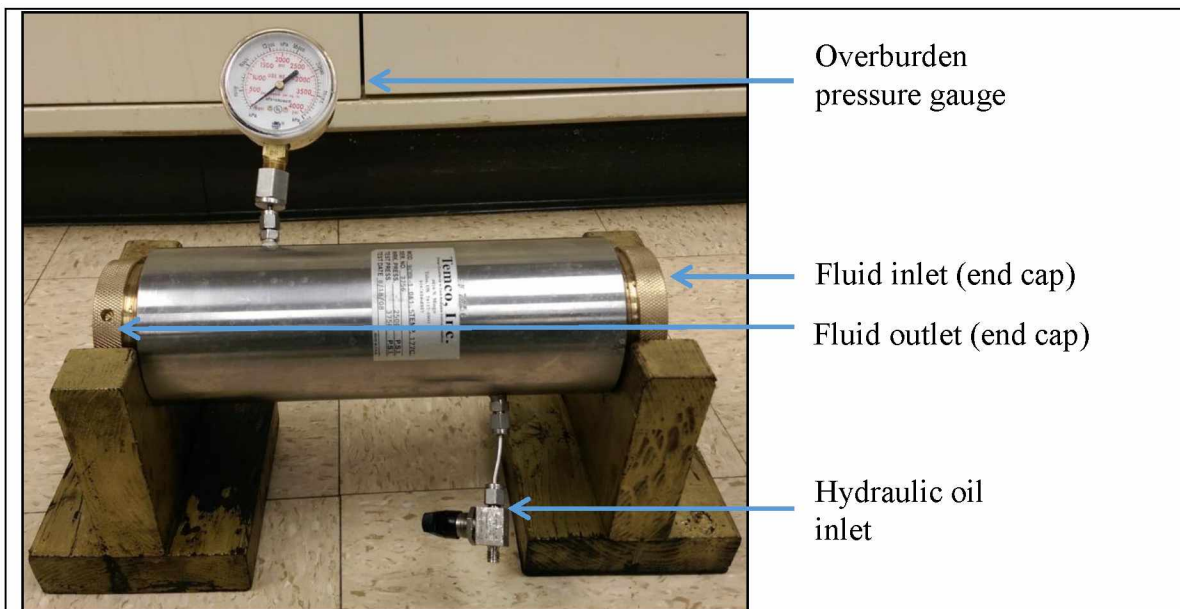
Figure 3.9 Photographic Representation of the Temco, Inc. RCHR Series Core Holder

3.3.5 Hand Pump (Overburden Pressure)

Enerpac hand pump rated at maximum pressure of 10,000 psi was used to apply reservoir overburden pressure (Figure 3.10). The hand pump was operated by filling the hydraulic oil in the reservoir/chamber and engaging the non-return valve (NRV). The hydraulic oil outlet port was connected with a fluid line to the inlet port of the core holder. Through this inlet port, the hydraulic oil was pumped in the annulus of the core holder.

Figure 3.10 Photographic Representation of a Hand Pump used in Experiment

3.3.6 Differential Pressure Transducer

Heise PM Model digital pressure transducer was used to measure pressure drop across the core plugs in the experiment. It can record pressure readings up to maximum of 10,000 psi. Figure 3.11 shows a photographic representation of Heise type digital pressure transducer used in the experiments.
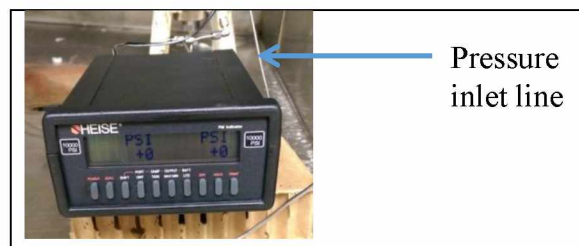
Figure 3.11 Photographic Representation of Heise Type Digital Pressure Transducer

3.3.7   Back Pressure Regulator

The back pressure regulator in the reservoir coreflooding experiment was incorporated to maintain/simulate the actual reservoir pressure in the entire coreflood rig to keep the gas in solution when recombined oil was used. The back pressure regulator utilized has a maximum working pressure of 10,000 psi and temperature of 350 °F (see Figure 3.12).
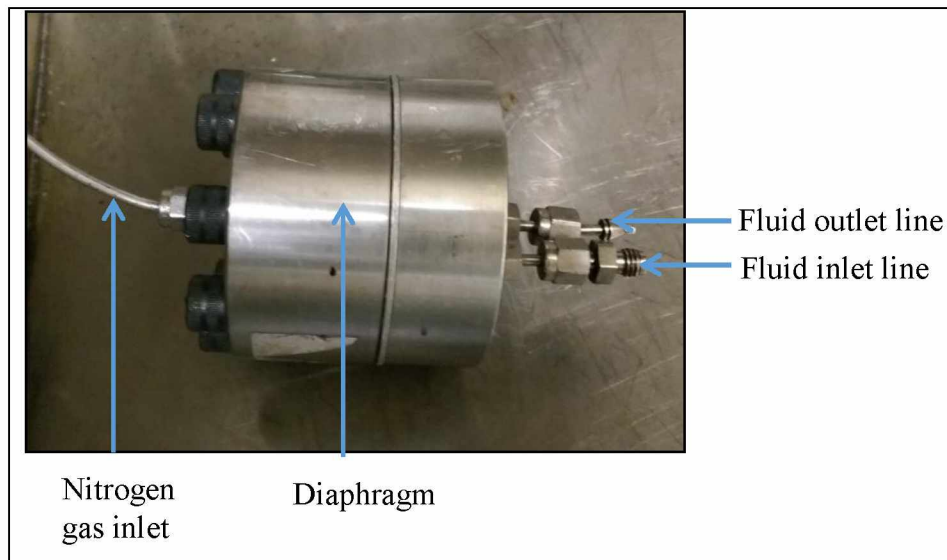
Figure 3.12 Photographic Representation of Back Pressure Regulator

3.4   Overview of the Surface Level Investigation using Optical Microscope Experiment
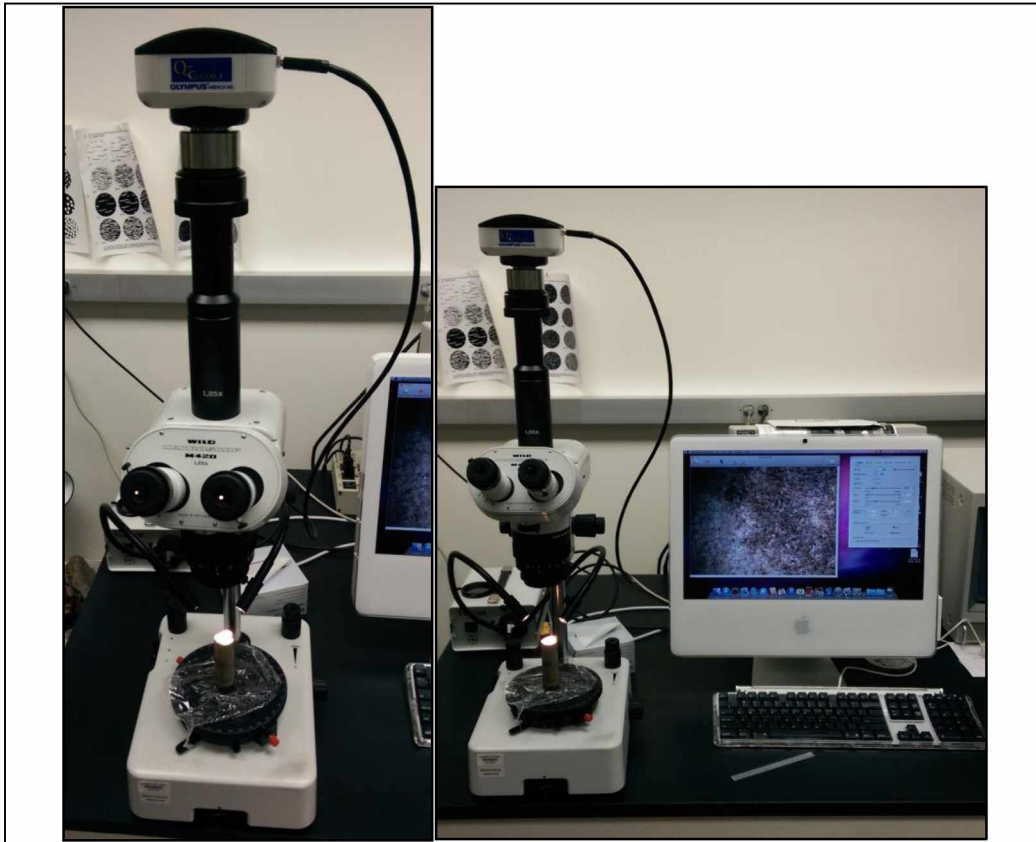
Figure 3.13 Photographic Representation of an Optical Microscope

The Wild M420 photo microscope (Figure 3.13) is a physically large microscope that was utilized for the surface level investigation of core samples. The M420 is designed to observe and photograph subjects primarily in a magnification range between 7.9 X and 40 X. It is a composite microscope, i.e., its objective produces an intermediate image in a focus plane in the air inside the microscope, and an ocular further enlarges it. The M420 also produces a non-inverted image in the oculars. The core samples were placed under the microscope and observed through a computer screen. The microscope was directly attached to a computer where images can be recorded.

Chapter 4 Experimental Description and Procedure

4.1 Experimental Description

As part of current research work, the experiments were designed to evaluate the effect of low salinity water on Alaska North Slope (ANS) reservoir core samples and to investigate the mechanism behind it. Determination of the mechanism behind low salinity water effect was based on qualitative analysis. Another important aspect of the research was to determine the effect of low salinity water on different clays. Four sets of experiments were conducted in this research study: (1) Direct visualization of the release of crude oil from clay surfaces (substrate type test), (2) Amott type spontaneous displacement test to determine the effect of low salinity water on different clays, (3) Evaluate the effect of low salinity water on oil recovery (for ANS reservoir cores, Berea sandstone cores and cores prepared or reconstituted in the lab) using dead oil sample, (4) Conduct a pseudo reservoir condition coreflood (using recombined oil) with low salinity water and compare the results, and observe on surface level the effect of low salinity water using microscope. The synthetic formation brine was prepared in the lab based on ANS reservoir brine composition. Reduction in salinity was achieved by decreasing the amount of total dissolved solids (TDS) using de-ionized (DI) water and mixing it with synthetic brine in proper proportion.

Flood rates used in the substrate experiments were 50, 100 and 200 cc/min, while the brine rate and oil rate in the coreflooding experiment varied as per the core sample (brine rate ranging from 2-5 cc/min and oil rate from 0.25-0.75 cc/min). A reservoir temperature of 155 $^{\circ}$F was maintained and 500 psi overburden pressure was used throughout all the coreflooding experiment.

Preparation of the core samples was the first step in all the coreflooding experiments. The core plugs were cleaned in the Dean-Stark apparatus using toluene, followed by acetone and heating in the oven. Subsequently porosities and absolute permeabilities of all the core samples were

determined. In all sets of corefloods, the core sample was flooded to initial water saturation. The core sample was then flooded with high salinity brine followed by low salinity brine (at reservoir temperatures and ambient outlet pressure) to determine the oil recovery. Slug-wise injection of low salinity brine was implemented to compare the results with continuous injection. Surface level investigation of core samples under microscope was conducted at various stages (dry sample, saturated sample, spontaneous displacement with high salinity brine, followed with low salinity brine).

4.2 Brine Sample

The experiments conducted as a part of this research work were designed to examine the effect of low salinity water on the core samples and clays. Synthetic brine of high salinity as well as low salinity was used in the experiments. High salinity brine was prepared by mixing various salts in the de-ionized (DI) water in proper proportion. The ANS reservoir formation water composition used was 23,881 ppm (TDS). Reduction in the brine salinity was achieved by ten times diluting high salinity brine by DI water. The desired concentration of low salinity water used in the experiments was about 2500 ppm (TDS).

The following procedure was adopted to prepare synthetic brine in the laboratory:

1. A reservoir brine recipe of about 23,881 ppm was obtained. Exact quantities of each salt was determined and weighed using a scale sensitive to 1 ten-thousandth of a gram.

2. These quantities were calculated based on 1 liter of DI water, so these salts were then added to the water, capped in an air tight container.

3. Low salinity brine of 2,500 ppm (TDS) was prepared by diluting high salinity brine approximately 10 times using DI water.

4. The density of brine measured using Anton-Paar Densitometer was 1.015 g/cc at 20 °C (68 °F) and 1.0024 g/cc at 68.33 °C (155 °F). Variation in the density of brine was minor.

5. Viscosity of brine was measured using Anton-Paar Viscometer at various temperatures (see Figure 4.1 and Table 4-1).

Table 4-1 Viscosity of Brine

Temperature (^{o}C)	Temperature (^{o}F)	Viscosity (cP)
20	68	1.0230
30	86	0.8315
40	104	0.6806
50	122	0.5663
68.33	155	0.4864
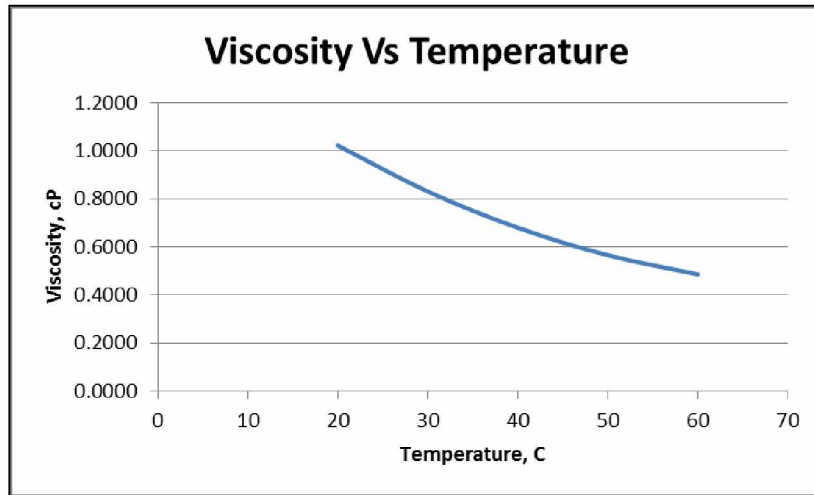
Figure 4.1 Graph of Viscosity of Brine vs Temperature

4.3   Dead Crude Oil

The dead crude oil samples were obtained from ANS reservoir for the experiment. The oil samples used were from two different wells and taken at different time. The density and viscosity measurement of crude oil was determined by using Anton-Paar Densitometer and Viscometer.

Procedure to prepare and measure the density and viscosity of oil:

1. Crude oil was first filtered using filter paper (200 micron) and centrifuged to remove impurities (if any).

2. Both density and viscosity measurements were carried out at 20 °C (68 °F) and 68.33 °C (155 °F). The values are reported in Table 4-2. Figure 4.2 is a plot of density of treated oil sample Well 1 versus temperature.

Table 4-2 Density and Viscosity of Crude Oil (Untreated)

Temperature	Temperature	Well 1		Well 2	
°C	°F	Density, g/cc	Viscosity, cP	Density, g/cc	Viscosity, cP
20	68	0.9414 to 0.9582	1620 to 1720	0.9619 to 0.9453	1700 to 1780
68.33	155	0.9155 to 0.9463	158 to 178	0.9501 to 0.9315	223 to 315

3. As seen from the Table 4-2, the density and viscosity value has a wide range. A high value of viscosity might be due to emulsification. To remove water from oil, an emulsion breaker was used (2-3 drops in 100 ml oil). After addition of emulsion breaker, oil was centrifuged for 24 hours (see Table 4-3 and Figure 4.3).

4. The aim was to cut down the viscosity value of oil to 3 cP (at 155 °F) using toluene (~35% by volume) for use in the coreflood experiment.

Table 4-3 Density and Viscosity of Crude Oil after Addition of Emulsion Breaker and Centrifugation

Temperature	Temperature	Well 1		Well 2	
°C	°F	Density, g/cc	Viscosity, cP	Density, g/cc	Viscosity, cP
20	68	0.9430	245	0.9428	244.1
68.33	155	0.92665	32.86	0.9266	32.85
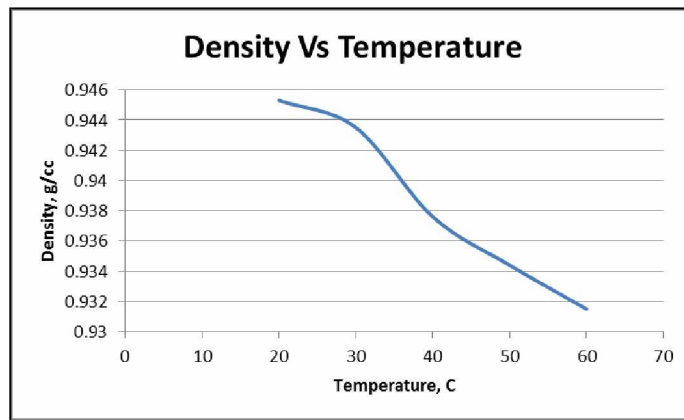
Figure 4.2 Graph of Density of Oil vs Temperature (Treated Oil Sample Well 1)

Figure 4.3 Picture of Filtered and Centrifuged Oil after Addition of Emulsion Breaker, which shows the Removed Water (Sample from Well 2)

4.4   Recombination of Oil (Pseudo Live oil)

Conducting a coreflood at full reservoir condition requires oil to be recombined with a reservoir gas to represent actual reservoir conditions. Recombination of oil was performed using methane as most of the gas produced in the reservoir contains methane in higher proportions. PVT data for the well was obtained from AOGCC website.

(http://aogweb.state.ak.us/WebLink8/DocView.aspx?id=32411&dbid=0)

The gas-oil ratio (GOR) was 340 scf/stb and corresponding bubble point pressure was 2328 psi. The above GOR could not be used to recombine methane with oil because the maximum pressure that coreflooding equipment can handle was 2500 psi and moreover procuring a separator gas sample closely matching the reported composition was going to take a long time to ship. Therefore, the following procedure was adopted for the recombination of oil to produce a pseudo live oil,

1. Bubble point pressure of 100 psi was assumed and corresponding GOR was calculated using CMG WINPROP (only methane gas was used for recombination).

2. The CMG WINPROP calculated 5.5 scf/stb GOR for a bubble point pressure of 100 psi. Similarly for comparison purposes (to evaluate if addition of more gas would have any influence on oil recovery due to LSWF), GOR of 7 scf/stb and 10 scf/stb was used to calculate the bubble point pressure using CMG WINPROP.

3. The methane gas moles (amount of gas) were calculated by converting the above GOR values to the conditions used during the experiment (see Table 4-4).

4. Dead oil mixture was then recombined in an accumulator at 100 psi (GOR 5.5 scf/stb) for 2 days to prepare recombined oil. The accumulator was kept pressurized at 500 psi using ISCO pump during the process. Pressure was continuously monitored during the process and

48

stabilized value of pressure ensured that all the gas was in solution and recombined oil in single phase.

5. The accumulator was then heated to 155 °F before conducting the experiment.

6. The density and viscosity of oil was calculated using CMG WINPROP with methane gas and adding toluene (~35% by volume) to it. The density of recombined oil was 45.3 lb/ft3 (at 155 °F) and viscosity was 2.7 cP (at 155 °F).

Table 4-4 Pseudo Live Oil Preparation

GOR (scf/stb)	Bubble point pressure (psi)	Amount of gas used (cc) @ 60 °F and 100 psi
5.5	100	71
7	118	90
10	160	130

4.5   Core Sample Preparation

All the core plugs for coreflooding experiment were obtained from Geologic Material Center (GMC), Alaska and Berea Sandstone Company (Figure 4.4). The core samples were chosen from different wells having different percentage of Glauconite clay in it. The core plugs were 1 inch in diameter and have lengths varying from 2 inch to 6 inch. Some core plugs were already broken during transportation and some cores were highly unconsolidated and hence broke apart after using them in Dean-Stark (see Figure 4.5 and Table 4-5).

All the core samples were cleaned with Dean-Stark process which involves flushing of the cores with toluene followed by acetone. Toluene was used to clean out any hydrocarbon-based material that might have been in the core, while acetone dissolves the toluene and/or water present in the core. Then the core samples were dried in the oven at 100 °F and after drying, the core samples

were weighed to determine if they achieved a steady reading, indicating the sample is thoroughly cleaned and dried.

After cutting and cleaning of the core samples, air permeability was measured using Tiny Perm II (portable air permeameter). The values of air permeabilities are listed in Table 4-5. Following the permeability measurement, core plugs were kept for saturation under vacuum in high salinity formation brine for several weeks. After two days of saturation under vacuum, it was observed that most of the core samples broke down into pieces because they were highly unconsolidated and muddy in nature (Figure 4.6). Hence second batches of core samples were obtained (Table 4-6).

Table 4-5 First Batch of Core Plug Data after Cutting and Cleaning

Core #	Depth (ft)	Dimension (L, in x Dia, in)	Dry wt. (gm)	K, air vertical (md)	K, air horizontal (md)
Core 1	2885.60	2.5 x 1"	64.06	31.4282	6.6219
Core 2	3024.40	2.5 x 1"	50.07	67.9892	21.5182
Core 3	Broken	2 x 1"	Broken	-	-
Core 4	3100.35	2 x 1"	44.4	14.3254	3.6735
Core 5	2446.60	2.5 x 1"	37.79	29.8523	9.5369
Core 6	2404.50	2.5 x 1"	43.02	7.3567	6.1733
Core 7	3077.65	3 x 1"	59.37	44.0102	71.9138
Core 8	Broken	3 x 1"	Broken	-	-
Core 9	3290.20	1.5 x 1"	43.01	2.0378	2.2799
Core 10	Not used	1.5 x 1"	Not used	-	-
Core 11	6539.30	1.5 x 1"	41.93	2.0958	2.2168
Core 12	6595.40	1 x 1"	32.18	39.3377	33.2423
Core 13	Not used	2.5 x 1"	Not used	-	-
Core 14	Broken	2.5 x 1"	Broken	-	-

Table 4-6 Second Batch of Core Plug Data after Cutting and Cleaning

Core #	Depth (ft)	Dimension (L, in x Dia, in)	Dry wt. (gm)
Core 15	2867.50	4 x 1"	74.43
Core 16	2915.40	4 x 1"	116.98
Core 17	3041.60	4 x 1"	71.72
Core 18	3126.80	2.5 x 1"	46.87
Core 19	3245.05	2.5 x 1"	57.2
Core 20	2471.40	2.5 x 1"	38.92
Core 21	2812.35	3 x 1"	49.83
Core 22	2892.75	3 x 1"	67.04
Core 23	3100.50	3 x 1"	41.89
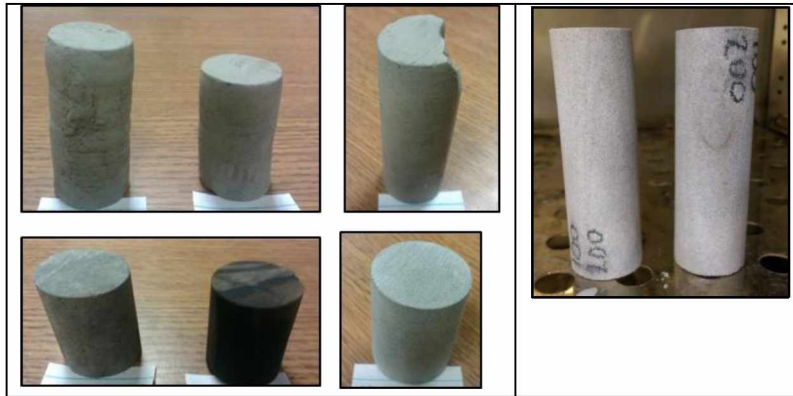
Figure 4.4 Core Samples from ANS Wells and Berea Sandstone

Figure 4.5 Core Sample Disintegrated into Sand after Dean-Stark Experiment and Already Broken Core Samples (in transportation)

Figure 4.6 Pictures of Damaged Core Samples after Saturating in High Salinity Brine

4.6   Laboratory Preparation of Synthetic Core Samples

As discussed earlier, to compare the effect of low salinity water on different clays, two clay types, Montmorillonite (Core A) and Kaolinite (Core B), were used to prepare the core samples. A cylindrical shaped mold (1" in diameter and 1.5" in length) was utilized. The cores were made up of clay, sand, oil, and water. The exact quantities of the core's composition can be seen in Table 4-7. U.S. mesh size of 200 (74 micron) was used for which the permeability was 200 mD and porosity of about 20-30%.

The following procedure was incorporated to prepare core samples:

1. In a ceramic bowl, 25 g of clay (Montmorillonite/Kaolinite), 15 ml treated dead oil (with addition of toluene), 10 ml high salinity brine and 40 g sand (200 mesh size) were mixed together.

2. This mixture was then packed into a mold and kept in the oven for drying, to make up the solid core (see Figure 4.7 (a)).

Table 4-7 Core Composition

Component	Quantity
Oil	15 ml
Connate water	10 ml
Sand	40 g
Clay	25 g

a)Mixture   b) Mold of core

c) Montmorillonite d) Kaolinite
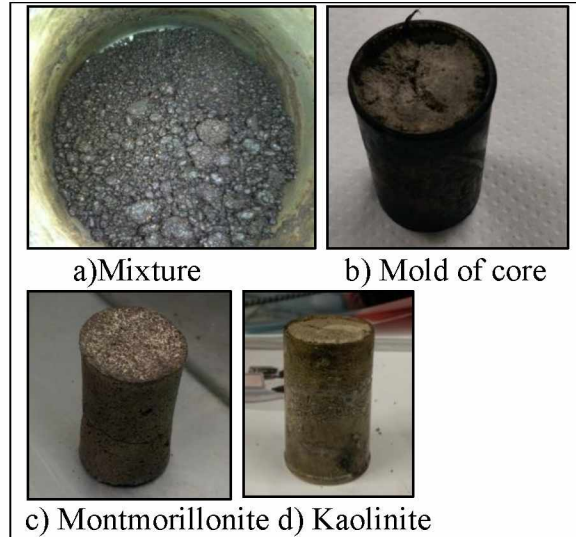
Figure 4.7 Laboratory Preparation of Core Sample

4.7   Calculation of Pore Volume (PV) and Porosity

Saturation method was used to calculate porosity of the core samples.

$$PV = \frac{M_{wet} - M_{dry}}{\rho_{brine}}$$

Where M_{dry} is the dry weight of the core sample, M_{wet} is the weight of the core sample after saturation and ρ_{brine} is the density of brine. Bulk volume is calculated as follows,

$$BV = \frac{\pi D^2 L}{4}$$

Where D is diameter of core sample and L is length of core sample. Porosity in percent is then calculated by following expression,

$$Porosity = \frac{PV}{BV} \times 100$$

4.8 Absolute Permeability Determination

The absolute permeability of a core sample was determined by conducting a coreflood experiment. A pressure drop across the core sample was measured using a digital pressure transducer. Accurate determination of absolute permeability depends on achieving steady state condition within the core sample. Steady state condition was attained when the pressure drop across the core sample does not change with time. Figure 4.8 shows a typical plot of pressure drop vs. number of injected pore volumes (PV) of brine.
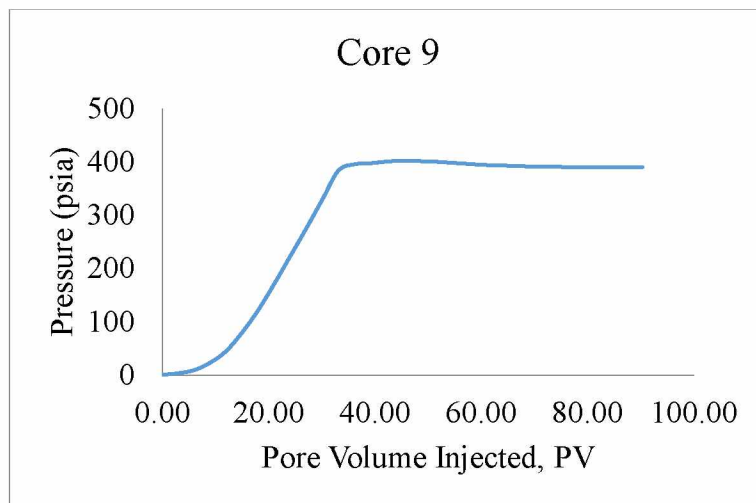
Figure 4.8 Graph of Pressure Drop vs PV Injected for Core 9

Calculation of absolute permeability (k) using Darcy's law is as follows,

$$k = \frac{Q \times \mu \times L}{1.1271 \times A \times dP}$$

where, k is permeability (mD), Q is flow rate (bbl/day), μ is viscosity (cP), L is length of core (ft), A is area (ft2) and dP is pressure drop across the core (psi).

The entire core sample's data used in coreflooding experiment is given in the Table 4-8. Figure 4.9 shows the comparison between porosity, air permeability and absolute permeability for the core samples. Core 16 was not used in the coreflooding experiments due to very low porosity value but it was utilized for surface level investigation as the core sample consist of Glauconite clay in it. Unfortunately, after establishing initial water saturation, Core 11 broke into pieces due to application of higher pressure.

Table 4-8 Data for the Core Samples used in the Experiment

Core #	Depth (ft)	Dimension (L, in x Dia, in)	Dry wt. (gm)	Wet wt. (gm)	Porosity (%)
Core 9	3290.2	1.5 x 1"	41.94	43.62	9.99
Core 11	6539.3	1.5 x 1"	41.93	45.06	9.16
Core 12	6595.4	1 x 1"	32.18	33.54	10.41
Core 16	2915.4	4 x 1"	95.41	96.17	2.06
Core 23	3100.5	3 x 1"	41.88	44.79	12.98
Berea 1	-	3 x 1"	83.27	88.96	14.70
Berea 2	-	3 x 1"	83.39	89.00	14.71
Montmorillonite (Core A)	-	1.5 x 1"	41.34	46.7	27.70
Kaolinite (Core B)	-	1.5 x 1"	39.9	44.34	22.94
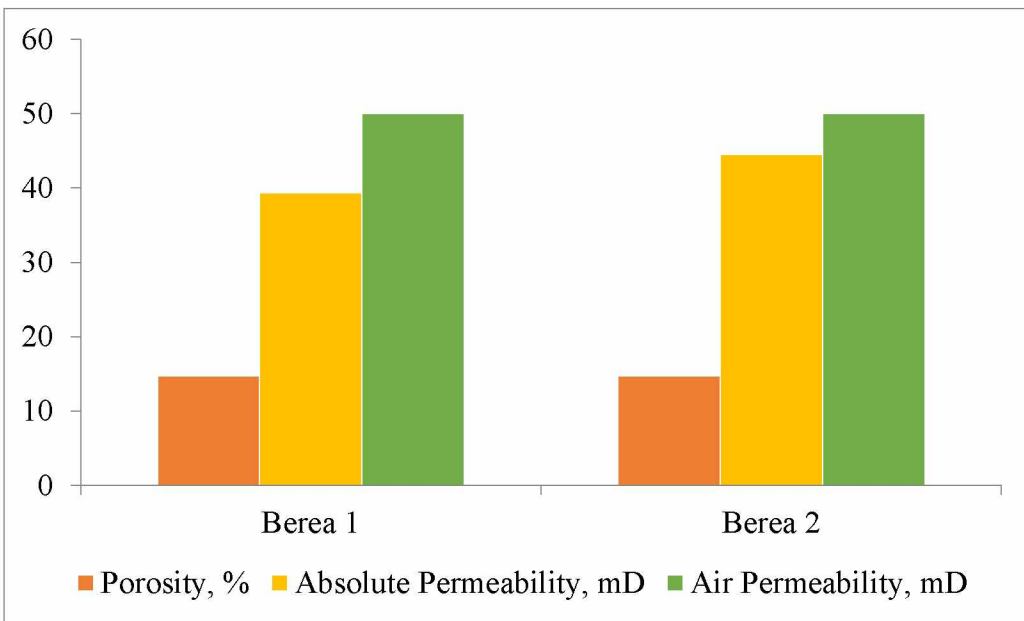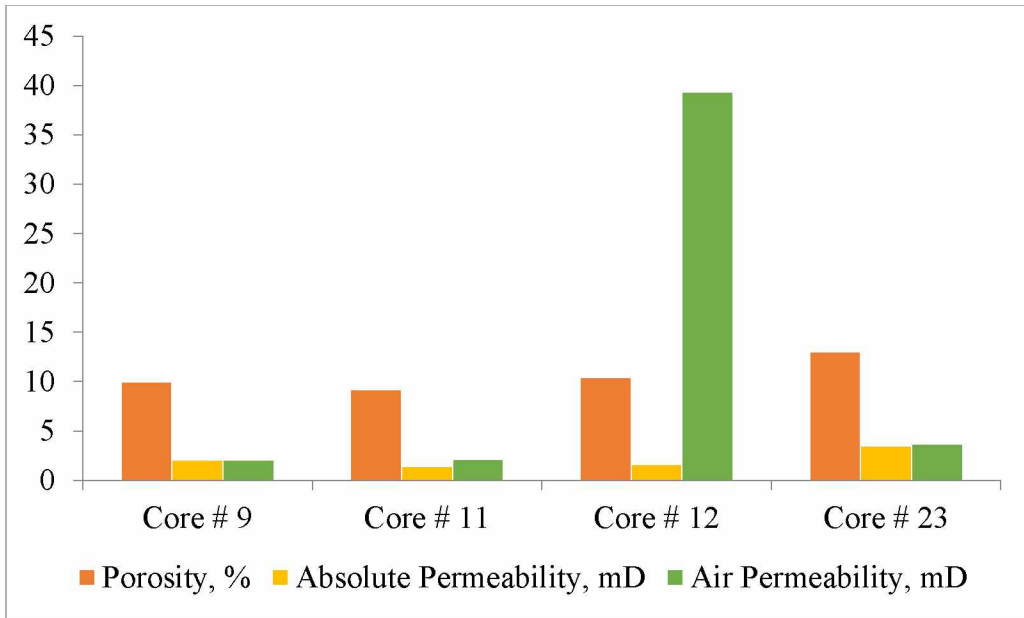
Figure 4.9 Graphical Representation of Porosity and Permeability Data for ANS Core Samples and Berea Core Samples

4.9   Establishment of Initial Water Saturation

In order to establish the initial water saturation, after the absolute permeability calculation, the core sample (brine saturated) was weighed and again confined in core holder to flood it with treated crude oil (3 cP). An overburden pressure of 500 psi was applied radially to the core sample. The entire coreflood experiment was conducted at reservoir temperature (155 ^{o}F) inside a Thermotron oven. After starting the oil flood, water started producing and volume of water was recorded. The dead line volume calculated with known PV sample was subtracted to get accurate results. The attainment of initial water saturation in the core sample was achieved when the displacement of water by oil continued until no more water was produced. The volume of water produced was then used to calculate initial water saturation (see Figure 4.10).
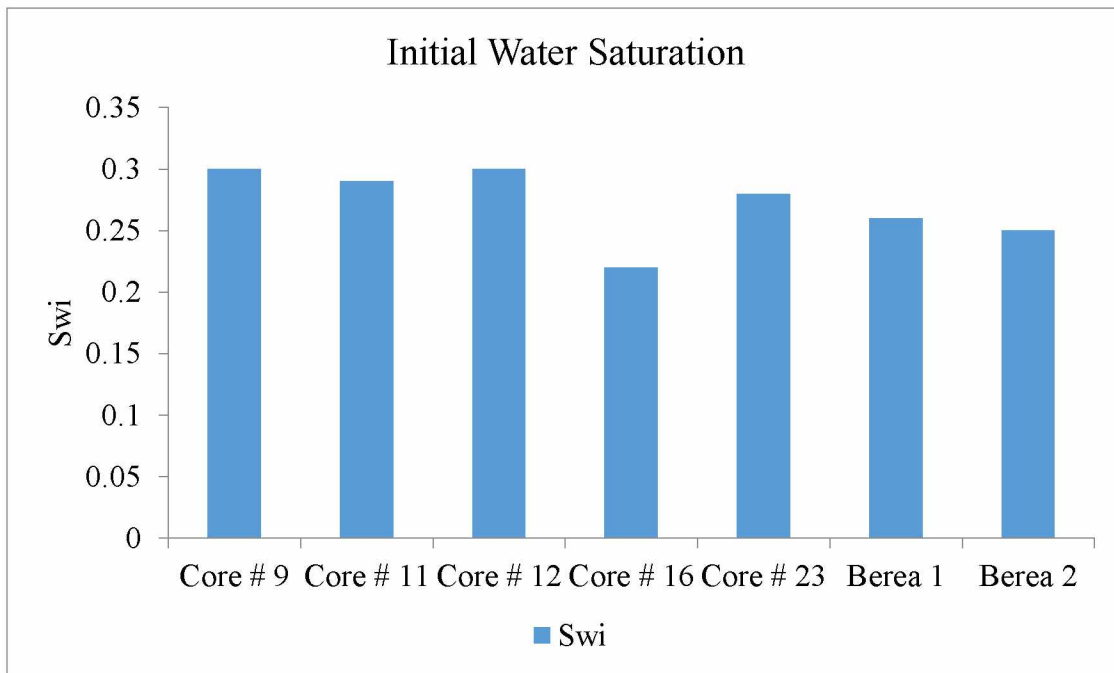
Figure 4.10 Initial Water Saturation in Core Samples after Oil Displacement

4.10 Substrate Type Test Experimental Procedure

In a flow cell, a flow of brine with specified composition was achieved by pumping it with the help of ISCO pump at either constant rate or constant pressure (in this case constant flow rate). The brine was flowed over a clay surface where oil droplets were firmly attached. Two different fluid accumulators were used to store high salinity and low salinity brine. The inlet and outlet valves used into and away from the accumulators help isolate high salinity brine and low salinity brine during injection. The microscopic glass slides were used to make substrates where clay particles were glued to glass slides using 2-component glue (epoxy glue, available through Gorilla). Oil droplets were attached using a syringe needle (ϕ 0.65 x 0.80 mm) to the substrate. The substrates were then put inside a flow cell made with slide holders which allowed a closed flow inside a flow cell. The plastic tubing was used for inlet and outlet flow from the flow cell. Figure 4.11 and Figure 4.12 shows the actual experimental setup used for conducting the experiment.

Figure 4.11 Photographic Representation of a Flow Cell Apparatus

Figure 4.12 Video Camera Setup and Substrates of Kaolinite and Glauconite clay

Substrate slides were prepared using three different types of clays, Glauconite, Kaolinite and Montmorillonite. The procedure used to conduct substrate type experiment was as follows:

1. As discussed earlier, reservoir brine recipe of about 23,881 ppm high salinity and 2500 ppm low salinity was prepared. Brine sample was then filled in accumulators.

2. The substrate slides were prepared in four different ways as follows,

i. The clays were mixed with high salinity brine and then glued on microscopic glass slide. The substrates were then kept for drying in an oven at 100 °F for about half an hour. Oil droplets were then firmly attached to substrate using a syringe needle (about 3 ml). It was ensured that the size, number and amount of droplets on each slide tested were consistent. Figure 4.13 shows the example of sample prepared by mixing with high salinity brine.
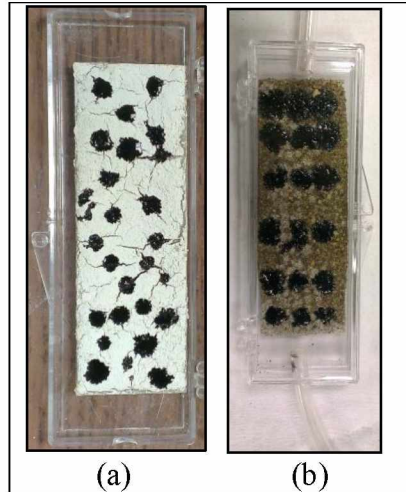
Figure 4.13 Substrate Prepared by Mixing with High Salinity Brine (Kaolinite and Glauconite)

ii. The substrate was prepared using clay samples mixed with high salinity brine and then glued on microscopic glass slide. Oil droplets were attached in a similar way. This substrate was then saturated in high salinity brine for 24 hours (see Figure 4.15(a) and (b)).

iii. The clay sample was directly sprinkled on the microscopic glass slide having glue on it. The clay particles that were not firmly attached were blown off by air. Oil droplets were attached in a similar way using a syringe needle as the first method. Figure 4.14 and 4.15 c) shows the example of substrate in which clays were directly sprinkled on the glass slide.

Figure 4.14 Substrate Prepared by Directly Sprinkling Clay on the Slide (Glauconite)

iv. To get a realistic approach to the method of substrate preparation, oil was mixed with clays and high salinity brine. After preparing the paste, it was glued on clay surface in a similar way as method i.

3. The substrates were then kept inside a flow cell and closed tightly. The flow cell was placed underneath the camera to record if there was any release of oil while water flows over it.

4. ISCO pump was filled with distilled water by closing the accumulator side valve, opening the fill side valve, and then pressing "Refill" on the ISCO pump controller. The ISCO pump was used to create a steady state flow of high as well as low salinity brine at a flow rate of about 50-200 ml/min. The experiment was conducted at various flow rates of 50 ml/min, 100 ml/min and 200 ml/min to see the effect of flow rate on experiment. All other conditions i.e. flow speed, salinity of brine kept constant.

5. With the camera on and directly over the flow cell, set the flow rate using the ISCO pump controller at 50 ml/min. Ensure that the accumulator side valve on the ISCO pump was open, the low salinity brine accumulator valves were closed, and the high salinity brine accumulator valves were open. Once a flow rate has been chosen, press start and flood the test cell with high salinity brine until the first release of oil droplet. After several minutes of high salinity flood (about 10-15 min), a steady state was reached where all oil droplets were stable and no more release of oil.

6. After the brief high salinity brine flood, as there was no more release of oil open the valves to the low salinity brine accumulator and close the valves to the high salinity brine accumulator to switch to low salinity brine flood. The typical substrate type experiment lasts for about 30-40 min.

7. Finally record the observation during experiment. Review the video to see if there was any release of crude oil from the clay surface with low salinity water. Amount of oil collected in beaker was then separated from water using centrifuge and it was measured. Another way of calculating the amount of oil released was using images from the experiment by calculating volume of the oil droplet before and after experiment performed and the difference in volume gives the amount of oil recovered.

The above procedure was followed for each clay Glauconite, Kaolinite and Montmorillonite and results were recorded for comparison. The results and discussion of the experiment are reported in section 5.1.
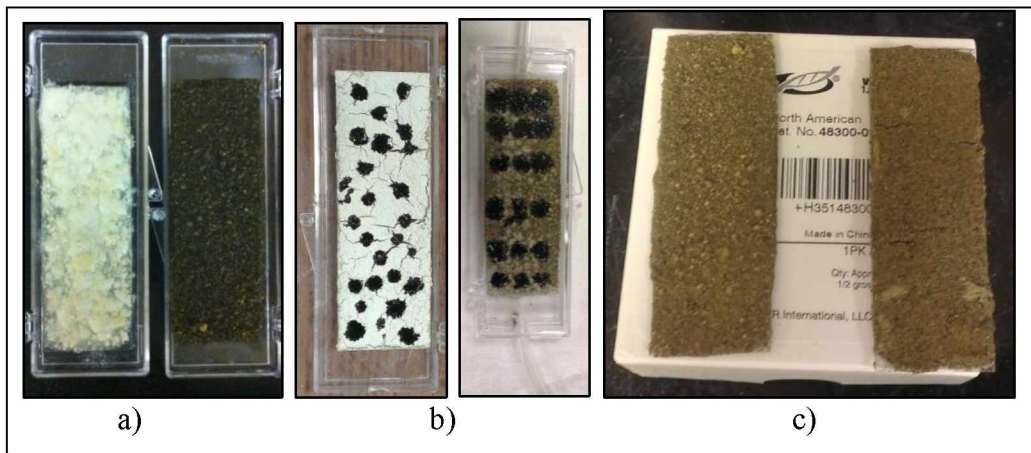
Figure 4.15 Different Methods of Substrate Preparation

4.11 Amott Type Spontaneous Displacement Test Experimental Procedure

As stated earlier, the spontaneous displacement test of a core sample was conducted after establishing initial water saturation. The procedure to conduct Amott type spontaneous displacement test was as follows:

1. The Amott cells were firmly mounted on a stand as shown in Figure 4.16. Initially Amott cells were filled with high salinity brine.

2. After completion of oil flood, core sample was immersed in Amott cell containing high salinity brine. The core sample kept in Amott cell for more than 24 hours for spontaneous displacement of oil by high salinity brine. Oil drops were collected at top because of difference in densities. The amount of oil released was noted.

3. The high salinity brine was then replaced by low salinity brine when there was no more oil production. Again the core kept in low salinity brine for spontaneous displacement for another 24 hours and amount of oil released was recorded until no more oil was produced.

(a)   (b)   (c)
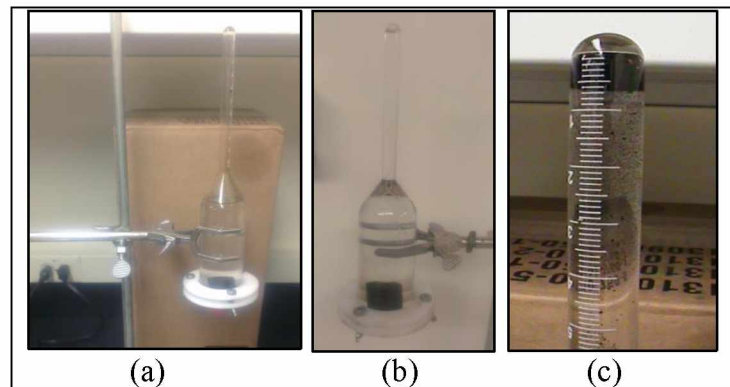
Figure 4.16 Photographic Representation of (a) Amott Cells Setup (b) Spontaneous Displacement of Oil by Brine and (c) Oil Produced with Displacement by Low Salinity Brine

Results of the Amott test are discussed in section 5.2.

4.12 Experimental Procedure for Dead Crude Oil Floods

As discussed earlier, the coreflooding experiments involving dead oil were designed to evaluate the effect of low salinity water injection on oil recovery and also find out the effect of slug-wise injection on the same. Dead oil coreflood with continuous and cyclic injection were employed in all samples. All the coreflooding experiments with dead oil were conducted at reservoir temperature of 155 °F and an overburden pressure of 500 psi. Depending on the core sample, the brine flow rate used was in a range of 2-5 cc/min and oil flow rate varied from 0.5-0.75 cc/min. All the corefloods with dead oil were conducted in a tertiary injection mode. The following procedure was adopted in the coreflooding experiment:

1. Accumulators were filled with brine and dead oil (mixed with toluene).

2. After achieving initial water saturation, the core sample was confined in core holder with overburden pressure of 500 psi and entire coreflood rig was accommodated in Thermotron oven to conduct experiment at reservoir temperature (155 °F).

3. The ISCO pump was operated at constant flow rate (depending on core sample in use) to flood the core sample with high salinity brine. Oil started producing because of forced displacement by brine. High salinity brine was flooded until no more oil was produced. Volume of oil collected in beaker was measured.

4. Then in the next step, the flow was switched to low salinity brine at constant flow rate and additional oil was produced until the water was seen at outlet and oil has stopped producing. Volume of additional oil recovered was recorded.

4.13 Slug Wise Injection Procedure

As mentioned earlier, slug-wise injection of low salinity brine was conducted to compare the results with continuous injection. All the coreflood experiments with slug-wise injection were conducted at tertiary injection mode. The conditions kept similar as in case of dead oil corefloods. Following procedure was incorporated for slug-wise injection of low salinity brine:

1. Initial water saturation was established with core sample as discussed in section 4.9.
2. Core sample was then flooded with high salinity brine until the stabilized pressure was achieved.
3. In the next step, the slugs of low salinity brine were injected followed by injection with high salinity brine (PV injected was based on core sample).
4. The slugs of low salinity brine were injected till no more oil was produced. The amount oil produced was noted at every step.

4.14 Coreflooding at Reservoir Condition

The actual reservoir conditions were not completely simulated by corefloods with dead oil. In field reservoir conditions, solution gas present in the oil may affect oil production and recovery for low salinity water flood. Thus, it was necessary to incorporate actual reservoir conditions of temperature and pressure during the coreflooding experiment. As discussed in section 4.4 recombined oil was prepared and flooded in a similar manner as described in section 4.12 with an addition of back pressure regulator into the system.

Procedure incorporated during the corefloods for modified or simplified reservoir condition was as follows:

1. Saturated core samples were flooded with recombined oil (live oil) to bring the samples to initial water saturation. The reservoir temperature used was 155 °F and bubble point pressure of 100 psi. The back pressure regulator was pressurized using nitrogen gas to ensure that the oil remained in single phase during the floods.

2. After achieving initial water saturation, the core sample was confined in core holder with overburden pressure of 500 psi.

3. The ISCO pump was operated at constant flow rate (depending on core sample in use) to flood the core sample with high salinity brine. Oil started producing because of forced displacement by brine. High salinity brine was flooded until no more oil was produced. Volume of oil collected in beaker was measured.

4. Then in the next step, the flow was switched to low salinity brine at constant flow rate and additional oil was produced until the water was seen at outlet and oil has stopped producing. Volume of additional oil recovered was recorded.

5. The calculation for oil produced was adjusted with the use of GOR because gas was liberated during the production.

Results of all experiments conducted using dead and recombined oil are presented in section 5.3.

4.15 Experimental Procedure- Surface Level Investigation using Microscope

As discussed earlier, the optical microscope (M420) was utilized to investigate on surface level the effect low salinity waterflooding. The optical microscope was directly connected to a computer where the images can be observed and recorded. A simple procedure was followed (given below) to capture the surface images of a core sample.

1. Take the dry sample and place it under optical microscope. Zoom the microscope using computer operations to desired level and pictures can be taken by simply pressing a record button.

2. Next step was to saturate the core sample in high salinity brine under vacuum for several days. Take the saturated sample and place under the microscope. Follow the same procedure as in step 1.

3. Then achieve the initial water saturation condition by oil flooding the same core sample (saturated in brine) used in step 2. Spontaneously displace the core sample with high salinity brine by Amott test and observe the core sample under microscope. Similar procedure was followed as in step 1.

4. Next step was to spontaneously displace the core sample with low salinity brine and follow the similar procedure as in step 1 and 3 to capture the microscopic images.

The above procedure was repeated for ANS reservoir core sample and Berea core sample. Results of the surface level investigation are discussed in section 5.4.

Chapter 5 Results and Discussion

5.1   Results of Substrate Type Test

The main goal of the substrate experiment was to provide a direct evidence of the release of crude oil with low salinity water. The results of all the successful experiments are listed in Table B-1 through Table B-3. Figure 5.1 shows a typical result of the substrate test after a low salinity waterflood. It was evident from the Figure 5.1 that the low salinity brine causes oil droplets to detach from the surface of clay. It was because of the adhesion force between oil droplets and clay particles which are reduced by the low salinity brine (Berg et al. 2009).

As seen from the results given in Appendix B (below), the amount of oil recovered was more in case of (a) substrate prepared by mixing with high salinity brine, (b) substrate prepared by mixing high salinity brine and oil together, at a flow rate of 100 ml/min with a little or no substrate damage (see Figure 5.2 and Figure 5.3). It was observed that oil recovery was more in case of high brine flow rate (200 ml/min) but there was more damage to the substrate and hence results were unfavorable.

Substrate prepared with saturating in high salinity brine and substrate prepared by directly sprinkling on the slide were not as favorable method as the two methods discussed above because of clay swelling, fines migration and substrate damage. Hence these methods were neglected while comparing results.

Figure 5.4 and Figure 5.5 shows a comparison between different types of clays on low salinity waterflooding with different method of substrate preparation. Unfortunately, an experiment with Montmorillonite clay cannot be considered as successful due to high clay damage. Also the oil recovered was high in case of Montmorillonite clay because of higher substrate damage as compared to other clays. It was observed that, the oil recovery was more in Kaolinite but with clay

swelling. On the other hand, Glauconite showed less damage than Kaolinite and comparable oil recovery with Kaolinite. Based on the results, Kaolinite and Glauconite clay can be considered more favorable than Montmorillonite (see Figure B.1 through Figure B.4).

(a) Kaolinite   (b) Glauconite
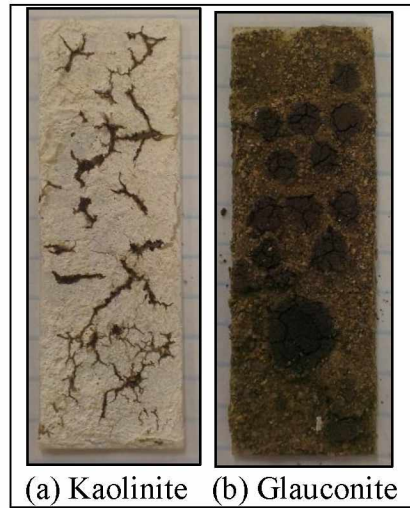
Figure 5.1 Picture of Substrate after Completion of the Experiment
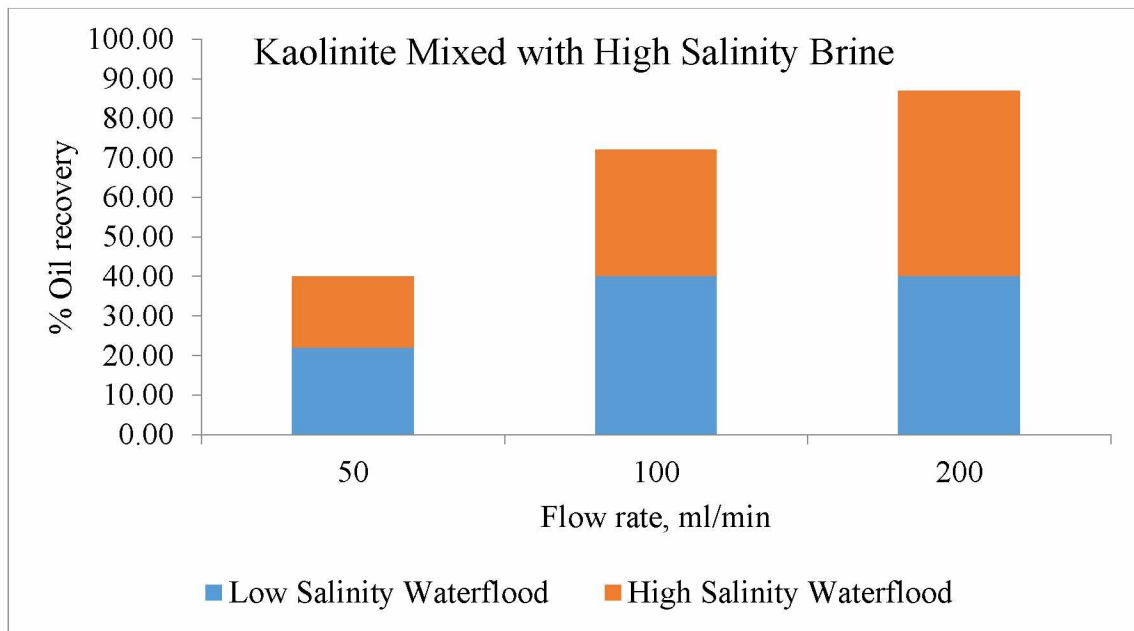
Figure 5.2 Results of Successful Substrate (Mixed with High Salinity Brine) Tests with Kaolinite at Different Flow Rates
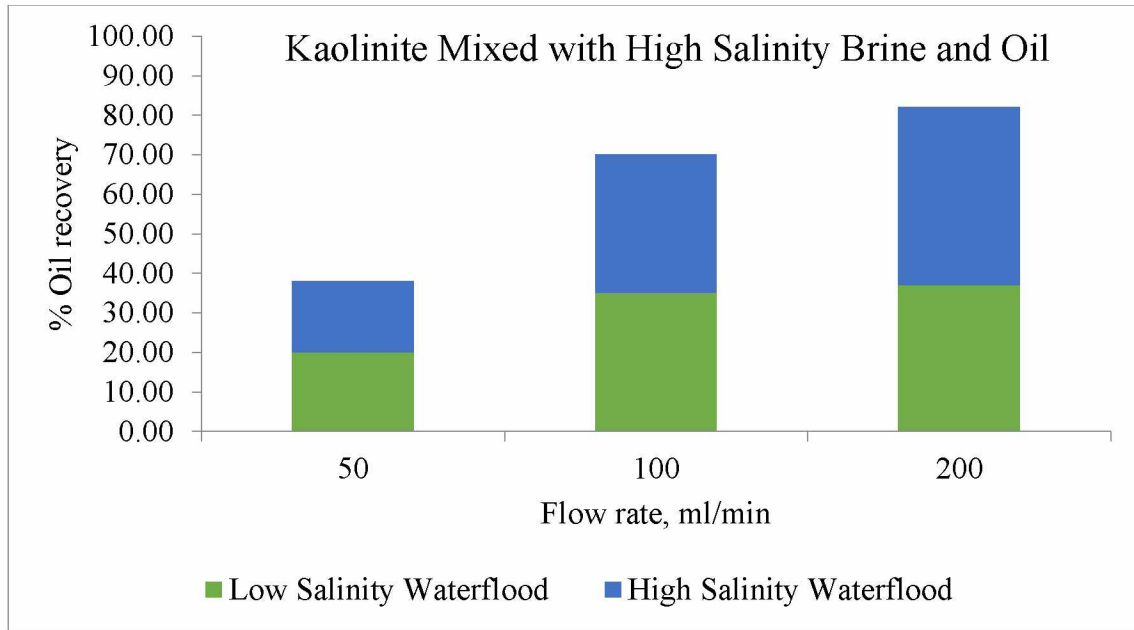
Figure 5.3 Results of Successful Substrate (Mixed with High Salinity Brine and Oil) Tests with Kaolinite at Different Flow Rates
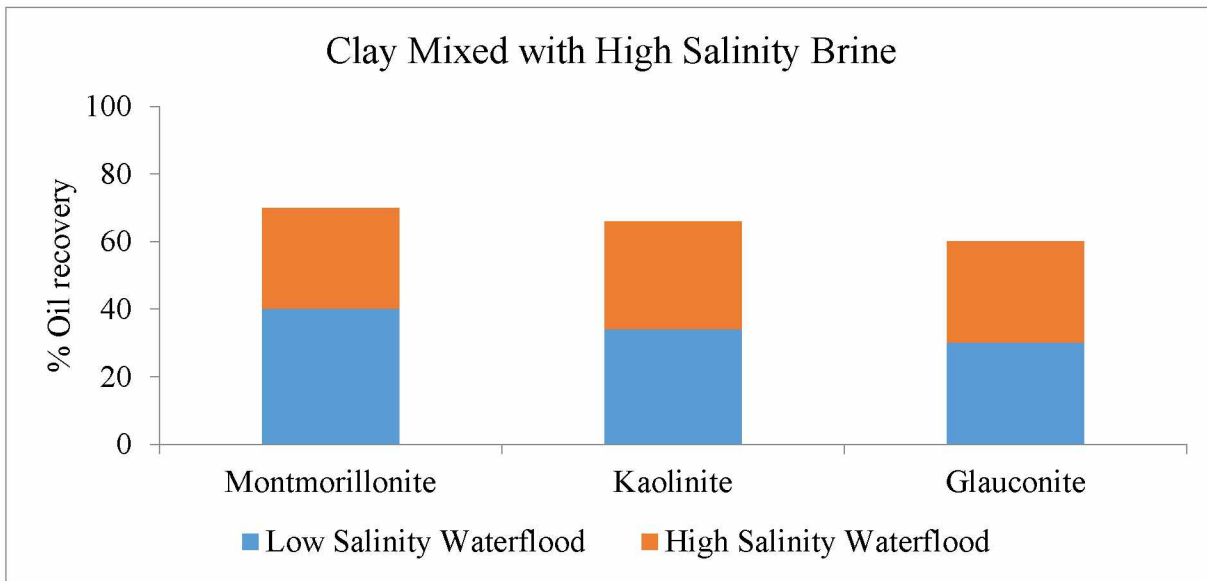
Figure 5.4 Average Oil Recoveries for Different Types of Clays (Mixed with High Salinity Brine)
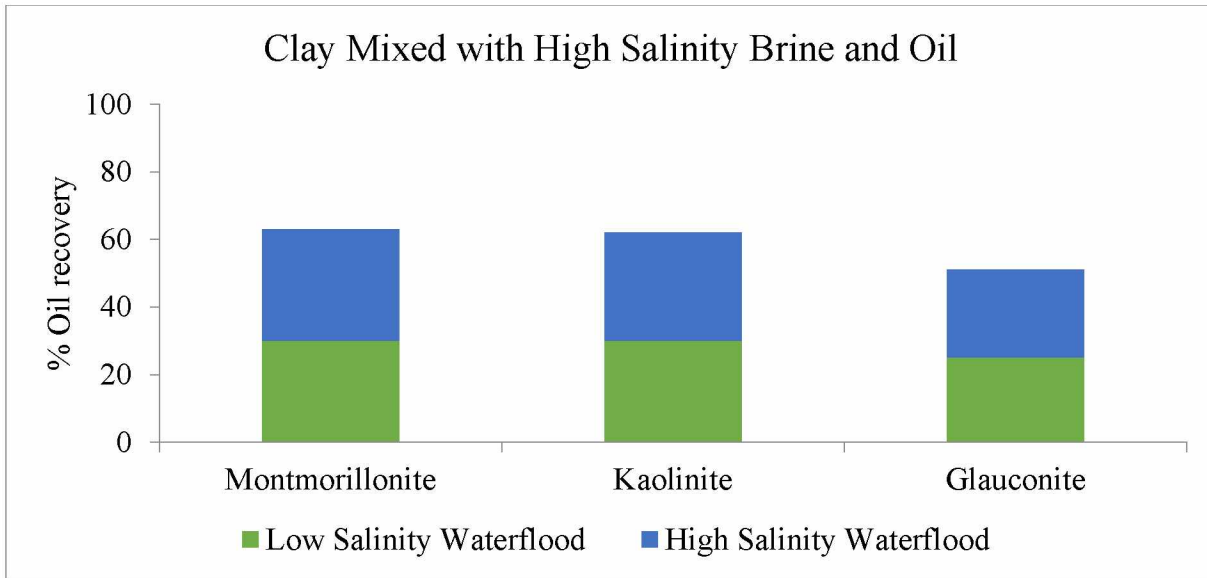
Figure 5.5 Average Oil Recoveries for Different Types of Clays (Mixed with High Salinity Brine and Oil)

5.2 Results of Amott Type Spontaneous Displacement Test

The main objective of performing Amott test was to spontaneously displace the oil in the core with high salinity brine followed by low salinity brine and quantitatively determine the effect of low salinity water on the clay type. The Amott test was conducted on a) four ANS reservoir core samples having different percentage of Glauconite in it (Core 9, Core 11, Core 12 and Core 23), b) two Berea core samples (having kaolinite in it) and c) two core samples prepared in lab having Montmorillonite and Kaolinite in it. As discussed earlier, spontaneous displacement test with high and low salinity water was performed after forced displacement of oil (establishing initial water saturation). Results of the entire Amott test conducted are given in Appendix C (below).

As seen from the Figure 5.6 (and Table C-1 through Table C-4), core samples having high percentage of Glauconite (Core 23= 20.47%) recovers more oil than the core samples having low percentage of Glauconite in it (Core 12= 5.73%). Core 9 having intermediate percentage of Glauconite shows oil recovery in a range of Core 12 and Core 23. Oil recovery was higher in case

71

of core Core 11 having low percentage of Glauconite (0.12%) because it was broken into two pieces after keeping it in Amott cell containing high salinity brine.

The similar results were seen from the Berea core samples (Table C-5 and Table C-6). Core A containing Montmorillonite recovers less oil with low salinity water than Core B having Kaolinite. Montmorillonite clay damaged in low salinity water, hence it can be considered as unfavorable. Therefore clay type and clay content have a significant effect in low salinity water. Amott test qualitatively demonstrates that high percentage of Glauconite have potential in oil production with low salinity water.
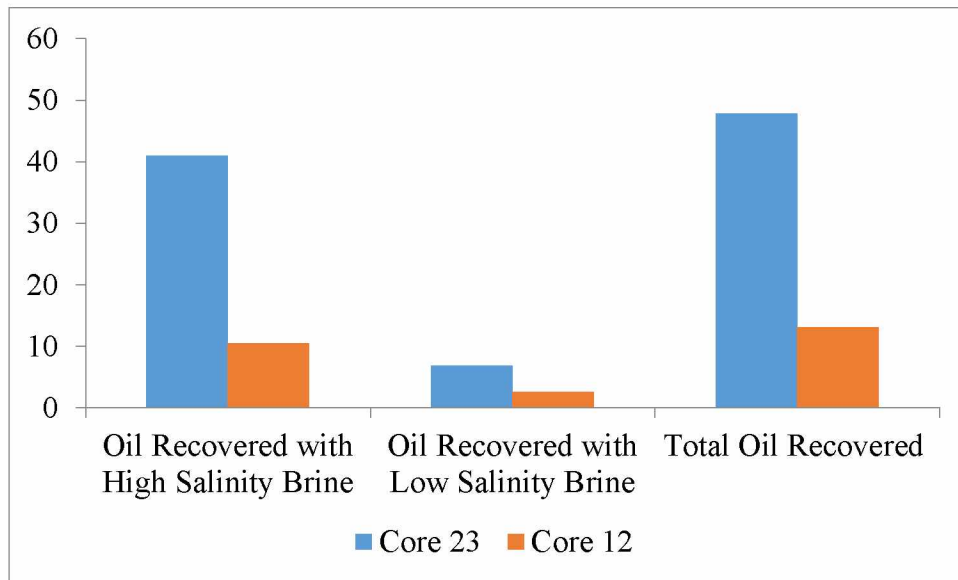
Figure 5.6 Graphical Representation of Oil Recoveries for Core 23 and Core 12

5.3   Results of Coreflooding Experiment

5.3.1   Coreflooding Performed with Dead Oil

The low salinity water coreflooding experiment was conducted in tertiary recovery mode with continuous injection of low salinity water after high salinity waterflood. Three ANS reservoir core samples (Core 9, Core 12 and Core 23) and two Berea core samples were utilized for conducting the experiment. Results of all the coreflooding experiments are listed in Appendix D (below). Table 5-1 shows data for water flood and oil flood and Figure 5.7 is a typical plot for waterflood and oil flood. As seen from the Table 5-1, the improvement in oil recovery was observed with reduction in brine salinity. Low salinity water has an impact on improving oil recovery may be because of wettability alteration as suggested by Agbalaka (2006), Patil (2007) and Kulathu (2009).

The coreflood results for ANS reservoir core sample gave similar results as Amott test in which core containing high and intermediate amount of Glauconite clay recovers more oil than the core having low content of Glauconite in it. Likewise, low salinity waterflood has equal impact on Berea core samples that contains Kaolinite clay. Figure 5.9 is an oil recovery profile for Core 9. It is seen from the plot that injecting 24 PV's of high salinity brine, almost 0.22 PV of oil was recovered and further injecting 48 PV's of low salinity brine, additional 0.20 PV of oil was recovered. Oil recovery profile for remaining core samples are given in Appendix D (below). The incremental oil recoveries with low salinity waterflood ranges from 5% to 30% for ANS reservoir core samples and about 15% for Berea sandstone core samples.

Table 5-1 Coreflooding Experiment Data for Core 9

Core 9		
Glauconite clay = 10.89 % by volume		
Pore Volume (PV)	1.66	cc
Porosity (ϕ)	9.99	%
Flow Rate (Q)	5	ml/min
Differential Pressure (ΔP)	390	psia
Viscosity of Brine (μ_b)	1.00	cP
Absolute Permeability (k_{abs})	2.03	mD
Initial Water Saturation (S_{wi})	0.30	
Oil-flood Data		
Flow Rate (Q)	0.5	ml/min
Differential Pressure (ΔP)	490	psia
Viscosity of Oil (μ_o)	3.00	cP
Effective Permeability to Oil at S_{wi} (k_{eff})	0.48	mD
Waterflood Data		
Effective Permeability to high salinity brine at S_{or}	0.48	mD
Effective Permeability to low salinity brine at S_{or}	0.47	mD

Core 9		
Glauconite clay = 10.89 % by volume		
Initial Oil in the Core-plug	1.16	cc
Oil Recovered with High Salinity Brine	31.86	%
Oil Recovered with Low Salinity Brine	29.63	%
Total Oil Recovered	61.49	%
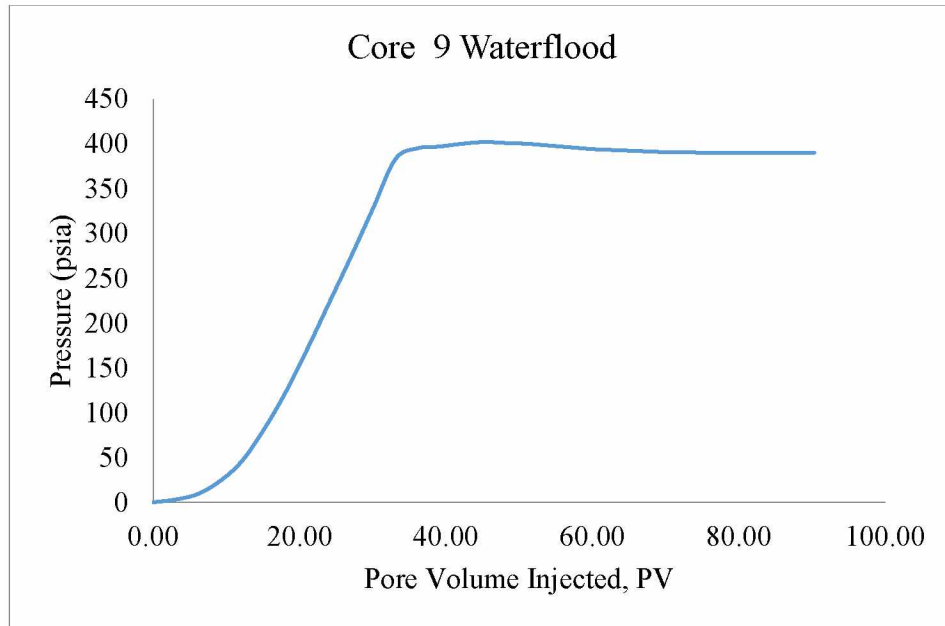
Figure 5.7 Graphical Representation of Pressure Profile during Waterflood (Core 9)
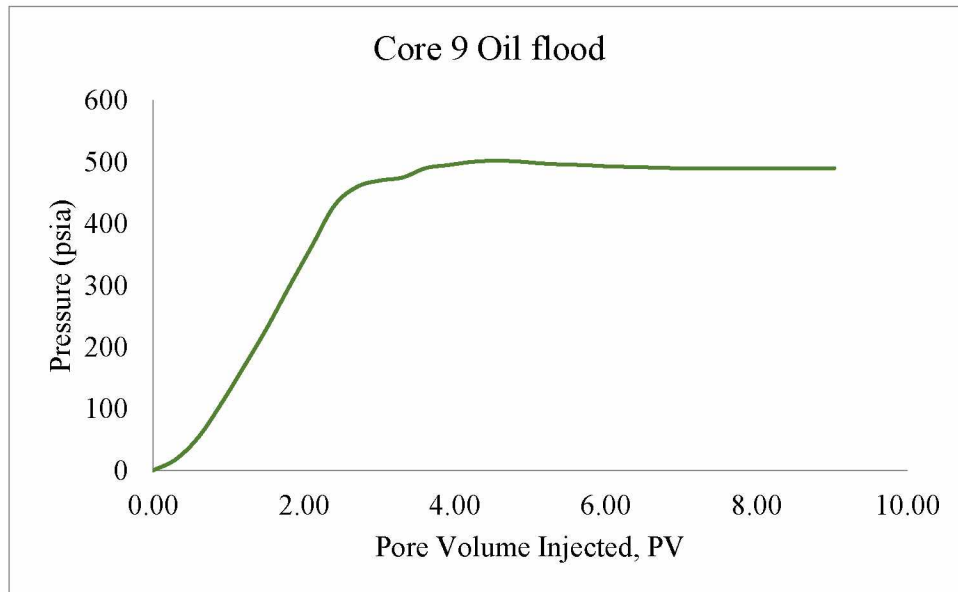
Figure 5.8 Graphical Representation of Pressure Profile during Oil-flood (Core 9)
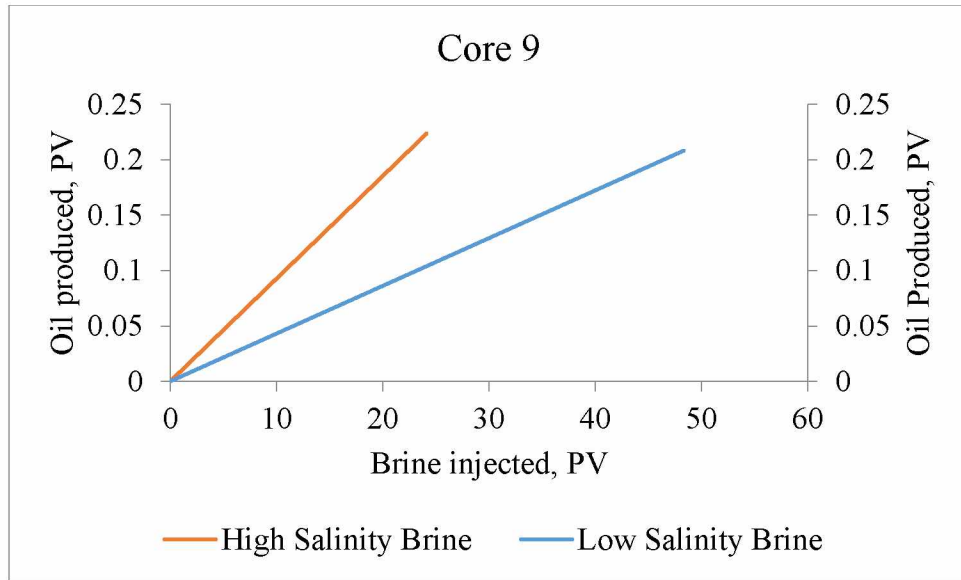
Figure 5.9 Oil Recovery Profile for Core 9
Primary Y-axis: High salinity brine and Secondary Y-axis: Low salinity brine

5.3.2 Reservoir Condition Corefloods

The reservoir condition corefloods were conducted with recombined oil at reservoir temperature and bubble point pressure. Continuous flooding of low salinity water was conducted in a tertiary recovery mode. Only one ANS reservoir core sample (Core 9) and one Berea sandstone core sample was utilized for performing the experiment. Unfortunately, other samples got destroyed during the process of coreflooding with dead oil. Figure 5.10 and Figure 5.11 compares the results between low salinity waterflood with dead oil and recombined oil. A slightly higher oil recovery was observed in the case of pseudo live oil when the gas is in solution. Oil recovered with low salinity waterflood was almost similar in both cases because initial oil saturation was same. There was about 5% increase in the total oil recovery in case of recombined oil for Core 9 and almost 10% in case of Berea sandstone core sample. The effect with low salinity water on recombined oil was similar in case of both samples.

The Core 9 was reused to perform the studies by using a GOR of 5 scf/stb, 7 scf/stb and 10 scf/stb. Figure 5.12 examines the effect of varying the GOR on oil recoveries with high salinity waterflood and low salinity waterflood. With the increase in GOR (at least in the fairly narrow tested range), the amount of oil recovered remained same in case of both waterfloods.
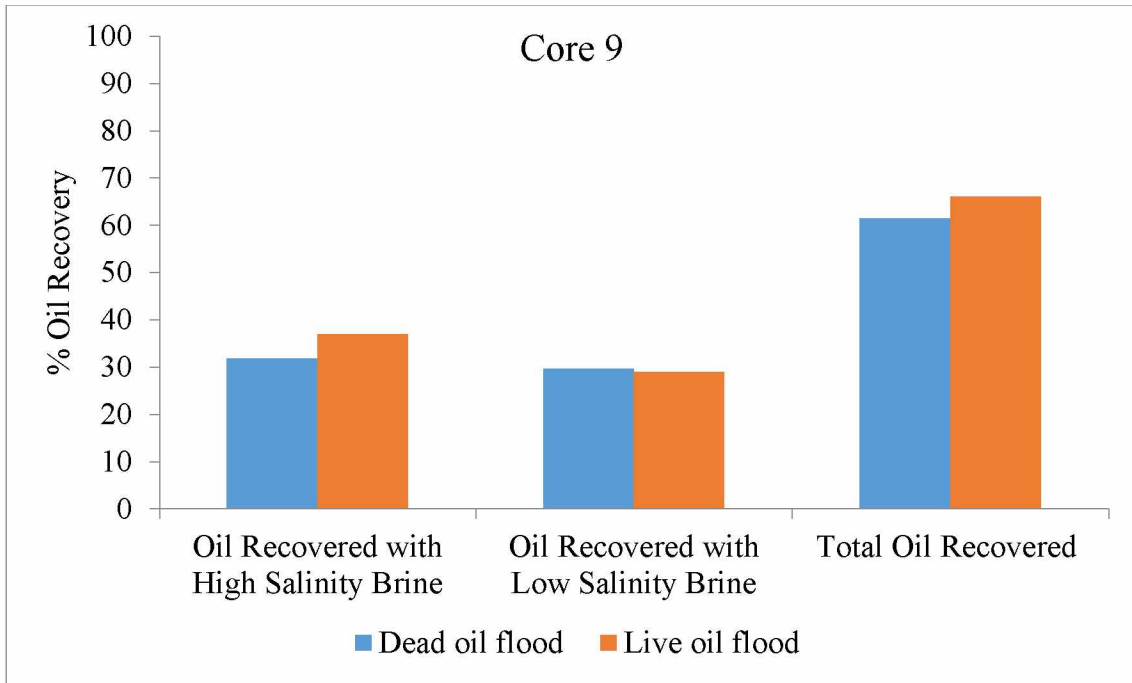
Figure 5.10 Graphical Representation of Comparison between Dead Oil Coreflood vs Pseudo Live Oil Coreflood for Core 9
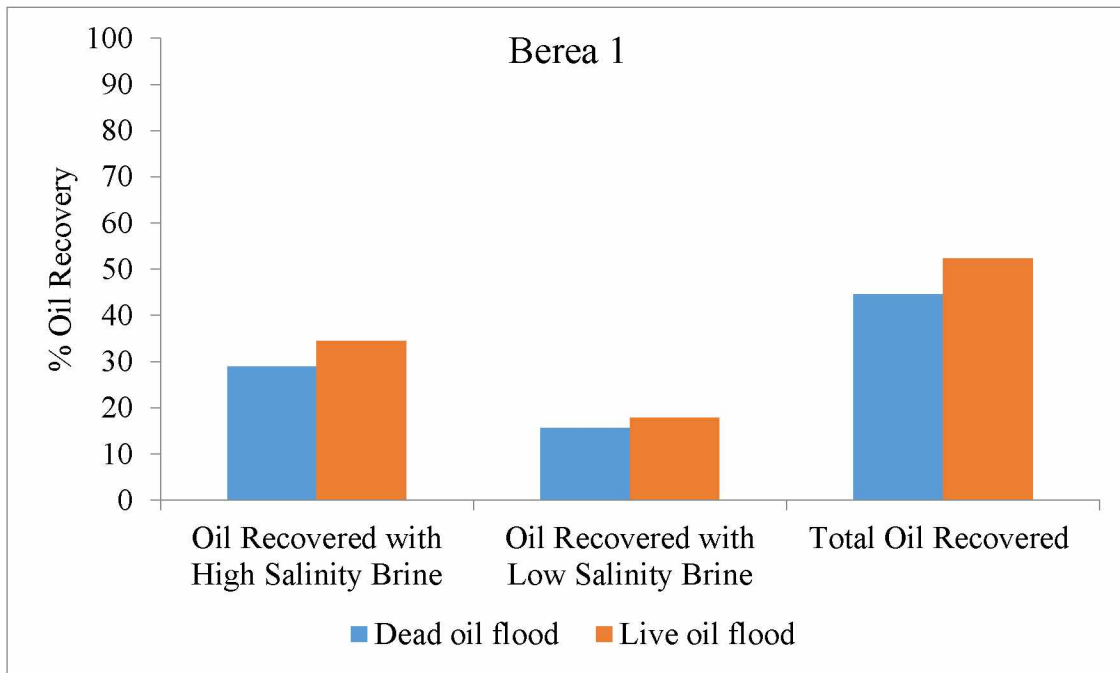
Figure 5.11 Graphical Representation of Comparison between Dead Oil Coreflood vs Pseudo Live Oil Coreflood for Berea 1
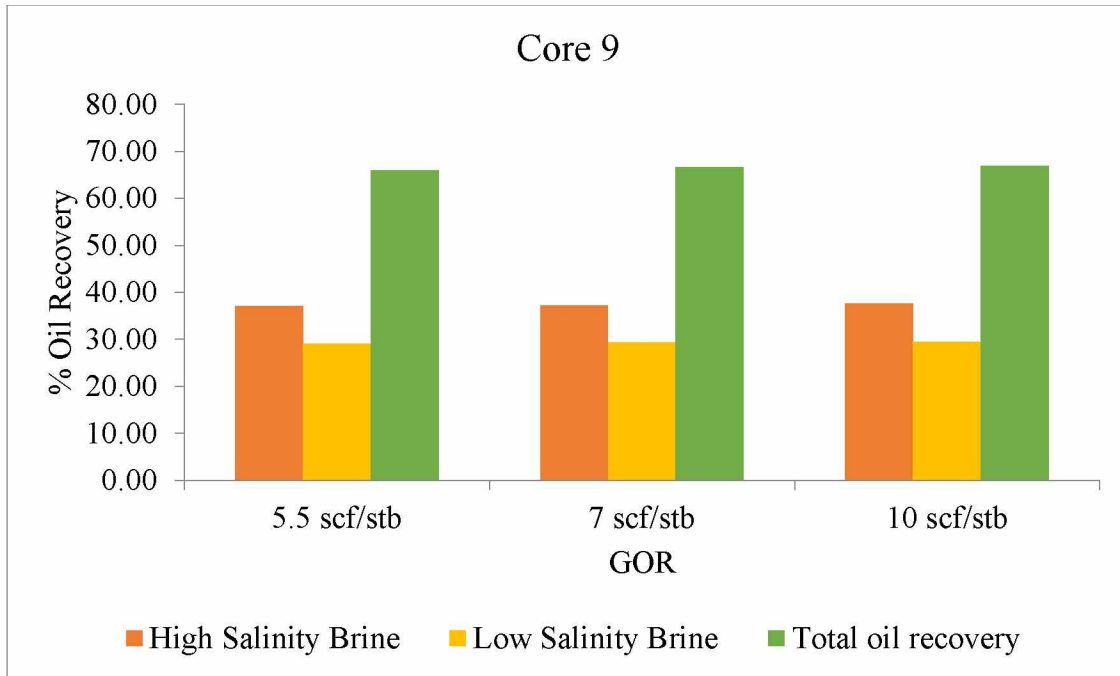
Figure 5.12 Graphical Representation of Comparison of Oil Recoveries with Variation in GOR

5.3.3   Continuous Injection vs. Slug Wise Injection

The two set of core samples (Core 9 and Berea 1) were used to perform slug-wise injection of low salinity water. The main objective of this task was to compare the effect of slug-wise injection with continuous injection. The slugs of low salinity water were injected followed by high salinity water. In case of Core 9, the slug size of 2 PV was used while for Berea 1 slug size of 1 PV was used. Figure 5.13 and Figure 5.14 gives the comparison between the continuous injection and slug-wise injection. Results showed that 29.6% oil was recovered with 45 PV of low salinity water injection, whereas, it took only 30 PV (total injection 40 PV) of low salinity water to recover 28.3% of oil. In case of Berea sandstone core sample, only 6 PV (total injection 7 PV) of slug-wise injection of low salinity water recovered 15.2% oil as compared to 9 PV of continuous injection to recover 15.6%. Hence, slug-wise injection was efficient in producing similar amount of oil with less PV of low salinity water which might favor the economics of the project.

79
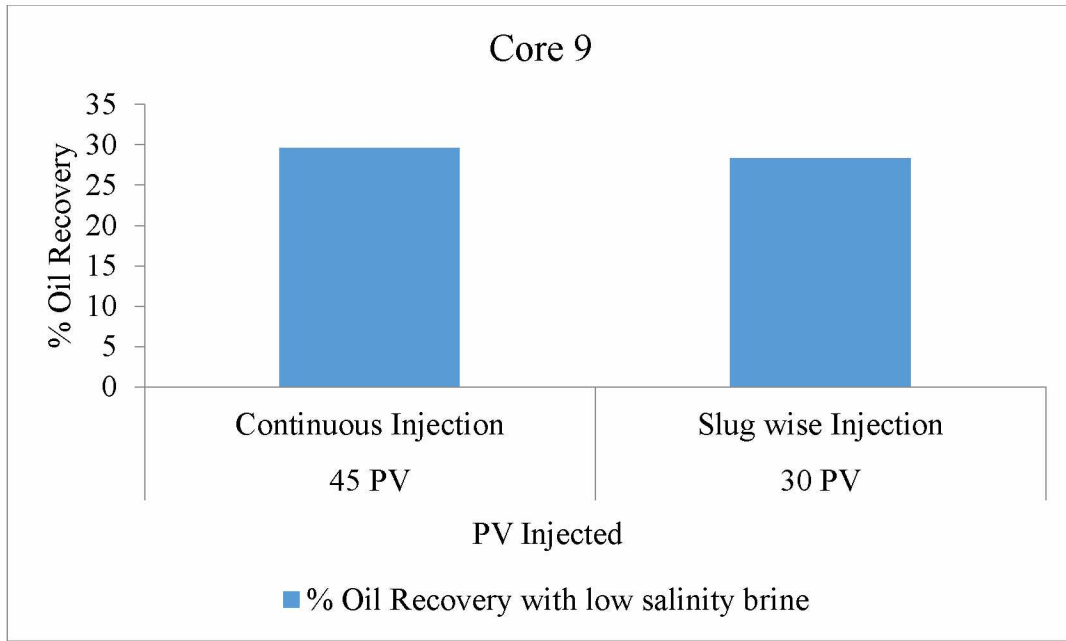
Figure 5.13 Graphical Representation of Continuous Injection vs Slug-wise Injection for Core 9
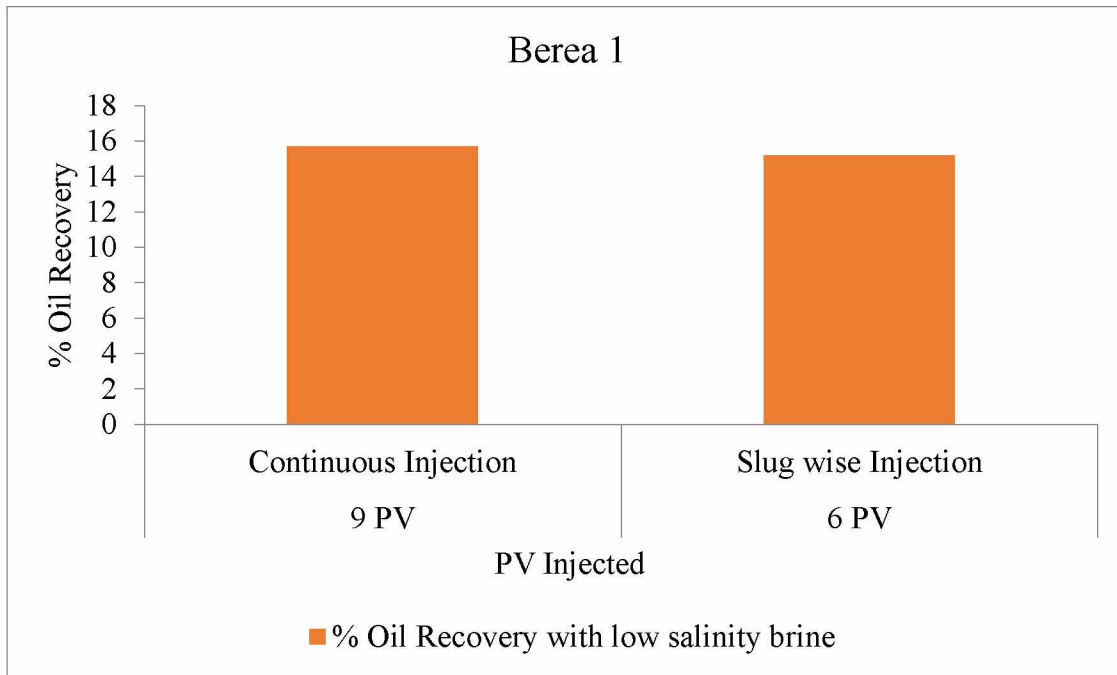
Figure 5.14 Graphical Representation of Continuous Injection vs Slug-wise Injection for Berea1

5.4   Results of Surface Level Investigation using Microscope

The surface level investigation of the core sample was performed to determine the effect of using

the low salinity water. The study was based on the qualitative analysis of the microscopic images

of the Core 9, Core 16 and Berea 1 core samples. Figure 5.15 shows the microscopic images of the Core 9 at four different conditions (a) core sample when it is dry, (b) core sample after saturating in brine, (c) core sample after spontaneously displaced with high salinity brine and (d) core sample after spontaneously displaced with low salinity brine. Results of the Core 16 and Berea 1 are given in Appendix E (below). The difference can be seen when the sample was dry and saturated. It may be due to because the microscope image for the saturated sample slightly showed reflection from water (Figure 5.15 (a) and Figure 5.15 (b)). In similar manner, the oil seen at the surface was darker and reflective after spontaneous displacement with high salinity brine (Figure 5.15(c)); on the other hand, after spontaneous displacing with low salinity brine, the surface of the core sample was lighter and less oily, possibly giving an indication of the swept oil. Based on the qualitative analysis of the core samples from Figure E.1 and Figure E.2, it can be suggested that low salinity water might change the wetting state of core sample or it might react with the core sample to detach the oil from the surface to recover more oil. Hence, low salinity water has potential in producing oil for the samples having clay in it.

(a) Dry Sample

(b) Saturated Sample

(c) Spontaneous Displacement with
High Salinity Brine

(d) Spontaneous Displacement with
Low Salinity Brine
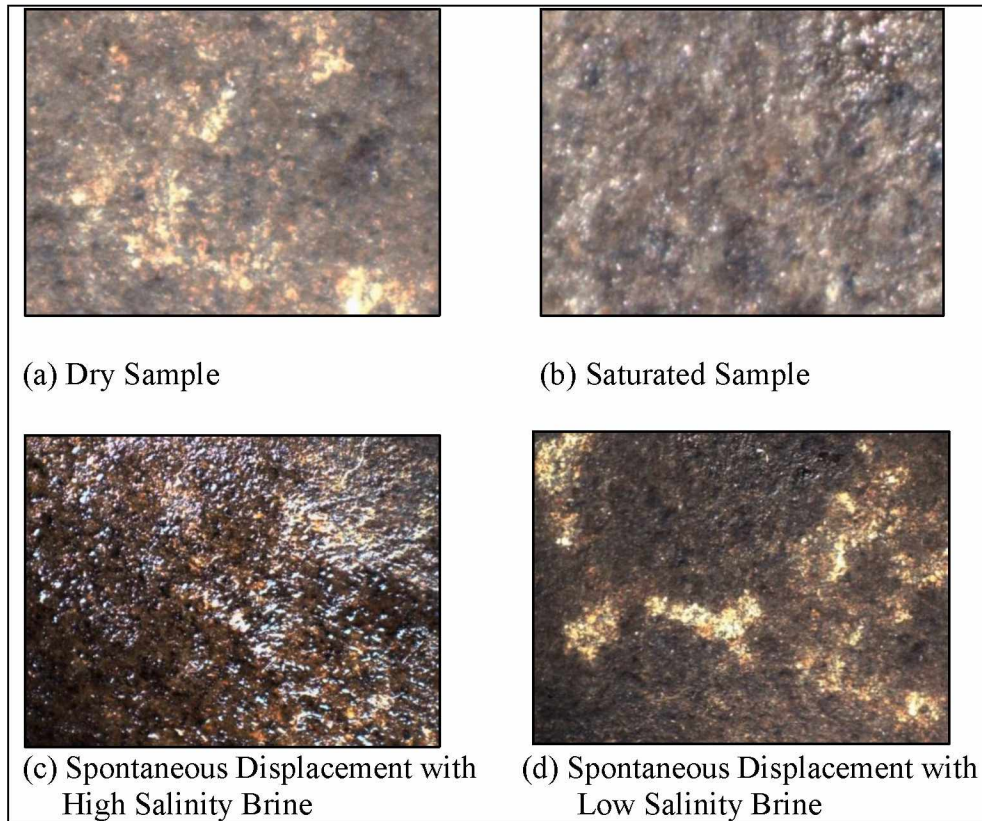
Figure 5.15 Microscopic Images for Core 9

Chapter 6 Conclusions and Recommendations

6.1 Conclusions

As yet there is no exact primary mechanism behind low salinity waterflooding, but wettability modification due to p^H alteration and salinity changes, cation exchange capacity (CEC) and electric double layer expansion/MIE are widely discussed mechanisms in the literature. Commonly researched topics, as they relate to LSWF, include presence of clay, wettability and water chemistry (see Figure A.1). Reservoirs that are oil-wet or mixed wet have shown to be more attractive candidates for LSWF. Optimum injected water salinity will depend on the composition of the reservoir brine, and LSWF benefits have been highest in injection water salinity ranging between 2,000 ppm and 5,000 ppm TDS. Slug wise injection appears to be the most economical injection method for LSWF.

Clay type is one of the most discussed topics in published works referencing LSWF. Some have proposed that Kaolinite would be the least favorable clay, but many positive results have come from sandstones containing kaolinite. Many experiments have been conducted with kaolinite clays, but little with other clays.

Two other observations from the literature review are: (1) Lab and field experiments generally seem to match each other, though field wide benefits are slightly lower than laboratory studies. (2) There is a lack of study relating oil properties (such as API gravity and viscosity) and rock properties (such as porosity, pore size, and permeability) to the benefits of LSWF. Despite the different explanations of how LSWF mechanism works, many parameters that may play role are given as follows,

1. Clays should be present and clay content must be high.
2. Formation water and/or seawater (high salinity) from prior flooding has to be present.

3. The injected brine salinity should be in the range of the optimum salinity, i.e., in between 2000 ppm to 5000 ppm.

4. A polar component has to be present in oil.

5. The reservoir has to be oil-wet or mixed-wet (or intermediate-wet)

The general conclusion for the current research is given as follows:

1. There are several factors to consider when selecting reservoir candidates for LSWF. A preliminary screening criterion based on literature review was proposed, as shown in Table 6-1.

Table 6-1 Preliminary Screening Criteria

Proposed LSWF Screening Criteria		
Variable	Favorable	Unfavorable
Clay Present	Yes	No
Clay Content	High	Low
Salinity of Brine	2000-5000 ppm	>7000 ppm
p^H of the medium	>7	<7
Oil Composition	Polar Components	Non-Polar Components
Wettability	Strongly Oil-Wet	Strongly Water-wet
Connate Water	Brackish (Yes)	Fresh (No)
EOR Mode	Secondary	Tertiary

2. The current literature on LSWF does not include any studies on core containing glauconite clays. However, the work that has been conducted as part of this research project indicates that low salinity waterflooding has a potential application in improving oil recovery for ANS reservoir.

3. In substrate type experiment, the direct experimental evidence of the release of crude oil from the clay surface by low salinity water was recorded. It can be seen from the results that the presence of clay and clay type play an important role in low salinity waterflood. The oil recovery is more in case of Kaolinite than Glauconite but as far as the damage and swelling is concerned Glauconite is more effective than Kaolinite. Hence Glauconite can be considered as favorable clay in low salinity waterflood projects.

4. Amott type spontaneous displacement test resulted in about 10-40% oil production with high salinity brine whereas incremental oil produced with low salinity brine was in the range of 3-7%.

5. In case of coreflooding experiments, continuous injection of low salinity waterflood recovers more oil but requires several PV's. Whereas, during slug-wise injection of low salinity water, nearly the same amount of oil was recovered with less PV injection.

6. (Modified) Reservoir condition corefloods recovered slightly more oil than the dead oil corefloods, which further supports the favorable potential of LSWF for ANS.

7. Surface level investigation conducted on core sample using microscope helped in qualitative understanding and some type of visual confirmation of the LSWF potential.

8. Based on the quantitative and qualitative analysis of the experimental results, the hierarchy for the clay minerals favorable for low salinity waterflooding is proposed as follows:

<div align="center">Kaolinite > Glauconite > Montmorillonite</div>

6.2   Recommendations

1. Conducting a sensitivity experimental study on each parameter, for example, API gravity, oil viscosity, pore size, porosity, permeability will help to better identify which mechanisms contribute the most to the benefits of LSWF.

2. LSWF response is unique to each reservoir, therefore, careful planning and understanding, on a case by case basis, is necessary in order to determine the potential of LSWF for field-wide implementation.

3. A comprehensive study comparing the clay type and amount of clay could provide evidence into the optimum clay characteristics amenable to LSWF.

4. Utilize good quality core samples, with larger pore volumes, for performing coreflood experiments. Also the effect of higher aging temperature of core samples with LSWF can be determined.

5. Actual reservoir gas composition can be used for recombination of oil to match actual reservoir conditions.

6. Use of technology such as nuclear magnetic resonance (NMR), scanning electron microscope (SEM) will help investigate LSWF effect at pore level.

7. Economics of the low salinity waterflood project can be investigated for a better comparison between continuous injection vs slug-wise injection of the low salinity water.

Chapter 7 References

Adamson, A.W. and Gast, A.P., 2007, "Physical Chemistry of Surfaces," 6th ed., Wiley.

Agbalaka, C. 2006. "Review and Experimental Studies to Evaluate the Impact of Salinity and Wettability on Oil Recovery Efficiency," MS Thesis, University of Alaska Fairbanks, May

Agbalaka, C.C., Dandekar, A.Y., Patil, S.L., Khataniar, S., and Hemsath, J.R. 2009. "Coreflooding Studies to Evaluate the Impact of Salinity and Wettability on Oil Recovery Efficiency." Transport in Porous Media (1): 77-94

Ahmed: Reservoir Engineering Handbook: Elsevier Inc, 4th Edition (2010)

Alotaibi, M.B., and Naser-El-Din, H.A. 2011. "Wettability Studies Using Low-Salinity Water in Sandstone Reservoirs," Paper SPE 149942, presented at Offshore Technology Conference, Huston, Texas, 3-6 May

Amott, E.: ―Observations Relating to the Wettability of Porous Rock,‖ Trans American Institute of Mining Engineers, Vol. 216, 156-92, (1959)

Ashraf, A., Hadia, N., Torsater, N., and Tweheyo, M. 2010. "Laboratory Investigation of Low Salinity Waterflooding as Secondary Recovery Process: Effect of Wettability," Paper SPE 129012, presented at SPE Oil and Gas India Conference and Exhibition, Mumbai, India, 20-22 January

Austad, T., RezariDoust, A., and Puntervold, T. 2010. "Chemical Mechanism of Low Salinity Water Flooding in Sandstone Reservoirs," Paper SPE 129767, presented at SPE Improved Oil Recovery Symposium, Tulsa, Oklahoma, 24-28 April

Berg, S., Cense, A.W., Jansen, E., and Bakker, K. 2009, "Direct Experimental Evidence of Wettability Modification by Low Salinity," presented at International Symposium of the Society of Core Analysts, Noordwijk aan Zee, Netherlands, 27-30 September

Bernard, G. G. 1967. "Effect of Floodwater Salinity on Recovery of Oil from Cores Containing Clays," Paper SPE 1725, presented at thirty-eight Annual California Regional Meeting of SPE, Los Angeles, California, 26-27 October

Boussour, S., Cissokho, M., Cordier, P., Bertin, H., and Hamon, G. 2009, "Oil Recovery by Low Salinity Brine Injection: Laboratory Results on Outcrop and Reservoir Cores," Paper SPE 124277, presented at SPE Annual Technical Conference and Exhibition, New Orleans, Louisiana, 4-7 October

Buckley, J.S., Liu, Y., and Monsterleet, S. 1998. "Mechanism of Wetting Alteration by Crude Oils," Paper SPE 37230, presented at SPE International Symposium on Oilfield Chemistry, Houston, Texas, 18-21 February

Cissokho, M., Boussour, S., Cordier, P., Bertin, H., and Hamon, G. 2010. "Low Salinity Oil Recovery on Clayey Sandstone: Experimental Study," presented at International Symposium of the Society of Core Analysts, Noordwijk aan Zee, Netherlands, 27-30 September

Chen, Q., Mercer, D., and Webb, K. 2010. NMR Study on Pore Occupancy and Wettability Modification during Low Salinity Waterflooding. Paper SCA 2010-27 presented at the 24th International Symposium of Core Analysts, Halifax, Canada, 4–7 October.

Cuong, T. Q., Nghiem, L.X., Chen Z., Nguyen, Q.P., and Ngoc. T.B. Nguyen. 2013. "State-of-the Art Low Salinity Waterflooding for Enhanced Oil Recovery," Paper SPE 165903, presented at SPE Asia Pacific Oil and Gas Exhibition, Jakarta, Indonesia, 22-24 October

Cuong, T. Q., Nghiem, L.X., Chen Z., Nguyen, Q.P. 2013. "Modelling Low Salinity Waterflooding: Ion Exchange, Geochemistry and Wettability Alteration," Paper SPE 166447, at the SPE Annual Technical Conference and Exhibition held in New Orleans, Louisiana, 30 September - 2 October

Dandekar, A. Y.: Petroleum Reservoir Rock and Fluid Properties: CRC Press LLC. (2013)

Fjelde, I., Asen, S.M., and Omekeh, A. 2012. "Low Salinity Waterflooding Experiments and Interpretation by Simulations," Paper SPE 154142, presented at Eighteenth SPE Improved Oil Recovery Symposium, Tulsa, Oklahoma, 14-18 April

Fjelde, I., Omekeh, A.V., and Sokama-Neuyam, Y.A. 2014. "Low Salinity Waterflooding: Effect of Crude Oil Composition," Paper SPE 169090, presented at SPE Improved Oil Recovery Symposium, Tulsa, Oklahoma, 12-16 April

Hadia, N., Kumar, K.G., and Torsaeter, O. 2011, "Laboratory Investigation of Low Salinity Waterflooding on Reservoir Rock Samples from the Frøy Field," Paper SPE 14114, presented at SPE Middle East Oil and Gas Show and Conference, Manama, Bahrain, 25-28 September

Hamouda, A.A., Valderhaug, O.M., Munaev, R., and Stangeland, H. 2014. "Possible Mechanisms for Oil Recovery from Chalk and Sandstone Rocks by Low Salinity Water (LSW)," Paper SPE 169885, presented at SPE Improved Oil Recovery Symposium, Tulsa, Oklahoma, 12-16 April

Jerauld, G. R., Lin, C.Y., and Seccombe, J.C. 2008. "Modeling Low-Salinity Waterflooding," Paper SPE 102239, presented at SPE Annual Technical Conference and Exhibition, San Antonio, Texas, 24-27 September

Karabakal, U. and Bagchi, S.: "Determination of Wettability and Its Effect on Waterflood Performance in Limestone Medium," Energy and Fuels, Vol. 18, No. 2, (2003)

Kasmaei, A.K., and Rao, D.N. 2014. "Is Wettability Alteration the Main Case for Enhanced Oil Recovery in Low Salinity Waterflooding?," Paper SPE 169120, presented at SPE Improved Oil Recovery Symposium, Tulsa, Oklahoma, 12-16 April

Kulathu S. S.: "Low Salinity Cyclic Water Injection for Enhanced Oil Recovery in Alaska North Slope," MS Thesis University of Alaska Fairbanks (May 2009)

Kulathu, S., Dandekar, A.Y., Patil, S., and Khataniar, S. 2013. "Low Salinity Cyclic Waterfloods for Enhanced Oil Recovery on Alaska North Slope," Paper SPE 165812, presented at SPE Asia Pacific Oil and Gas Conference and Exhibition, Jakarta, Indonesia, 22-24 October

Lager, A., Webb, K.J., Collins, I.R., and Richmond, D.M. 2008. "LoSalTM Enhanced Oil Recovery: Evidence of Enhanced Oil Recovery at the Reservoir Scale," Paper SPE 113976, presented at SPE/DOE Symposium on Improved Oil Recovery, Tulsa, Oklahoma, 19-23 April

Lee, S. Y., Webb, K.J., Collins, I.R., Lager, A., Clarke, S.M., O'Sullivan M., Routh, A.F., and Wang X. 2010. "Low Salinity Oil Recovery- Increasing Understanding of the Underlying Mechanisms," Paper SPE 129722, presented at SPE Improved Oil Recovery Symposium, Tulsa, Oklahoma, 24-28 April

Ligthelm, D.J., Gronsveld,, J., Hofman, J.P., Brussee, F., Marcelis, F., and Van der Linde, H.A. 2009. "Novel Waterflooding Strategy by Manipulation of Injection Brine Composition," Paper SPE 119835, presented at SPE EUROPE/EDGE Annual Conference and Exhibition, Amsterdam, Netherlands, 8-11 June

Loahardjo, N., Xie, X., Yin, P., and Morrow, N.R. 2007. "Low Salinity Waterflooding of a Reservoir Rock," Paper SCA2007-29, presented at International Symposium of the Society of Core Analysts, Calgary, Canada, 10-12 September

Mahzari, P., and Sohrabi, M. 2014. "Crude Oil/Brine Interactions and Spontaneous Formation of Micro-Dispersions in Low Salinity Water Injection," Paper SPE 169081, presented at SPE Improved Oil Recovery Symposium, Tulsa, Oklahoma, 12-16 April

McGuire P.L., Chatham, J.R., Paskvan, F.K., Sommer, D.M., and Carini, F.H. 2005. "Low Salinity Oil Recovery: An Exciting New EOR Opportunity for Alaska's North Slope," SPE 93903, presented at SPE Western Regional Meeting, Irvine, California, 30th March-1st April

Morrow, N. 2011. "Improved Oil Recovery by Waterflooding and Spontaneous Imbibition," EORI TAB Meeting, presentation

Morrow, N. and Buckley, J. 2011. "Improved Oil Recovery by Low-Salinity Waterflooding," Paper SPE 129421, Distinguished Author Series

Nasralla, R. A., and Nasr-El-Din, H. A. 2011. "Impact of Electrical Surface Charges and Cation Exchange on Oil Recovery by Low Salinity Water," Paper SPE 147937, presented at SPE Asia Pacific Oil and Gas Conference and Exhibition, Jakarta, Indonesia, 20-22 September

Omekeh, A., Friis, H.A., Fjelde, I., and Evje, S. 2012. "Modeling of Ion-Exchange and Solubility in Low Salinity Waterflooding," Paper SPE 154144, presented at Eighteenth SPE Improved Oil Recovery Symposium, Tulsa, Oklahoma, 14-18 April

Patil, S.B.: "Experimental Investigation of Low Salinity Enhanced Oil Recovery Potential and Wettability Characterization of Alaska North Slope Cores", MS Thesis, University of Alaska Fairbanks (December 2007)

Patil, S., Dandekar, A.Y., Patil, S.L., and Khataniar, S. 2008. "Low Salinity Brine Injection for EOR on Alaska North Slope (ANS)," Paper IPTC 12004, presented at International Petroleum Technology Conference, Kuala Lumpur, Malaysia, 3-5 December

Pu, H., Xie, X., Yin, P., and Morrow, N.R. 2010. "Low Salinity Waterflooding and Mineral Dissolution," Paper SPE 134042, presented at SPE Annual Technical Conference and Exhibition, Florence, Italy, 19-22 September

Ramez, A. N. and Nasr-El-Din, H. A. 2014. "Double-Layer Expansion: Is It a Primary Mechanism of Improved Oil Recovery by Low Salinity Waterflooding?," Paper SPE 154334, Paper SPE 169081, presented at SPE Improved Oil Recovery Symposium, Tulsa, Oklahoma, 12-16 April

RezaeiDoust, A., Puntervold, T., Strand, S. and Austad, T. 2009. "Smart Water as Wettability Modifier in Carbonate and Sandstone: A Discussion of Similarities/Differences in Chemical Mechanism," Energy and Fuels 23(9): 4479-4485

Rivet, S.M., Lake, L.W., and Pope, G.A. 2010. "A Coreflood Investigation of Low-Salinity Enhanced Oil Recovery," Paper SPE 134297, presented at SPE Annual Technical Conference and Exhibition, Florence, Italy, 19-22 September

Robertson, E.P., Thomas, C.P., Zhang, Y., and Morrow, N.R. 2003. "Improved Waterflooding Through Injection Brine Modification," Idaho National Laboratory Report INEEL/EXT-02-01591, DOE Contract DE-AC07-99ID13727 (January 2003)

Robertson, E. P. 2007. "Low-Salinity Waterflooding to Improve Oil Recovery - Historical Field Evidence," Paper SPE 109965, presented at SPE Annual Technical Conference and Exhibition, November

Robertson, E. P. 2010. "Oil Recovery Increases by Low-Salinity Flooding: Minnelusa and Green River Formations," Paper SPE 132154, presented at SPE Annual Technical Conference and Exhibition, Florence, Italy, 19-22 September

Salathiel, R. A. 1973. "Oil Recovery by Surface Film Drainage In Mixed-Wettability Rocks," Journal of Petroleum Technology: 1216-1224, Paper SPE 4104

Sandengen, K., Tweheyo, M.T., Raphaug, M., Kjolhamar, A., Crescente, C., and Kippe, V. 2011. "Experimental Evidence of Low Salinity Waterflooding Yielding a More Oil-Wet Behavior," Paper SCA2011-16 presented at the International Symposium of the Society of Core Analysts, Austin, Texas, 18-21 September

Seccombe, J.C., Lager, A., Webb, K., Jerauld, G., and Fueg, E. 2008. "Improving Waterflood Recovery: LoSalTM EOR Field Evaluation," Paper SPE 113480, presented at SPE/DOC Improved Oil Recovery Symposium, Tulsa, Oklahoma, 19-23 April

Seccombe, J.C., Lager, A., Jerauld, G., Jhaveri, B., Buikema, T., Bassler, S., Denis, J., Webb, K., Cockin, A., Fueg, E., and Paskvan, F. 2010. "Demonstration of Low-Salinity EOR at Interwell Scale, Endicott Field, Alaska," Paper SPE 129692, presented at SPE Improved Oil Recovery Symposium, Tulsa, Oklahoma, 24-28 April

Shiran, B. S. and Skauge, A. 2012. "Wettability and Oil Recovery by Low Salinity Injection," Paper SPE 155651, presented at SPE EOR Conference at Oil and Gas West Asia, Muscat, Oman, 16-18 April

Skrettingland, K., Holt, T., Tweheyo, M.T., and Skjevrak, I. 2011. "Snorre Low-Salinity Water Injection - Coreflooding Experiments and Single-Well Field Pilot," Paper SPE 129877, presented at SPE Improved Oil Recovery Symposium, Tulsa, Oklahoma, 24-28 April

Sorbie, K. S. and Collins, I. R. 2010. "A Proposed Pore-Scale Mechanism for How Low Salinity Waterflooding Works," Paper SPE 129833, presented at SPE Improved Oil Recovery Symposium, Tulsa, Oklahoma, 24-28 April

Spildo, K., Johannessen, A.M., and Skauge, A. 2012. "Low Salinity Waterflood at Reduced Capillarity," Paper SPE 154236, presented at Eighteenth SPE Improved Oil Recovery Symposium, Tulsa, Oklahoma, 14-18 April

Tang, G. Q. and Morrow, N. R. 1997. "Salinity, Temperature, Oil Composition, and Oil Recovery by Waterflooding," Paper SPE 36680, presented at SPE Annual Technical Conference and Exhibition, Denver, Colorado, 6-9 October

Tang, G. Q. and Morrow, N. R. 1999. "Influence of Brine Composition and Fines Migration on Crude Oil/Brine/Rock Interactions and Oil Recovery," Journal of Petroleum Science and Engineering, 24(2-4): 99-11

Tchistiakov, A. 2000. "Colloid Chemistry of In-Situ Clay-Induced Formation Damage," SPE 58747, presented at SPE International Symposium on Formation Damage Control, Lafayette, Louisiana, 23-24 February

Vaidya, R.N., and Fogler, H.S. 1992. "Fines Migration and Formation Damage: Influence of pH and Ion Exchange," Paper SPE 19413, SPE Production Engineering, November

Vledder, P., Fonseca, J.C., Wells, T., Gonzalez, I., and Ligthelm, D. 2010. "Low Salinity Water Flooding: Proof of Wettability Alteration on A Field Wide Scale," Paper SPE 129564, presented at SPE Improved Recovery Symposium, Tulsa, Oklahoma, 24-28 April

Webb, K. J., Black, C.J.J., and Al-Ajeel, H. 2004. "Low Salinity Oil Recovery - Log-Inject-Log," Paper SPE 89379, presented at SPE/DOE Symposium on Improved Oil Recovery, Tulsa, Oklahoma, 17-21 April

Yousef, A. A., Al-Saleh, S., and Al-Jawfi, M. 2012. "Improved/Enhanced Oil Recovery from Carbonate Reservoirs by Tuning Injection Water Salinity and Ionic Content," Paper SPE 154076, presented at SPE Improved Oil Recovery Symposium, Tulsa, Oklahoma, 14-18 April

Zahid, A., Shapiro, A., and Skauge, A. 2012. "Experimental Studies of Low Salinity Water Flooding Carbonate: A New Promising Approach," Paper SPE 155625, presented at SPE EOR Conference at Oil and Gas West Asia, Muscat, Oman, 16-18 April

Zhang, Y., Xie, X., Morrow, N.R. 2007. "Waterflood Performance by Injection of Brine with Different Salinity for Reservoir Cores," Paper SPE 109849, presented at the SPE Annual Technical Conference and Exhibition, Anaheim, CA, USA, 11-14 November

Table A-1 Summary of LSWF publications

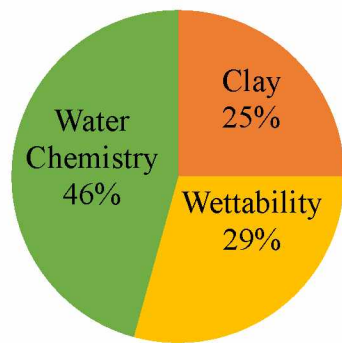| Paper No.	Year	DISCUSSED VARIABLES									
		Clay	Swi	Porosity	Permeability	Oil Type	API	Viscosity	Wettability	Water Chemistry	Temperature
SPE1725	1967	X							X	X	
SPE 4104	1973								X		
SPE 19413	1992	X								X	
SPE 36680	1997					X				X	X
SPE 37230	1998								X	X	
JPT 24(2-4): 99-11	1999									X	
SPE 58747	2000	X								X	X
Lab Report	2003	X				X				X	
SPE 89379	2004	X	X	X	X		X	X	X	X	
Elsevier 7365	2005									X	
SPE 93903	2005					X			X	X	
MS Thesis	2006								X	X	
SPE 109849	2007									X	
SPE 109965	2007										
Book	2007	X								X	
SCA2007-29	2007	X	X	X	X	X	X	X		X	X
SPE 113976	2008	X								X	
SPE 102239	2008		X						X	X	
IPTC 12004	2008								X	X	
SPE 113480	2008	X	X						X	X	
	2009								X	X	
	2009	X	X						X	X	
SPE 124277	2009	X	X							X	X
Energy & Fuels	2009								X	X	
SPE 119835	2009								X	X	
Petrophysics Vol. 51 No. 5 (314-322)	2009	X				X		X	X	X	
SPE 129722	2010	X								X	
SPE 129767	2010	X	X		X	X			X	X	X
SPE 129692	2010	X	X						X	X	
Petrophysics Vol. 51 No. 5 (305-313)	2010	X	X	X	X			X		X	X
SPE 129012	2010					X			X	X	
SPE 129833	2010	X								X	
SPE 132154	2010	X	X	X	X	X	X	X		X	X
SPE 134297	2010								X	X	
SPE 129877	2010	X	X	X	X	X			X		
SPE 134042	2010	X	X							X	
SPE 129564	2010								X		
SPE 149942	2011								X	X	
SPE 147375	2011		X		X	X	X	X		X	
IPTC 14507	2011										
Presentation	2011	X							X	X	
SPE 129421	2011		X						X	X	
SPE 147937	2011	X								X	
SPE 14114	2011	X	X								
SPE 147937	2011	X								X	
SPE 154334	2011	X								X	
SPE 129877	2011										
SPE 147410	2011										
SCA2011-16	2011								X	X	
SPE 152997	2012	X							X	X	
SPE 154037	2012	X								X	
SPE 154144	2012									X	
SPE 155625	2012	X									
SPE 154508	2012					X		X			X
SPE 154076	2012									X	
SPE 154142	2012		X						X	X	
SPE 154236	2012								X	X	
SPE 153993	2012										
SPE 154204	2012								X		
SPE 155651	2012								X	X	
SPE 165903	2013	X		X	X	X	X	X	X	X	
SPE 166447	2013	X		X	X				X	X	
SPE 165812	2013								X	X	
SPE 169885	2014	X	X						X	X	
SPE 169090	2014					X	X	X	X	X	
SPE 169081	2014								X	X	X
SPE 169120	2014								X	X	X
Total	65	29	14	6	7	11	4	7	34	53	8

Figure A.1 Most Studied Variables in the Literature

Appendix B Results of Substrate Test

Table B-1 Overview of all Experiments Conducted with Kaolinite

Clay type	Method of substrate preparation	Flow rate used (ml/min)	Time (min)	Oil released	% Total oil recovery	% release of oil with low salinity waterflood	Substrate damage
Kaolinite	Mixed with high salinity brine	50	30	Yes	40 %	22 %	Very little
		100	30	Yes	72 %	40 %	Yes
		200	30	Yes	87 %	40 %	High damage
Kaolinite	Saturated with high salinity brine	50	30	No	-	-	Damage
		100	30	Yes	30 %	12 %	Yes
		200	30	Yes	33 %	18 %	High damage
Kaolinite	Directly sprinkled	50	15	No	-	-	Damage
		100	15	Yes	40 %	27 %	Very little
		200	15	Yes	80 %	40 %	High damage
Kaolinite	Mixed with oil & brine	50	30	Yes	38 %	20 %	No damage
		100	30	Yes	70 %	35 %	Very little
		200	30	Yes	82 %	37 %	Moderate

Table B-2 Overview of all Experiments Conducted with Glauconite

Clay type	Method of substrate preparation	Flow rate used (ml/min)	Time (min)	Oil released	% Total oil recovery	% release of oil with low salinity waterflood	Substrate damage
Glauconite	Mixed with high salinity brine	50	30	Yes	30 %	15-18 %	No
		100	30	Yes	88 %	40-42 %	No
		200	30	Yes	74 %	30 %	Yes
Glauconite	Saturated with high salinity brine	50	30	No	-	-	Yes
		100	30	No	20 %	7-9 %	Yes
		200	30	Yes	70 %	10 %	High damage
Glauconite	Directly sprinkled	50	20	No	-	-	No
		100	20	No	-	-	Yes
		200	20	Yes	20 %	5-7%	High damage
Glauconite	Mixed with oil & brine	50	30	Yes	32 %	16 %	No
		100	30	Yes	75 %	45 %	Very little
		200	30	Yes	80 %	30 %	Yes

Table B-3 Overview of all Experiments Conducted with Montmorillonite

| Clay type	Method of substrate preparation	Flow rate used (ml/min)	Time (min)	Oil released	% Total oil recovery	% release of oil with low salinity waterflood	Substrate damage
Montmorillonite	Mixed with high salinity brine	50	10	Yes	44 %	25 %	Very little
		100	10	Yes	75 %	30 %	Damaged
		200	10	Yes	85 %	30 %	Damaged
Montmorillonite	Saturated with high salinity brine	50	15	No	-	-	Damaged
		100	15	No	-	-	Damaged
		200	15	No	-	-	Damaged
Montmorillonite	Directly sprinkled	50	5	Yes	42 %	30 %	Moderate
		100	5	Yes	60 %	25 %	Damaged
		200	5	Yes	80 %	20 %	Damaged
Montmorillonite	Mixed with oil & brine	50	10	No	-	-	Very little
		100	10	Yes	70 %	35 %	Moderate
		200	10	Yes	85 %	40 %	Damaged
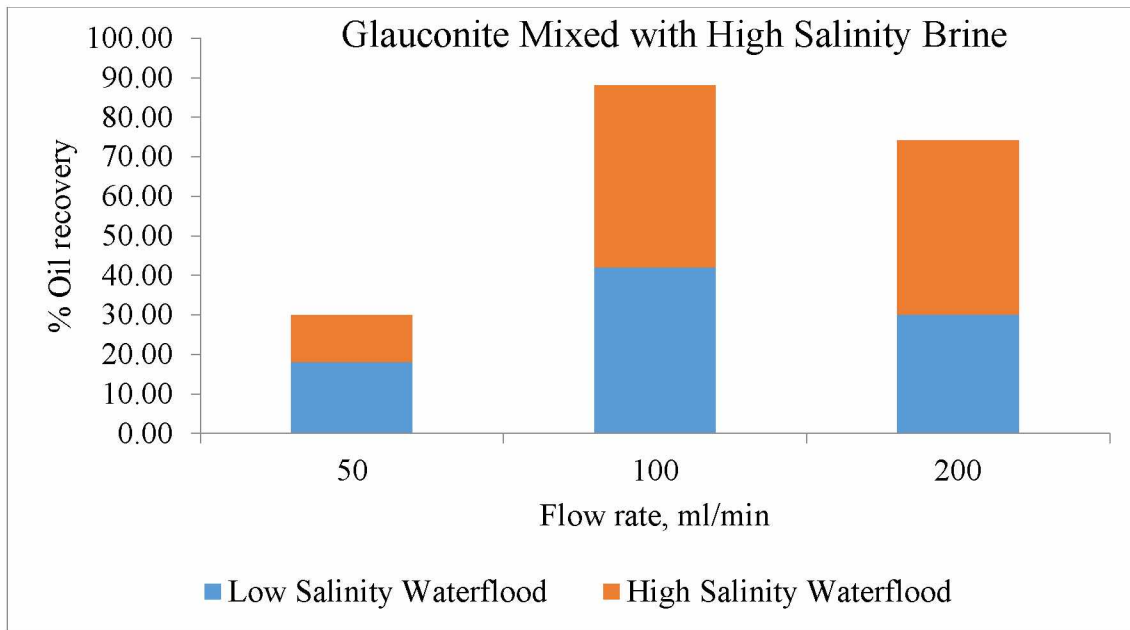
Figure B.1 Results of Successful Substrate (Mixed with High Salinity Brine) Tests with Glauconite at Different Flow Rates
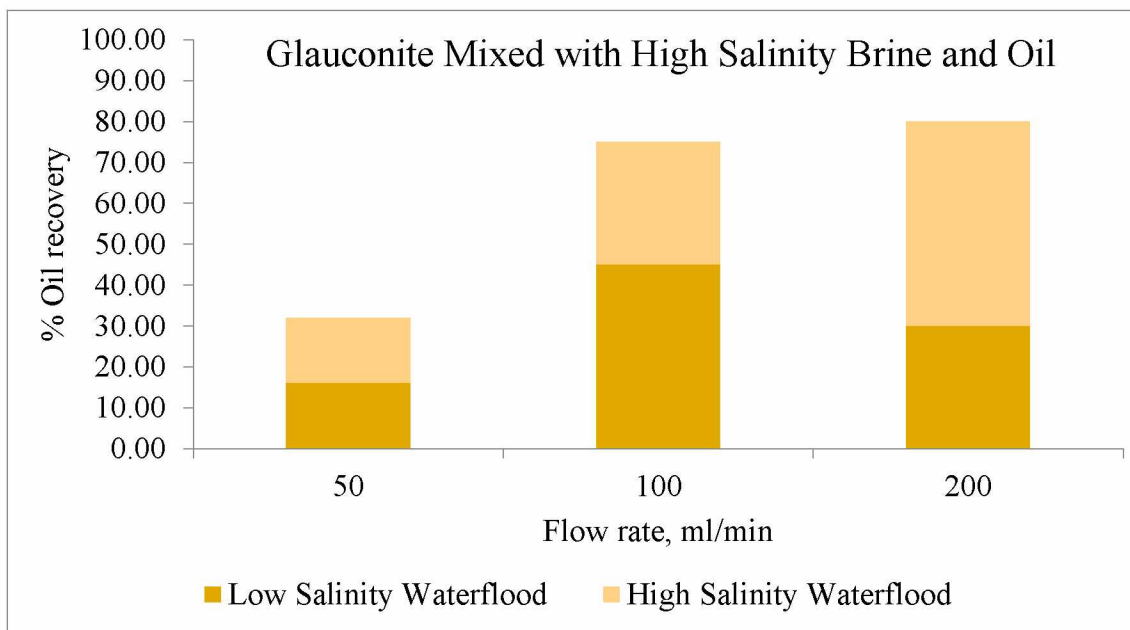

Figure B.2 Results of Successful Substrate (Mixed with High Salinity Brine and Oil) Tests with Glauconite at Different Flow Rates
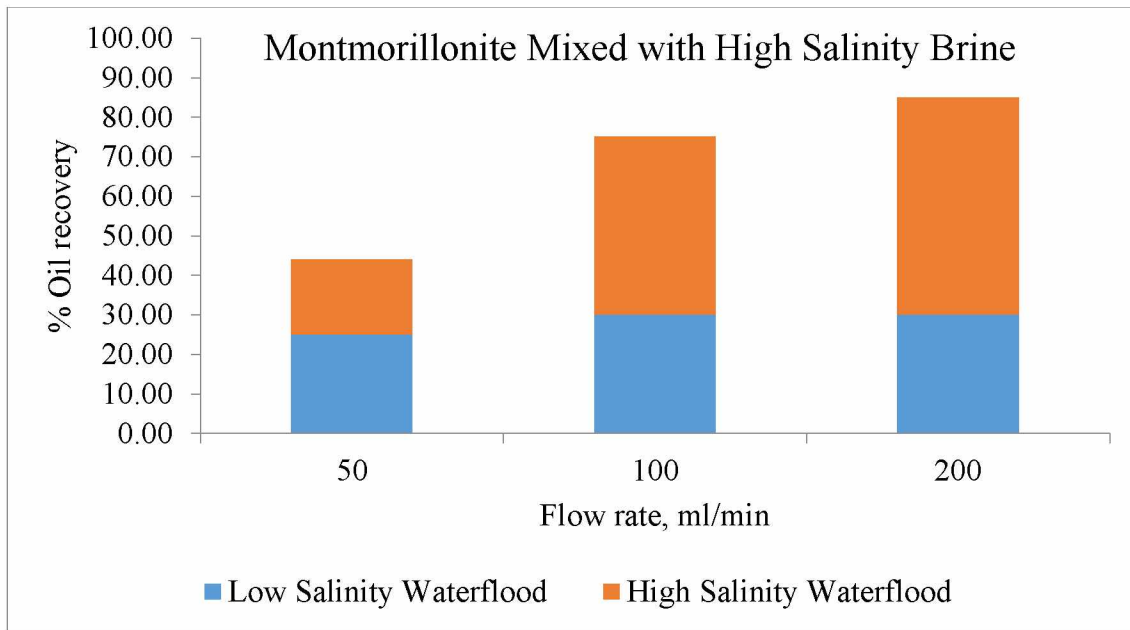
Figure B.3 Results of Successful Substrate (Mixed with High Salinity Brine) Tests with Montmorillonite at Different Flow Rates
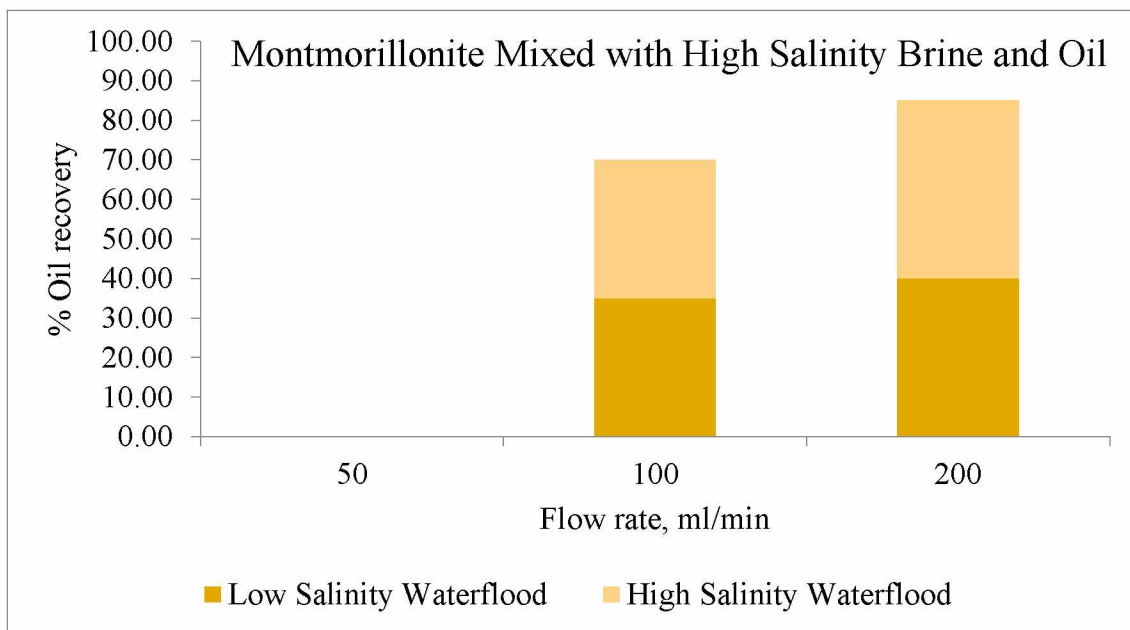

Figure B.4 Results of Successful Substrate (Mixed with High Salinity Brine and Oil) Tests with Montmorillonite at Different Flow Rates

Appendix C Results of Amott Tests

Table C-1 Amott Type Spontaneous Displacement Test Data for Core 9

Core 9		
Glauconite clay = 10.89 % by volume		
Initial Oil in the Core-plug	1.14	cc
Oil Recovered with High Salinity Brine	10.50	%
Oil Recovered with Low Salinity Brine	2.60	%
Total Oil Recovered	13.10	%

Table C-2 Amott Type Spontaneous Displacement Test Data for Core 11

Core 11		
Glauconite clay = 0.12 % by volume		
Initial Oil in the Core-plug	0.69	cc
Oil Recovered with High Salinity Brine	38.12	%
Oil Recovered with Low Salinity Brine	4.12	%
Total Oil Recovered	42.24	%

Table C-3 Amott Type Spontaneous Displacement Test Data for Core 23

Core 23		
Glauconite clay = 20.47 % by volume		
Initial Oil in the Core-plug	0.73	cc
Oil Recovered with High Salinity Brine	41.00	%
Oil Recovered with Low Salinity Brine	6.80	%
Total Oil Recovered	47.80	%

Table C-4 Amott Type Spontaneous Displacement Test Data for Core 12

Core 12		
Glauconite clay = 5.73 % by volume		
Initial Oil in the Core-plug	2.09	cc
Oil Recovered with High Salinity Brine	4.7	%
Oil Recovered with Low Salinity Brine	0.0	%
Total Oil Recovered	4.7	%

Table C-5 Amott Type Spontaneous Displacement Test Data for Berea 1

Berea 1		
Contains Kaolinite clay		
Initial Oil in the Core-plug	4.14	cc
Oil Recovered with High Salinity Brine	4.65	%
Oil Recovered with Low Salinity Brine	1.57	%
Total Oil Recovered	6.22	%

Table C-6 Amott Type Spontaneous Displacement Test Data for Berea 2

Berea 2		
Contains Kaolinite clay		
Initial Oil in the Core-plug	4.15	cc
Oil Recovered with High Salinity Brine	4.36	%
Oil Recovered with Low Salinity Brine	1.80	%
Total Oil Recovered	6.16	%

Table C-7 Amott Type Spontaneous Displacement Test Data for Core A

Core A		
Contains Montmorillonite clay		
Initial Oil in the Core-plug	5	cc
Oil Recovered with High Salinity Brine	40	%
Oil Recovered with Low Salinity Brine	17.8	%
Total Oil Recovered	57.8	%

Table C-8 Amott Type Spontaneous Displacement Test Data for Core B

Core B		
Contains Kaolinite clay		
Initial Oil in the Core-plug	5	cc
Oil Recovered with High Salinity Brine	37.8	%
Oil Recovered with Low Salinity Brine	19.6	%
Total Oil Recovered	57.4	%

Appendix D Results of Coreflooding Experiment

Table D-1 Coreflooding Experiment Data for Core 12

Core 12 (Glauconite= 5.73% by volume)		
Pore Volume (PV)	1.41	cc
Porosity (ϕ)	9.16	%
Flow Rate (Q)	5	ml/min
Differential Pressure (ΔP)	528	psia
Viscosity of Brine (μ_b)	1.00	cP
Absolute Permeability (k_{abs})	1.43	mD
Initial Water Saturation (S_{wi})	0.30	
Oil-flood Data		
Flow Rate (Q)	0.75	ml/min
Differential Pressure (ΔP)	577	psia
Viscosity of Oil (μ_o)	3.00	cP
Effective Permeability to Oil at S_{wi} (k_{eff})	0.58	mD
Waterflood Data		
Effective Permeability to high salinity brine at S_{or}	0.59	mD
Effective Permeability to low salinity brine at S_{or}	0.60	mD

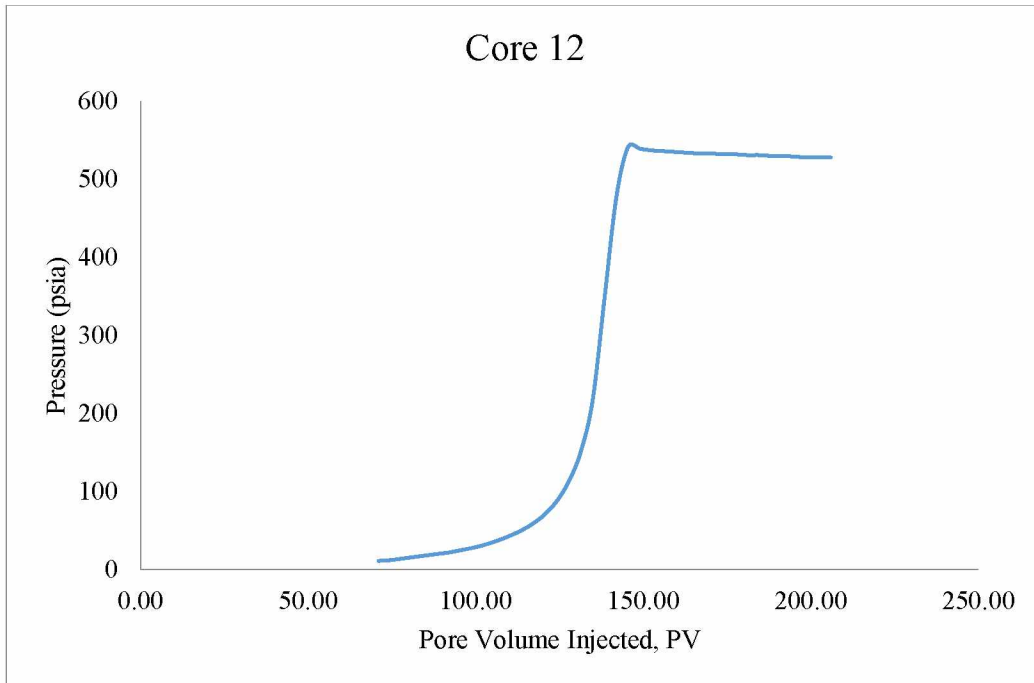| Core 12		
Glauconite clay = 5.73 % by volume		
Initial Oil in the Core-plug	2.09	cc
Oil Recovered with High Salinity Brine	2.33	%
Oil Recovered with Low Salinity Brine	0.0	%
Total Oil Recovered	2.33	%

Figure D.1 Graphical Representation of Pressure Profile during Waterflood (Core 12)
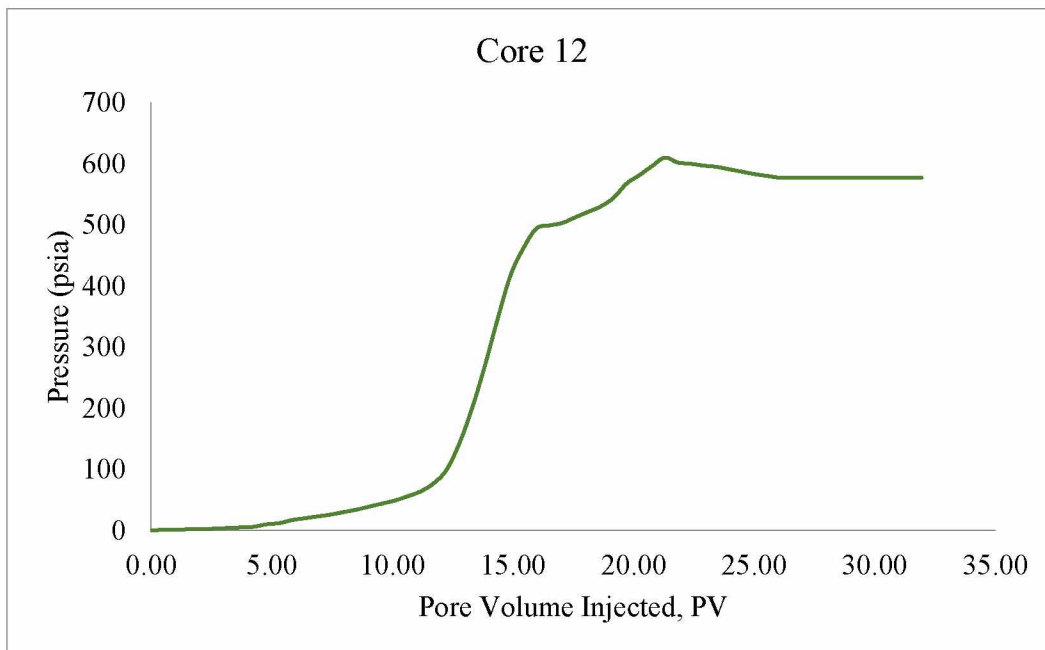

Figure D.2 Graphical Representation of Pressure Profile during Oil-flood (Core 12)
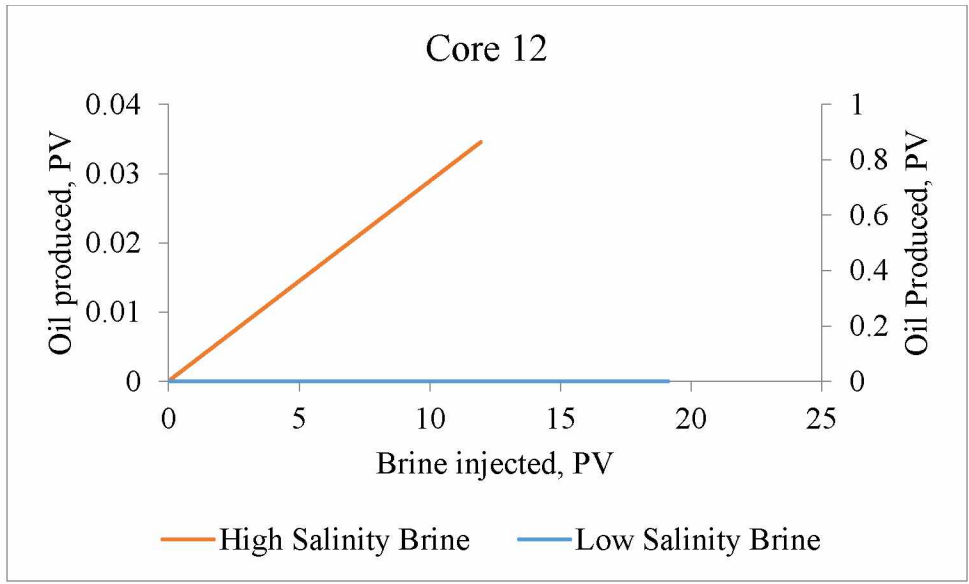
Figure D.3 Oil Recovery Profile for Core 12
Primary Y-axis: High salinity brine and Secondary Y-axis: Low salinity brine

Table D-2 Coreflooding Experiment Data for Core 23

Core 23 (Glauconite= 20.47 % by volume)		
Pore Volume (PV)	2.87	cc
Porosity (ϕ)	12.98	%
Flow Rate (Q)	2.5	ml/min
Differential Pressure (ΔP)	140	psia
Viscosity of Brine (μ_b)	1.00	cP
Absolute Permeability (k_{abs})	3.88	mD
Initial Water Saturation (S_{wi})	0.28	
Oil-flood Data		
Flow Rate (Q)	0.25	ml/min
Differential Pressure (ΔP)	203	psia
Viscosity of Oil (μ_o)	3.00	cP
Effective Permeability to Oil at S_{wi} (k_{eff})	0.80	mD
Waterflood Data		
Effective Permeability to high salinity brine at S_{or}	0.80	mD
Effective Permeability to low salinity brine at S_{or}	0.79	mD

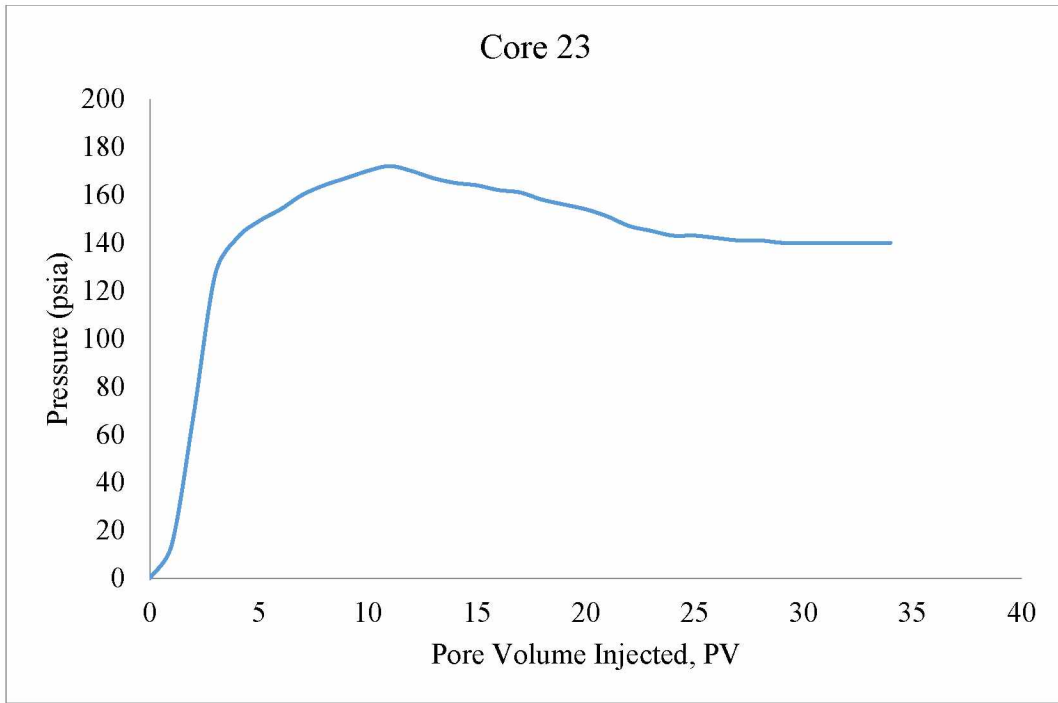| Core 23		
Glauconite clay = 20.47 % by volume		
Initial Oil in the Core-plug	0.98	cc
Oil Recovered with High Salinity Brine	30.81	%
Oil Recovered with Low Salinity Brine	5.13	%
Total Oil Recovered	35.94	%

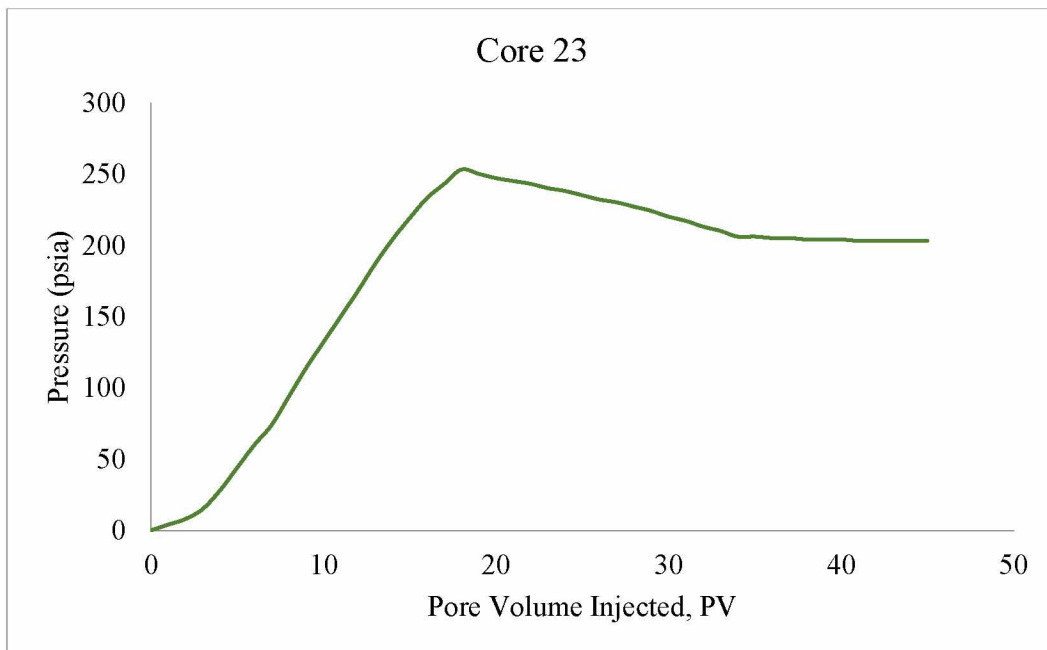Figure D.4 Graphical Representation of Pressure Profile during Waterflood (Core 23)

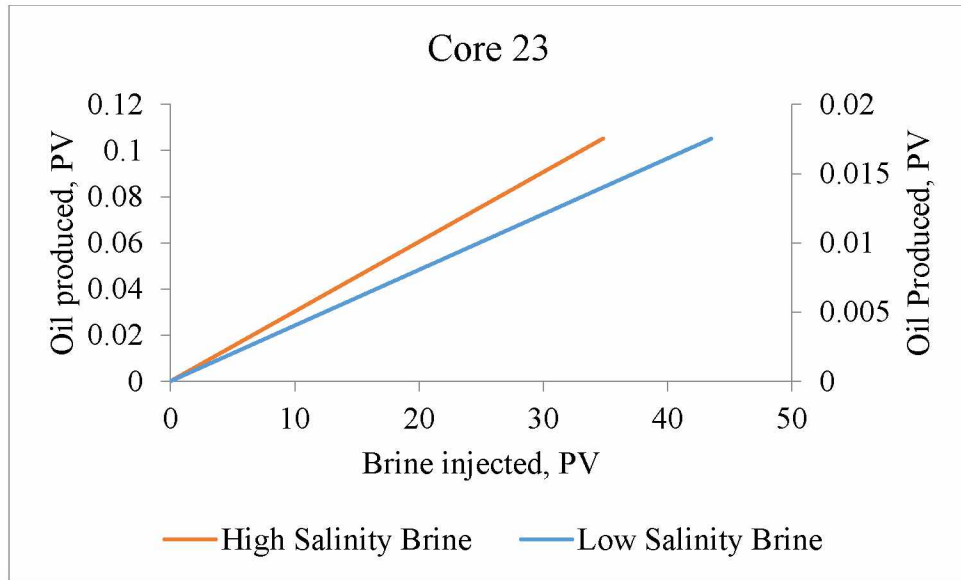Figure D.5 Graphical Representation of Pressure Profile during Oil-flood (Core 23)

108

Figure D.6 Oil Recovery Profile for Core 23
Primary Y-axis: High salinity brine and Secondary Y-axis: Low salinity brine

Table D-3 Coreflooding Experiment Data for Berea 1

Berea 1 (Kaolinite)		
Pore Volume (PV)	5.61	cc
Porosity (ϕ)	14.70	%
Flow Rate (Q)	2	ml/min
Differential Pressure (ΔP)	30	psia
Viscosity of Brine (μ_b)	1.00	cP
Absolute Permeability (k_{abs})	26.30	mD
Initial Water Saturation (S_{wi})	0.26	
Oil-flood Data		
Flow Rate (Q)	0.25	ml/min
Differential Pressure (ΔP)	20	psia
Viscosity of Oil (μ_o)	3.00	cP
Effective Permeability to Oil at S_{wi} (k_{eff})	14.77	mD
Waterflood Data		
Effective Permeability to high salinity brine at S_{or}	14.72	mD
Effective Permeability to low salinity brine at S_{or}	14.70	mD

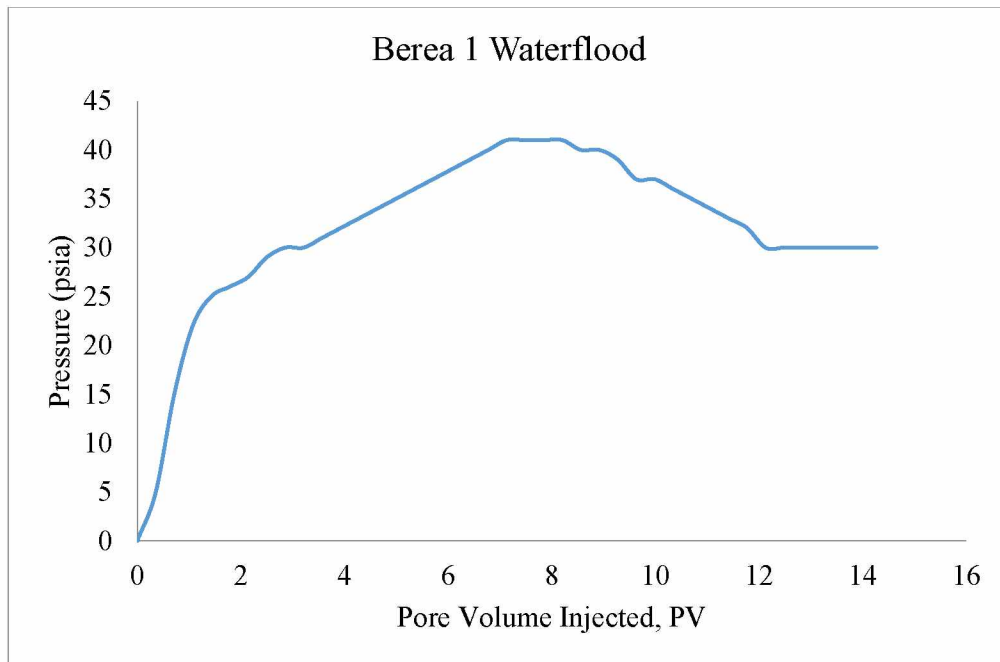| Berea 1		
Contains Kaolinite clay		
Initial Oil in the Core-plug	4.14	cc
Oil Recovered with High Salinity Brine	28.94	%
Oil Recovered with Low Salinity Brine	15.68	%
Total Oil Recovered	44.62	%

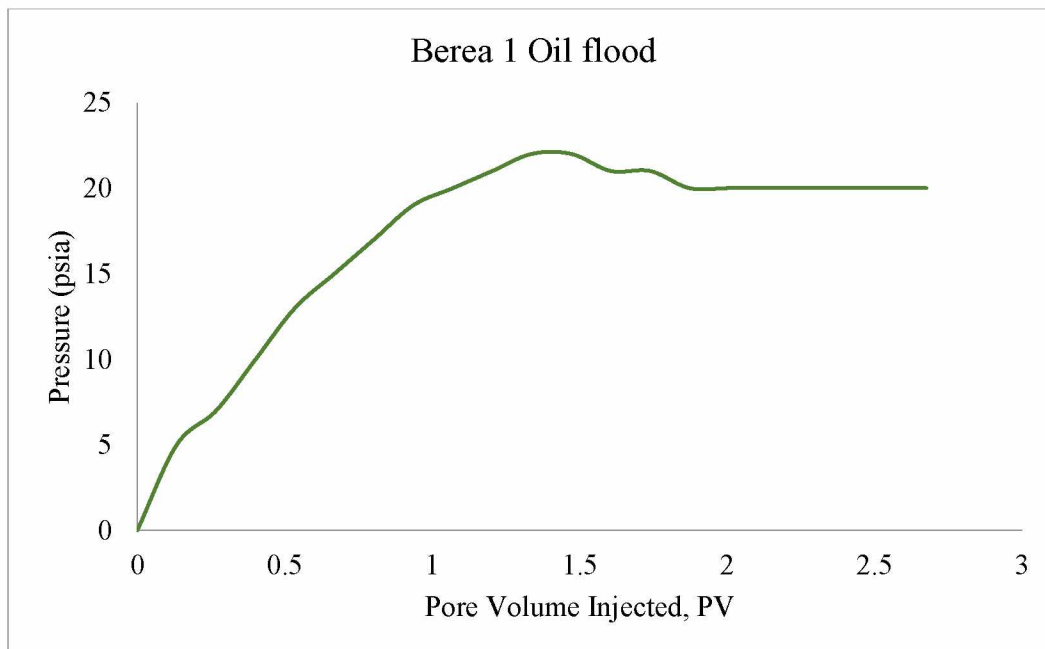Figure D.7 Graphical Representation of Pressure Profile during Waterflood (Berea 1)

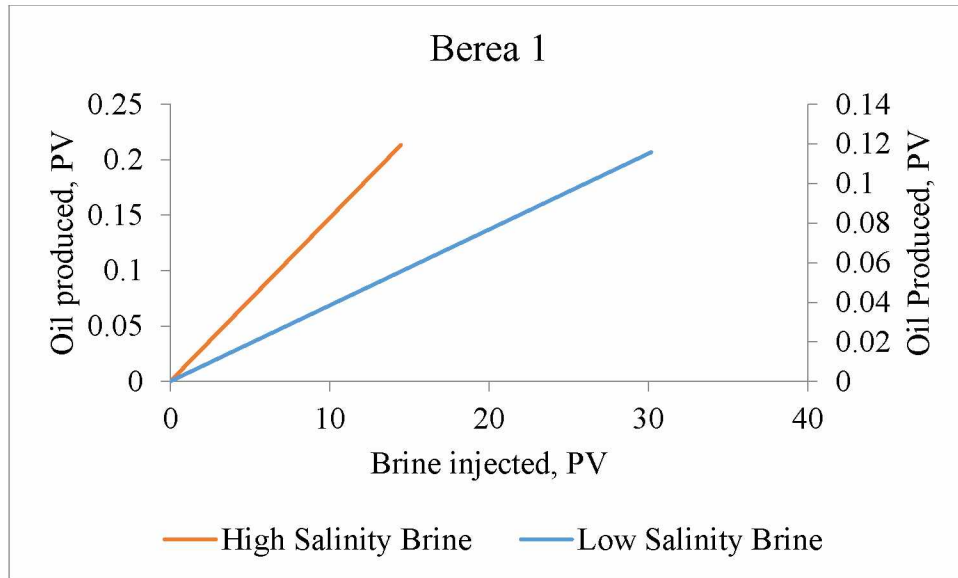Figure D.8 Graphical Representation of Pressure Profile during Oil-flood (Berea 1)

111

Figure D.9 Oil Recovery Profile for Berea 1
Primary Y-axis: High salinity brine and Secondary Y-axis: Low salinity brine

Table D-4 Coreflooding Experiment Data for Berea 2

Berea 2 (Kaolinite)		
Pore Volume (PV)	5.53	cc
Porosity (φ)	14.71	%
Flow Rate (Q)	2	ml/min
Differential Pressure (ΔP)	24	psia
Viscosity of Brine (μb)	1.00	cP
Absolute Permeability (k_{abs})	33.45	mD
Initial Water Saturation (S_{wi})	0.25	
Oil-flood Data		
Flow Rate (Q)	0.25	ml/min
Differential Pressure (ΔP)	18	psia
Viscosity of Oil (μo)	3.00	cP
Effective Permeability to Oil at S_{wi} (k_{eff})	16.70	mD
Waterflood Data		
Effective Permeability to high salinity brine at S_{or}	16.62	mD
Effective Permeability to low salinity brine at S_{or}	16.58	mD

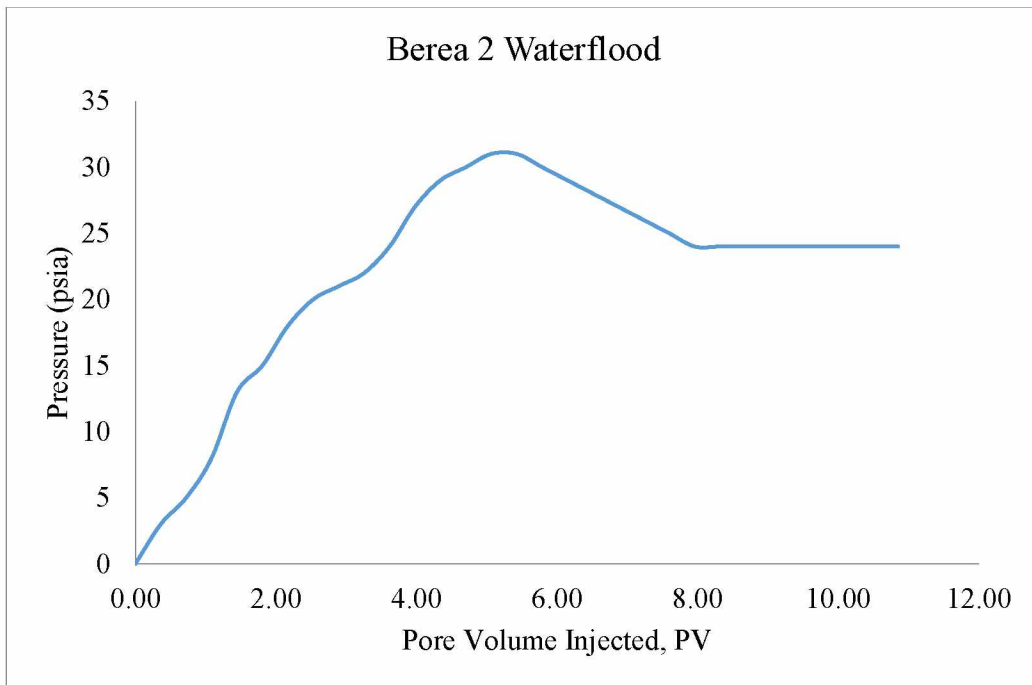| Berea 2		
Contains Kaolinite clay		
Initial Oil in the Core-plug	4.15	cc
Oil Recovered with High Salinity Brine	29.00	%
Oil Recovered with Low Salinity Brine	15.60	%
Total Oil Recovered	44.60	%

113

Figure D.10 Graphical Representation of Pressure Profile during Waterflood (Berea 2)
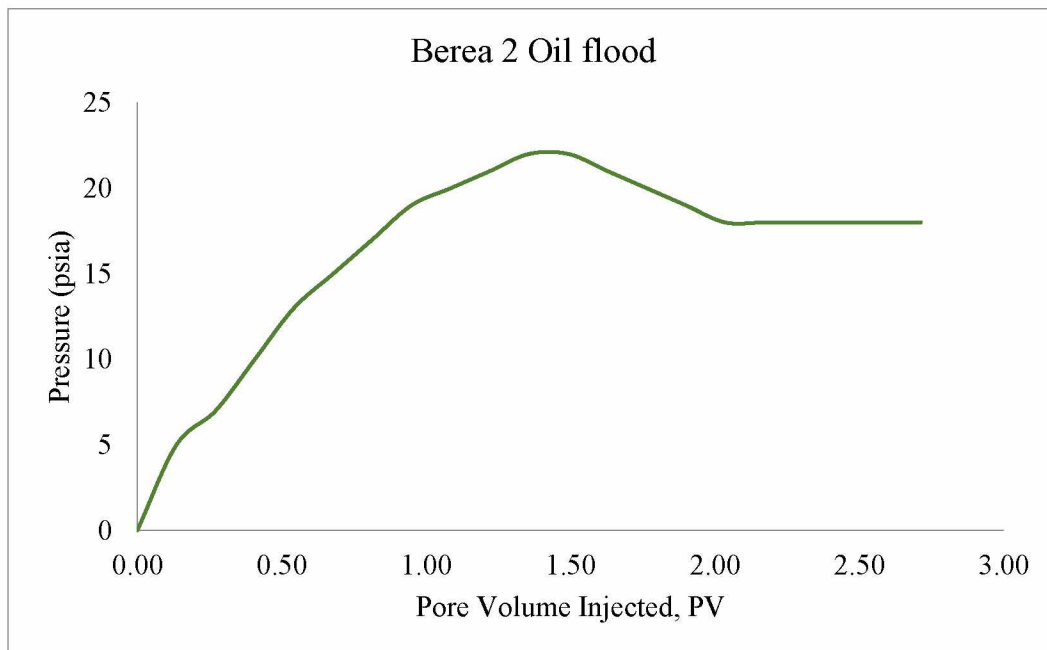

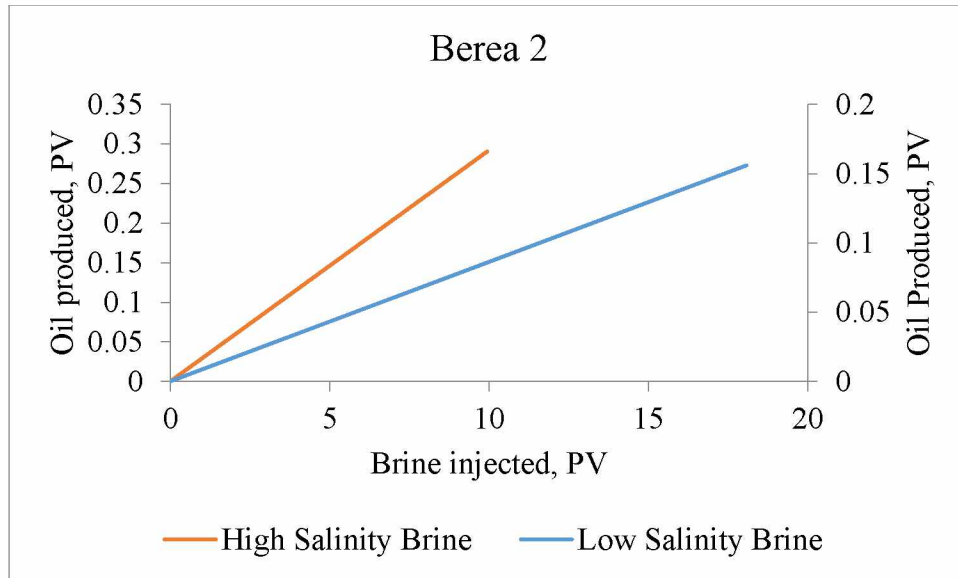Figure D.11 Graphical Representation of Pressure Profile during Oil-flood (Berea 2)

Figure D.12 Oil Recovery Profile for Berea 2
Primary Y-axis: High salinity brine and Secondary Y-axis: Low salinity brine

(a) Dry Sample

(b) Saturated Sample

(c) Spontaneous Displacement with High Salinity Brine

(d) Spontaneous Displacement with Low Salinity Brine
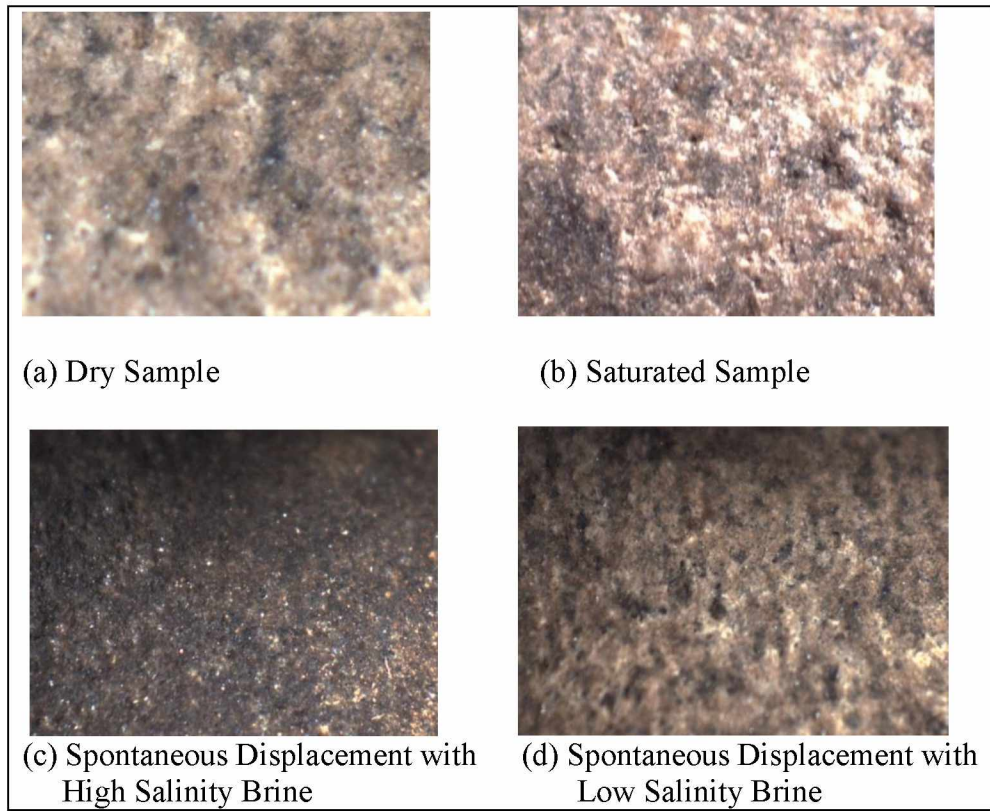
Figure E.1 Microscopic Images for the Core 16

(a) Dry Sample   (b) Saturated Sample

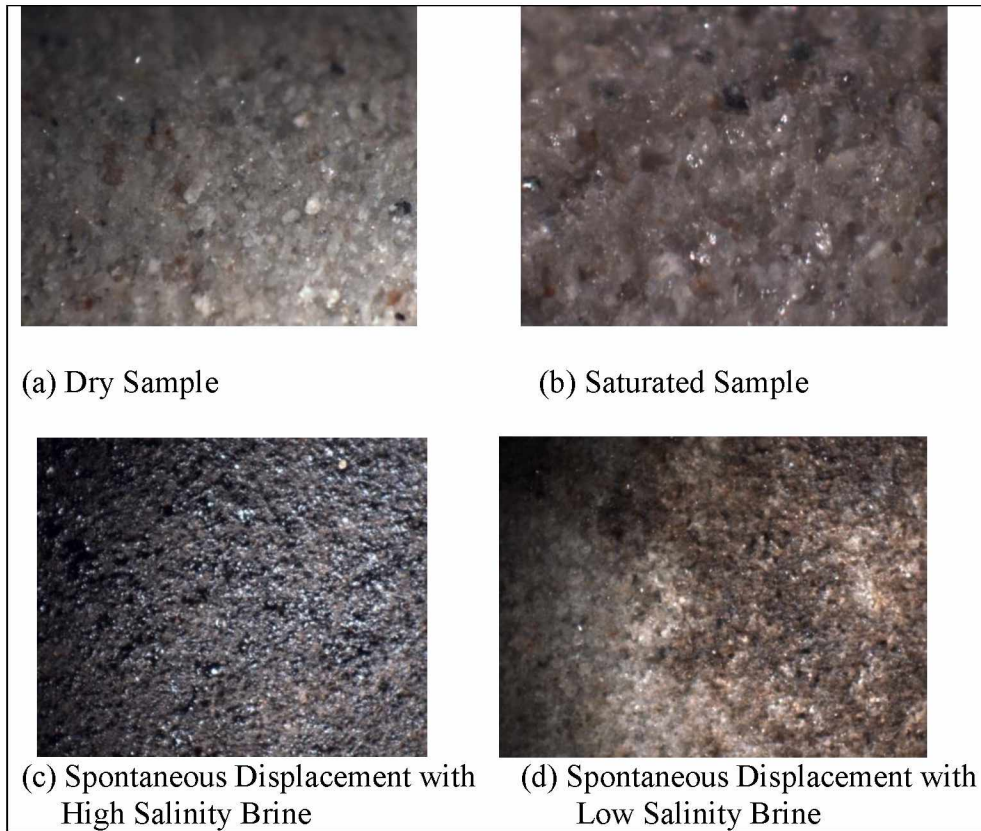(c) Spontaneous Displacement with High Salinity Brine   (d) Spontaneous Displacement with Low Salinity Brine

Figure E.2 Microscopic Images for the Berea Sandstone Core